A Dissertation Submitted to the University of Fukui
for the Degree of Doctor of Engineering

Study on Hydrogen and Deuterium Analysis Using Laser-Induced Plasma Spectroscopy

(レーザー誘起プラズマ分光法を用いた水素と重水素の分析に関する研究)

September 2012

Lie Zener Sukra

University of Fukui

Fukui, Japan

Study on Hydrogen and Deuterium Analysis Using Laser-Induced Plasma Spectroscopy

(レーザー誘起プラズマ分光法を用いた水素と重水素の分析に関する研究)

A Dissertation Submitted to the University of Fukui

for the Degree of Doctor of Engineering

In

Nuclear Power and Energy Safety Engineering

By

Lie Zener Sukra

September 2012

The dissertation of Lie Zener Sukra is approved

Committee Chairperson

_____

Professor Yoichi Tamagawa

Members:

_____ _____

Professor Kiichiro Kagawa Professor Tadashi Kanabe

_____

Professor Hideaki Niki

Abstract

Experimental study has been carried out for development of highly sensitive analysis of hydrogen and deuterium using laser-induced plasma spectroscopy. It should be stressed that highly sensitive and reliable analysis of hydrogen and deuterium is very difficult when we employed the ordinary laser-induced breakdown spectroscopy (LIBS) technique due to the undesirable effect of line broadening, the "mismatching effect", and the disturbance by ubiquitous water molecules (H_2O).

To overcome these difficulties, in this study, we offer two methods using laser-induced plasma; namely, one is laser-induced low-pressure plasma and the other one is laser-induced helium gas plasma at atmospheric pressure.

In low-pressure plasma, a 355 nm Nd:YAG laser irradiation on Ti sample was carried out to demonstrate its applicability to quantitative micro-analysis of deuterium impurities in titanium without the disturbance from ubiquitous surface water. This was achieved by adopting the optimal experimental conditions ascertained in this study, which were specified by 5 mJ laser energy and 10 Torr helium gas pressure. In this experimental study, we also demonstrated the potential applicability to three-dimensional quantitative micro-analysis of deuterium impurities in zircaloy using picoseconds laser (pulse width of 20 ps). The optimal experimental condition was specified as 7 mJ laser energy and 10 Torr helium gas pressure. By employing these operational parameters, a linear calibration line exhibiting a zero intercept was obtained from zircaloy sample doped with various concentrations of D with a limit of detection of approximately 10μg/g.

In high-pressure plasma, we intentionally used helium gas plasma to excite hydrogen or deuterium atoms to escape from "mismatching effect", which means H and D came out earlier than the shock wave generation, thus no excitations of H and D occurs in ordinary LIBS. For this purpose, special setup was offered by using ps and ns laser systems. In this technique, ps laser was operated for the ablation of the sample target and ns laser was operated for the generation of helium gas plasma with controlled relative timing. The desired sharp D emission (656.1 nm) was confirmed with effective suppression of interfering H emission from H_2O by operating the ps ablation laser at energy of approximately 26 mJ and at 1μs ahead of the helium plasma generation. Under this optimal experimental condition, a linear calibration line was obtained with practically zero intercept and a 20 μg/g detection

limit for D analysis in zircaloy sample, while in the same time creating a small size crater (only 10 μm in diameter).

It was confirmed again that the metastable helium atoms were very useful to excite hydrogen atom. In order to increase sensitivity of hydrogen analysis, it was required to make a lot of metastable helium atoms by inducing a big helium gas plasma. Therefore, a TEA CO_2 laser was used because of its specific characteristics of a TEA CO_2 laser, namely, long wavelength (1,064 nm) and long pulse duration (200 ns). In this study, we found that the H emission was still clearly detected from the zircaloy sample containing several hundred μg/g of H without the disturbance of host elements when only the TEA CO_2 laser was focused onto the sample. Namely, zircaloy sample was faintly melted and only H atoms come out from the sample surface and subsequently move into the helium gas plasma to be excited through metastable helium atoms. We called this technique the "selective detection of H". In order to suppress the H disturbance from H_2O, a small helium gas plasma (diameter of approximately 5 mm) was produced on the zircaloy sample surface by irradiating a TEA CO_2 laser (energy of 250 mJ). This gas plasma was completely covered by fresh helium gas using a big pipe (5mm in diameter) and a by flowing high current of He (10 Lpm). As the result, high-sensitivity H analysis can be performed in zircaloy sample containing hydrogen in low concentration level (11-100 μg/g) with a limit of detection of approximately 5 μg/g. Basically, we also have demonstrated that our methods can potentially be applied to H analysis in steel samples, where less 1 μg/g H of analysis was required without employing heating process, by removing H_2O on the sample surface using synchronized defocus TEA CO_2 laser pre-irradiation and photomultiplier detection methods with an aid of interference filter at hydrogen emission line, H_α.

Moreover, we also showed the evidence of mismatching effect and the mechanism of the excitation process of the atoms in laser-induced helium gas plasma. To prove the mismatching effect, helium metastable atoms probing technique was used. Helium gas plasma was produced in front of the sample surface by focusing a fundamental Nd:YAG laser (110 mJ), and a 532 nm Nd:YAG laser was irradiated on the sample surface with a suitable delay time to send the atoms to the cooled helium gas plasma, where the metastable helium atoms exist. When the ground-state atoms entered the cooled helium gas plasma, atomic emission took place by colliding with metastable helium atoms. By this method, it was clearly demonstrated that H atoms came out from the sample surface were faster than other elements.

In order to examine the mechanism of excitation process of atoms, Teflon sample was used. We proved that not only impurity atoms and host atoms of the target but also helium atoms were also excited through helium metastable atoms, which were produced at the initial stage of the helium gas plasma production through recombination process between helium ions and electrons. It was also concluded that during the recombination process, mostly triplet metastable helium atoms were produced. Thus, it is reasonable to think that not singlet helium metastable atoms, but triplet helium metastable atoms are major contributor in the excitation process.

List of Contents

List of Scientific Publications

International Publication

1. Ali Khumaeni, **Zener Sukra Lie**, Yong Inn Lee, Kazuyoshi Kurihara, Koo Hendrik Kurniawan, Ken-ichi Fukumoto, Kiichiro Kagawa, and Hideaki Niki, *Emission Characteristics of Ca and Mg Atoms in Gas Plasma Induced by the Bombardment of Transversely Excited Atmospheric CO_2 laser at 1 atm*, Jpn. J. Appl. Phys. **51** (2012) pp.082403 1-9

2. **Zener Sukra Lie**, Ali Khumaeni, Hideaki Niki, Kazuyoshi Kurihara, Koo Hendrik Kurniawan, Rinda Hedwig, Ken-ichi Fukuimoto, Kiichiro Kagawa, Yong Inn Lee, *A Comprehensive Study of H Emission in TEA CO_2 Laser-induced Helium Gas Plasma for Highly Sensitive Analysis of Hydrogen in Metal Samples*, Journal of the Korean Physical Society **61**, 1 (2012) pp. 49-54

3. Maria M. Suliyanti, Affi N. Hidayah, Marincan Pardede, Eric Jobiliong, Syahrun N. Abdulmadjid, Nasrullah Idris, Muliadi Ramli, Tjung J. Lie, Rinda Hedwig, May O. Tjia, Koo H. Kurniawan, **Zener S. Lie**, Hideaki Niki, Kichiro Kagawa, *Double pulse spectrochemical analysis using orthogonal geometry with very low ablation energy and He ambient gas*, spectrochim. Acta Part B: At. Spectrom **59** (2012) pp. 56-60

4. Ali Khumaeni, **Zener Sukra Lie**, Hideaki Niki, Yong Inn Lee,Kazuyoshi Kurihara, Motoomi Wakasugi, Touru Takahashi, andKiichiro Kagawa, *Comparative study of Nd:YAG laser-induced breakdown spectroscopy and transversely excited atmospheric CO_2 laser-induced gas plasma spectroscopy on chromated copper arsenate preservative-treated wood*, Appl. Opt.**51** (2012) pp. B121-B129

5. H. Suyanto, **Z.S. Lie**, H. Niki, K. Kagawa, K. Fukumoto, R. Hedwig, S.N. Abdulmadjid, A.M. Marpaung, M. Pardede, M.M. Suliyanti, A.N. Hidayah, E. Jobiliong, T.J. Lie, M.O. Tjia, K.H. Kurniawan, *Quantitative Analysis Of Deuterium In Zircaloy Using Double-Pulse Laser-Induced Breakdown Spectrometry (LIBS) And*

Helium Gas Plasma Without A Sample Chamber, Anal. Chem. **84** (2012) pp. 2224-2231

6. **Zener Sukra Lie**, Ali Khumaeni, Kazuyoshi Kurihara, Koo Hendrik Kurniawan, Yong Inn Lee, Ken-ichi Fukumoto, Kiichiro Kagawa, And Hideaki Niki, *Excitation Mechanism of H, He, C, and F Atoms in Metal- Assisted Atmospheric Helium Gas Plasma Induced by Transversely Excited Atmospheric- Pressure CO_2 Laser Bombardment,* Jpn. J. Appl. Phys. **50** (2011) pp. 122701 1-7

7. A.M. Marpaung, **Z.S. Lie**, H. Niki, K. Kagawa, K. Fukumoto, M. Ramli,. S.N. Abdulmadjid, N. Idris, R. Hedwig, M.O. Tjia, M. Pardede, M.M. Suliyanti, E. Jobiliong, K.H. Kurniawan, *Deuterium Analysis in Zircaloy using ps Laser-Induced Low Pressure Plasma,* J. Appl. Phys., **110** (2011) pp. 063301 1-6.

8. **Z. S. Lie**, H. Niki, K. Kagawa, May On Tjia, R. Hedwig, M. Pardede, E. Jobiliong, M. M. Suliyanti, S. N. Abdulmadjid, and K. H. Kurniawan, *Observation of exclusively He-induced H emission in cooled laser plasma*, J. Appl. Phys. **109** (2011) pp. 103305 1-5

9. Ali Khumaeni, **Zener Sukra Lie,** Hideaki Niki, Koo Hendrik Kurniawan, Yong Inn Lee, Kazuyoshi Kurihara, and Kiichiro Kagawa, *Direct Analysis of Powder Sample Using Transversely Excited Atmospheric CO_2 Laser-Induced Gas Plasma at 1 Atm By Introducing The Powder Particles Into The Plasma,* Journal of Analytical and Bioanalytical Chemistry **400** (2011) pp. 3279-3287

10. **Zener Sukra Lie,** Ali Khumaeni**,** Tadashi Maruyama, Ken-ichi Fukumoto, Hideaki Niki and Kiichiro Kagawa**,** *Emission characteristics of Hydrogen in atmospheric helium gas plasma induced by TEA CO_2 laser bombardment on zircaloy sample containing hydrogen,* Journal of Analytical Atomic Spectrometry **26** (2011) pp. 1451-1456

11. Ali Khumaeni, **Zener Sukra Lie**, Yong Inn Lee, Kazuyoshi Kurihara, Hideaki Niki, and Kiichiro Kagawa, *Rapid Analysis of Tiny Amount of Powder Samples Using Transversely Excited Atmospheric CO_2 Laser-induced He Gas Plasma with the Aid of*

High-Vacuum Silicon Grease as a Binder on Metal Subtarget, Applied Spectroscopy **65**, 2, (2011) pp. 236-241

12. Ali Khumaeni, **Zener Sukra Lie**, Hideaki Niki, Kenichi Fukumoto, Tadashi Maruyama, and Kiichiro Kagawa. *A novel double-pulse laser plasma spectroscopy technique for H analysis in metal samples utilizing transversely excited atmospheric-pressure CO_2 laser induced metastable He atom.* Journal of optical review 17, (2010) pp. 285-289

13. **Zener Sukra Lie**, Ali Khumaeni, H. Niki, K. Fukumoto, and K. Kagawa *Hydrogen analysis in metal samples by selective detection method utilizing TEA CO_2 laser-induced He gas plasma*, Applied Physics A, Springer 101, (2010) pp. 555-558

14. S.N. Abdulmadjid, **Z.S. Lie,** H. Niki, M. Pardede, R. Hedwig, T.J. Lie, E. Jobiliong, K.H. Kurniawan, K.Fukumoto, K. Kagawa, M.O. Tjia, *Quantitative Deuterium Analysis of Titanium Samples in UV Laser-Induced Low-Pressure Helium Plasma,* Appl. Spectrosc. **64**, 4, (2010) pp. 365-369

15. R. Hedwig, **Z.S. Lie**, K.H. Kurniawan, A.N. Chumakov, K. Kagawa, M.O. Tjia, *Toward Quantitative Deuterium Analysis with Laser-Induced Breakdown Spectroscopy Using Atmospheric-Pressure Helium Gas,* J. Appl. Phys. **107**, 2 (2010) pp. 023301 1-5

16. **Z.S. Lie**, M. Pardede, R. Hedwig, M.M. Suliyanti, E. Steven, Maliki, Koo H. Kurniawan, M. Ramli, S.N. Abdulmadjid, N. Idris, K. Lahna, K. Kagawa and M.O. Tjia, *Intensity Distributions of Enhanced H Emission from Laser-Induced Low-Pressure He Plasma and a Suggested He-Assisted Excitation Mechanism,* J. Appl. Phys., **106**, 3 (2009) pp. 043303 1-6

17. **Zener S. Lie**, M. Pardede, R. Hedwig, M.M. Suliyanti, K.H. Kurniawan, Munadi, Y.I. Lee, K. Kagawa, I. Hattori, M.O. Tjia, *Spectrochemical Analysis of Powder Using 355 nm Nd-YAG Laser-Induced Low Pressure Plasma*, Anal and Bioanal. Chem, **390** (2008) pp. 1781-1787

18. Munadi, M. Pardede, R. Hedwig, M.M. Suliyanti, T.J. Lie, **Z.S. Lie**, Koo H. Kurniawan, K. Kagawa, M. Ramli, K. Fukumoto, T. Maruyama, M.O. Tjia, *Study of Hydrogen and Deuterium Emission Characteristics in Laser Induced Low Pressure Helium Plasma for the Suppression of Surface Water Contamination,* Anal. Chem, **80**, 4 (2007) pp. 1240-1246

19. M. Ramli, K. Fukumoto, H. Niki, S.N. Abdulmadjid, N. Idris, T. Maruyama, K. Kagawa, M.O. Tjia, M. Pardede, K.H. Kurniawan, R. Hedwig, **Z.S. Lie**, T.J. Lie, D.P. Kurniawan, *Quantitative Hydrogen Analysis of Zircaloy-4 in Laser-Induced Breakdown Spectroscopy with Ambient Helium Gas,* Appl. Opt. **46** (2007) pp. 8298-8304

20. M. Pardede, R. Hedwig, M.M. Suliyanti, **Z.S. Lie**, T.J. Lie, D.P. Kurniawan, K.H. Kurniawan, M. Ramli, K. Fukumoto, H. Niki, S.N. Abdulmadjid, N. Idris, T. Maruyama, K. Kagawa, M.O. Tjia, *Comparative Study of Laser-Induced Plasma Emission of Hydrogen from Zircaloy-2 Samples in Atmospheric and Low Pressure Ambient Helium Gas,* Appl. Phys. B. **89**, 2-3 (2007) pp. 291 - 298

21. K.H. Kurniawan, M. Pardede, R. Hedwig, **Z.S. Lie**, T.J. Lie, D.P. Kurniawan, M. Ramli, K. Fukumoto, H. Niki, S.N. Abdulmadjid, N. Idris, T. Maruyama, K. Kagawa, M.O. Tjia, *Quantitative Hydrogen Analysis of Zircaloy-4 Using Low-Pressure Laser Plasma Technique,* Anal. Chem. **79**,7 (2007) pp. 2703-2707

22. M. Ramli, K. Kagawa, S.N. Abdulmadjid, N. Idris, W.S. Budi, M.A. Marpaung, K.H. Kurniawan, T.J. Lie, M.M. Suliyanti, R. Hedwig, M. Pardede, **Z.S. Lie**, M.O. Tjia, *Some Notes on the Role of Meta-Stable Excited State of Helium Atom in Laser-Induced Helium Gas Breakdown Spectroscopy,* Appl. Phys. B. **86**, 4 (2007) pp. 729-734

NATIONAL PUBLICATION

1. Kiichiro Kagawa, **Zener Sukra Lie**, Ali Khumaeni, Kazuyoshi Kurihara, *Laser-Induced Breakdown Spectrosopy*, Journal of the Japan Society of Abrasive Technology. **56**, 8 (2012) pp.515-518

International Conference

1. **Zener Sukra Lie**, Ali Khumaeni**,** Hideaki Niki, Yong Inn Lee, Kazuyoshi Kurihara, Koo Hendrik Kurniawan, Ken-ichi Fukumoto, Kiichiro Kagawa, *Excitation Mechanism in Metal Assisted-Atmospheric He Gas Plasma Induced by TEA CO2 Laser Bombardment,* EMSLIBS 2011, Turkey, September 11-15, 2011

2. **Zener Sukra Lie**, Ali Khumaeni**,** Hideaki Niki, Yong Inn Lee, Kazuyoshi Kurihara, Ken-ichi Fukumoto, Kiichiro Kagawa, *Effective techniques to suppress H emission from H_2O in TEA CO_2 laser-induced helium gas plasma for highly sensitive hydrogen analysis in metal sample* **,** OIE'11, Finland, September 8-10, 2011

3. Ali Khumaeni**, Zener Sukra Lie**, Hideaki Niki, Kazuyoshi Kurihara, Kiichiro Kagawa, *Analysis of Pre-Treated Wood Using Transversely Excited Atmospheric CO2 Laser-Induced Gas Plasma*, NASLIBS 2011, Florida, July 18-20, 2011

4. A.M. Marpaung, **Z.S. Lie**, H. Niki, K. Kagawa, K. Fukumoto, M. Ramli, S.N. Abdulmadjid, N. Idris, R. Hedwig, M.O. Tjia, M. Pardede, E. Jobiliong, M.M. Suliyanti, K.H. Kurniawan, *Metastable Excited He Assisted Optical H and D Emission in Laser Induced Plasma Spectroscopy*, International Symposium on Modern Optics and Its Applications – 2011, Bandung, Indonesia, July 4-7, 2011

5. Ali Khumaeni, **Zener Sukra Lie**, Hideaki Niki, Yong Inn Lee, Kazuyoshi Kurihara, and Kiichiro Kagawa, *A Unique Technique for Rapid Analysis of Tiny Amount of Powder Sample Using Transversely Excited Atmospheric CO2 Laser-induced He Gas Plasma at 1 atm*, Pachifichem 2010, Honolulu, Hawaii, USA, December 15-20, 2010.

6. Kiichiro Kagawa, **Zener Sukra Lie**, Ali Khumaeni, Kazuyoshi Kurihara, Hideaki Niki, and Kenichi Fukumoto, *Review on Hydrogen Analysis Using TEA CO2 Laser-Induced He Gas Plasma at 1 atm*, Pachifichem 2010, Honolulu, Hawaii, USA, December 15-20, 2010.

7. **Zener Sukra Lie**, Ali Khumaeni, Hideaki Niki, Ken-ichi Fukumoto, Kazuyoshi Kurihara, and Kiichiro Kagawa, *Highly Sensitive Hydrogen Analysis on Metal Samples Utilizing Photomultiplier Detection Method in LIBS Using TEA CO2 Laser-*

Induced He Gas Plasma, Pachifichem 2010, Honolulu, Hawaii, USA, (December 15-20, 2010)

8. Ali Khumaeni, **Zener Sukra Lie**, Hideaki Niki, Yong Inn Lee, Kazuyoshi Kurihara, and Kiichiro Kagawa, *Direct Analysis of Powder Sample Using Transversely Excited Atmospheric CO_2 Laser-induced Metal Assisted Gas Plasma at 1 atm by Introducing the Powder Particles into the Plasma***,** 6th International Conference on Laser-Induced Breakdown Spectroscopy, Memphis, USA, (September 13-17, 2010), pp.158

9. **Zener Sukra Lie**, Ali Khumaeni, Hideaki Niki, Kazuyoshi Kurihara, Ken-ichi Fukumoto, and Kiichiro Kagawa, *Highly Sensitive Analysis of Hydorogen in Metal Samples Using Selective Detection Method in TEA CO_2 Laser-Induced Helium Gas Plasma by Utilizing Effective Techniques to Suppress H Emission from H_2O*, 6th International Conference on Laser-Induced Breakdown Spectroscopy, Memphis, USA, (September 13-17, 2010), pp.57

10. **Z. S. Lie,** Ali Khumaeni, K. Fukumoto, H. Niki, and K. Kagawa, *Spectrochemical Analysis Using TEA CO2 laser-Induced He Gas Plasma at 1 atm*. International and commemorative symposium in establishing the applied laser technology, Institute at Tsuruga Head Office, JAEA (ICSL 2010), February 17-18 (2010)

11. **Z.S. Lie**, Ali Khumaeni, H. Niki, K. Fukumoto, and K. Kagawa, *Hydrogen Analysis in Metal Samples by Selective Detection Method Utilizing TEA CO2 Laser-Induced He Gas Plasma***,** 10th International Conference on Laser Ablation, Nov 22-27, Singapore, (2009) pp.339

12. K. Kagawa, Ali Khumaeni, **Z.S. Lie**, K.H. Kurniawan, H. Niki, K. Fukumoto, *Hydrogen Analysis in Metal Samples by Selective Detection Method Utilizing TEA CO2 Laser-Induced He Gas Plasma*, 2nd North American Symposium on Laser-Induced Breakdown Spectroscopy, July 13-15, New Orleans, LA, USA (2009) pp.118

13. K.H. Kurniawan, **Zener S. Lie**, T.J. Lie, M.O. Tjia, K. Kagawa, *Excitation Mechanism of Hydrogen Emission in the Plasma Induced by Nd-YAG Laser at*

Atmospheric Pressure of Helium Gas, Second Asia Pacific Winter Conference on Plasma Spectrochemistry, Bangkok, Thailand (November 26 - December 2, 2006) pp. 113-114.

National Conference

1. Ali Khumaeni, **Zener Sukra Lie**, Kazuyoshi Kurihara, Ken-ichi Fukumoto, Kiichiro Kagawa, and Hideaki Niki, *High Sensitive Analysis of Atoms on Metal Surface by Using Transversely Excited Atmospheric Pressure CO2 Laser,* Annual Meeting of AESJ (Atomic Energy Society of Japan), Fukui, Japan, March 19-21, 2012

2. 이 용인, **LIE Zener Sukra**, KHUMAENI Ali, NIKI Hideaki, KURNIAWAN Koo Hendrik, KICHIIRO Kagawa, KURIHARA Kazuyoshi, *Excitation Mechanism of H, He, C and F Atoms in Metal-Assisted Atmospheric Helium Gas Plasma induced by Transversely Excited Atmospheric-Pressure CO2 Laser Bombardment***,** the fall of 2011 academic paper , South Korean Physical Society Conference, October 19-21, 2011

3. **Zener Sukra Lie**, Ali Khumaeni, Hideaki Niki, Kazuyoshi Kurihara, Ken-ichi Fukumoto, Kiichiro Kagawa, Tadashi maruyama, *Highly sensitive hydrogen analysis in zircaloy sample utilizing TEA CO2 laser-induced He gas plasma,* Annual Meeting of AESJ (Atomic Energy Society of Japan),Fukui, Japan, March 28-30, 2011

4. Ali Khumaeni, **Zener Sukra Lie**, Yong Inn Lee, Kazuyoshi Kurihara, Kiichiro Kagawa, Hideaki Niki, *Direct analysis of powder samples using TEA CO_2 laser-induced metal-assisted gas plasma at 1 Atm*, Annual Meeting of AESJ (Atomic Energy Society of Japan),Fukui, Japan, March 28-30, 2011

5. Ali Khumaeni, **Zener Sukra Lie**, Hideaki Niki, and Kiichiro Kagawa, *Laser-induced plasma spectroscopy using TEA CO2 laser and its applications to rapid elemental analysis*, The 18th Indonesian scientific meeting in Japan, Nagoya, Japan, August 7-8, 2010

Acknowledgements

This thesis was completed with helps and advices of many people. First of all, the author would like to express sincere gratitude to Professor Hideaki Niki for accepting author as his doctoral student at the Department of Nuclear Power and Energy Safety Engineering in University of Fukui Japan and for his helpful guidance, valuable suggestion, and continual encouragement throughout this work. The author would like to express his indebtedness to Professor Kiichiro Kagawa for his advice and discussion during the the research work. The gratitude thanks are rendered to Professor Ken-ichi Fukumoto for his kind encouragement and his helped to prepare the zircaloy sample containing H and D in the research work. Also the author would like to express his thankfulness to Professor Kazuyoshi Kurihara for his kind support.

The author is also especially grateful to Dr. Hendrik Kurniawan for his kind support and helping the research in Maju Makmur Mandiri Research Center, Jakarta, Indonesia. Special thanks are rendered to Professor Yong Inn Lee, Chonbuk National University Republic of Korea for discussion related to my thesis subjects and his kind help in Journal submission. Special grateful thanks are delivered to President of University of Fukui for giving author a chance to pursue doctor program in University of Fukui Japan.

The author wishes to thank the Japanese Ministry of Education, Science, Sport and Culture (MEXT) for the scholarship support during my study as a doctor student at the Department of Nuclear Power and Energy Safety Engineering, Graduate School of Engineering, University of Fukui Japan.

I am greatly indebted and appreciate very much to my family for support. Thanks to Ali Khumaeni and colleagues as well as students for their kind help and good cooperation during my study and research works in University of Fukui. The author would like to express his deepest and heartiest thankfulness to all international friends for support and motivate during stayed in Fukui.

Biography

Personal Data

Name:	Lie Zener Sukra
Date of birth:	March 14, 1984
Place of birth:	Jakarta, Indonesia
Gender:	Male
Marital Status:	Single
Address:	Jl. Taman Chung no 10, Jakarta, Indonesia, 10130

Education Background

2009-2012	University of Fukui, Program of Nuclear Power and Energy Safety Engineering (doctoral)
2008- 2009	University of Indonesia (UI), Faculty of Electrical Engineering (Doctoral)
2006-2008	Bandung Institute of Technology, School of Electrical and Informatics Engineering (Graduate)
2002-2006	University of Indonesia (UI), Faculty of Electrical Engineering (Under Graduate)
1999-2002	SMUK 3 Penabur, Jakarta (senior high school)
1996-1999	SMPK 1 Penabur, Jakarta (junior high school)

Chapter 1

Introduction

A new method for rapid and near *in-situ* hydrogen analysis is urgently needed in many fields of investigation covering the field of material sciences as well as in industries. In a light-water nuclear power station, the enriched uranium fuel is contained in zircaloy pipes which immersed in a water tank. During the operation of the reactor, hot water reacts with the zircaloy surface to form zirconium oxide and hydrogen gas, which readily penetrates into and accumulates in the zircaloy pipe in the form of ZrH. The excessive presence of this trapped hydrogen is known to cause a certain type of structural damage, leading to reduce mechanical strength of the material and potentially endangering the operation of the power plants. Therefore, the hydrogen concentration in the zircaloy pipes must be examined periodically. The standard technique for detecting hydrogen involves melting a portion of the zircaloy tube in a carbon furnace and measuring the gas using a gas detector. However, this method is time-consuming, is destructive, cannot be used *in-situ*, and does not allow a mapping analysis to be performed. To overcome the problem, we applied a novel technique using laser plasma spectroscopy, which is believed to provide the solution, especially for rapid H analysis.

The invention of laser, made by Theodore Maiman in 1960 [1-2], has significantly changed the direction of the development of science and technology. The lasers have created the ripples in the world of technology. One of very interesting laser characteristics is its ability to create a luminous spark which referred as laser-induced plasma (LIP). One of the appealing applications is elemental analysis on any kind of materials, which is known as laser-induced plasma spectroscopy (LIPS). LIPS, which is commonly called as laser-induced breakdown spectroscopy (LIBS), has recently become an increasingly popular technique for rapid and *in-situ* qualitative and quantitative elemental analysis of various samples in

different forms such as solids, liquids, and gases [3-12]. Because of the unique point of LIPS, it should be stressed that LIPS will be prospective as an applicable analytical tool for safety monitoring in nuclear industries, such as nuclear power station.

Despite many advantages of LIPS as analytical tool, there are still several problems to be solved for practical application, especially in hydrogen analysis. First, in the case of the ordinary LIPS method, the background of spectrum is rather high; this means that the minimum determinable concentration of the element is still high. Second, plasma emission highly fluctuates under the successive irradiation of the laser beam, which causes low precisions in quantitative analysis; during the laser irradiation, the crater shape on the sample surface always changes with each laser shot, resulting in the plasma emission fluctuation happens due to the change in the situation of gushing atoms. Third, due to the occurrence of the "mismatching effect" [13, 14], some elements which have very light or heavy mass compared to the host elements cannot be excited well. For instance, hydrogen containing in zircaloy tube is difficult to be excited in the laser plasma by employing ordinary LIBS due to the difference between the time when the hydrogen atom gushing occurs and the time when the shock wave starts being induced by the gashing of host elements, which have much higher mass than hydrogen [13].

One of the solutions to overcome these weak points is using low pressure technique. This technique has already been studied but still has some problems. At the initial of this study, we used Titan sample contained deuterium for the first time. Sample contained deuterium was used to avoid H emission which came from H_2O molecules. The best condition for H analysis was searched. Then, we concluded that at low energy (around 5mJ), an effective enhancement of the D impurity signal and effective elimination of the interfering hydrogen emission from the surface water was achieved with high reproducibility.

To demonstrate the potential applicability of three-dimensional quantitative micro-analysis, low pressure technique using picoseconds Nd:YAG laser was used in place of nanoseconds Nd:YAG laser. A linear calibration curve exhibiting a zero intercept was obtained from zircaloy sample doped with various concentration of D impurity. This result was due to escaping from the thermal effect, which induced segregation or migration of the D impurity inside the sample and resulting in changes in its local distribution.

It should be stressed that the implementation using low pressure technique was difficult to perform *in-situ* analysis. To realize the *in-situ* analysis requirement, laser induced helium plasma at atmospheric pressure was used. Two nanoseconds Nd:YAG lasers were applied in this study. Namely, a Nd:YAG laser was used to induce helium gas plasma and the

other laser was used to send the atoms to the helium gas plasma in order to solve the "mismatching effect". Using this technique, we also showed the evidence of the "mismatching effect". To obtain highly sensitive H analysis in atmospheric pressure, we used double pulse technique using picoseconds and nanoseconds laser. Picoseconds laser was used to send atoms to helium gas plasma region, and nanoseconds laser was used to produce meta-stable helium atoms, which play important role to excite atoms.

One solution to increase the sensitivity in the analysis using He gas plasma is to produce a lot of meta-stable helium atoms. To this end, we used the specific characteristics of a TEA CO_2 laser which is low frequency (long wavelength of 10.64 μm) and long pulse duration (200 ns) to produce a big helium gas plasma. In this study, we noticed that when the TEA CO_2 laser was focused on the zircaloy surface, H analysis can be done without ablating the sample. Namely, a strong helium gas plasma was produced and only H atoms came out from the sample. Then, the H atoms moved into the helium gas plasma to be excited through the meta-stable helium atoms. We call this technique "selective detection of H". Using this method, a nice linear calibration curve has successfully been made.

By applying "selective detection of H" method, the H_α, H_β, H_γ, and H_δ emission lines can be clearly detected with very low background spectrum and a very narrow spectral width using zircaloy sample which contains H. The excitation mechanism of hydrogen atoms in TEA CO_2 laser-induced helium gas plasma, emission characteristics of hydrogen and also those of helium and other elements were studied in detail. Based on these emission characteristics, the model of excitation mechanism (recombination model) was offered. Finally, to realize practical application of H analysis on zircaloy sample in nuclear power station, we suppressed the H emission disturbance to the level less than 10μg/g levels. Also, we clarified the origin of H emission disturbance coming from H_2O molecules. Namely, H emission disturbance came from H_2O molecules deposited on the sample surface, and not from H_2O populated in the surrounding gas.

The organization of this dissertation consists of six chapters. Chapter 1 contains the general introduction. Chapter 2 contains a review on basic concept and history of spectrochemical analysis using atomic emission spectroscopy including laser induced plasma spectroscopy. Detail experimental works and results will be described in the following chapters, from 3 to 5. Finally, the general conclusion will be presented in chapter 6.

References

1. T. H. Maiman, Stimulated optical radiation in ruby, Nature 187 (1960) 493-494.
2. T. H. Maiman, Optical and microwave-optical experiments in ruby, Phys. Rev. Lett. **4** (1960) 564-566.
3. R. Yoshiie, Y. Yamamoto, S. Uemiya, S. Kambara, H. Moritomi, Simple and rapid analysis of heavy metals in sub-micron particulates in flue gas, Powder Tech. **180** (2008) 135–139.
4. B. Bousquet, J. B. Sirven, L. Canioni, Towards quantitative laser-induced breakdown spectroscopy analysis of soil samples, Spectrochi. Acta part B **62** (2007) 1582–1589.
5. S. Y. Chan, N. H. Cheung, Analysis of solids by laser ablation and resonance-enhanced laser-induced plasma spectroscopy, Anal. Chem. **72** (2000) 2087-2092.
6. D.C.S. Beddowsa, O. Samekb, M. Lisˇkab, H.H. Telle, Single-pulse laser-induced breakdown spectroscopy of samples submerged in water using a single-fibre light delivery system, Spectrochi. Acta part B **57** (2002) 1461–1471.
7. D. Alamelu, A. Sarkar, S.K. Aggarwal, Laser-induced breakdown spectroscopy for simultaneous determination of Sm, Eu and Gd in aqueous solution, Talanta **77** (2008) 256–261.
8. F.J. Fortes, L.M. Cabalín, J.J. Laserna, Laser-induced breakdown spectroscopy of solid aerosols produced by optical catapulting, Spectrochi. Acta part B **64** (2009) 642–648.
9. J.E. Carranza, B.T. Fisher, G.D. Yoder, D.W. Hahn, On-line analysis of ambient air aerosols using laser-induced breakdown spectroscopy, Spectrochi. Acta part B **56** (2001) 851-864.
10. T. Čtvrtníčková, L. M. Cabalín, J. Laserna, V. Kanický, Comparison of double-pulse and single-pulse laser-induced breakdown spectroscopy techniques in the analysis of powdered samples of silicate raw materials for the brick-and-tile industry, Spectrochi. Acta part B 63 (2008) 42–50.
11. C. Gautier, P. Fichet, D. Menut, J. L. Lacour, D. L. Hermite, J. Dubessy, Quantification of the intensity enhancements for the double-pulse laser-induced breakdown spectroscopy in the orthogonal beam geometry, Spectrochi. Acta part B **60** (2005) 265– 276.
12. C. Gautier, P. Fichet, D. Menut, J. Dubessy, Applications of the double-pulse laser-induced breakdown spectroscopy (LIBS) in the collinear beam geometry to the elemental analysis of different materials. Spectrochi. Acta part B **61** (2006) 210–219.
13. K. H. Kurniawan, and K. Kagawa, Laser- Induced Shock Wave Plasma Spectroscopy, Applied Spectroscopy Reviews, **41** (2006), 1-36
14. N. Idris, S. Terai, T. J. Lie, H. Kurniawan, T Kobayashi, T. Maruyama, and K.Kagawa, Hydrogen Emission Induced by TEA CO_2 Laser Bombardment on Solid Samples at Low Pressure and Its Analytical Application, Appl. Spectroscopy, **59** (2005) 115-120

Chapter 2

Reviews on Laser-Induced Plasma Spectroscopy (LIPS)

2.1 Atomic Emission Spectroscopy (AES)

Spectroscopy is a technique, which uses the interaction of energy with a sample to perform an analysis; namely, the study of the absorption and emission of light and other radiation by matter [1]. Spectroscopy itself has several types, which are divided by the energy source; they are atomic emission spectroscopy, x-ray fluorescence spectroscopy, gamma-ray spectroscopy, etc. In this study, we concerned to the atomic emission spectroscopy which is the main part of spectrochemical analysis.

Atomic Emission Spectroscopy is a method of chemical analysis with the basic concept based on the light emission occurrence when electron in an upper energy state of atom drop to a lower level due to the fact that the atoms in the excited state have a natural tendency to de-excite and lose their excess energy [2]. Each atom has a characteristic emission spectrum, which is determined by its energy level, and in ordinary condition, all atoms are populated in the ground state of atomic energy level in thermal equilibrium. Once a suitable energy is given to the atom, the electron jumps up from the ground state to the excited state of the energy levels by absorbing the energy. Then, the electrons subsequently undergo a transition to the lower levels by emitting light which has special characteristics depending on kind of atoms.

To excite the atoms, high temperature plasma is required and many scientists have tried to create the exciting source. The first technique was made using a flame source, which is known as the oldest spectrochemical technique [3]. In flame, the sample to be analyzed is usually nebulized into the high temperature environment of the flame, where desolvation, volatilization, and atomization take place. Flame emission remains useful in determining alkali metals and others elements which easy to excited. In fact, common flames are not very

energetic and this limits detectability of elements with high excitation energies. Plasma source which has much more energetic (higher atomization efficiencies, high degrees of excitation and lower detection limit for many elements) than common flame, is required.

Next technique is arc and spark discharge excitation. The major used of the arc discharge is in qualitative and semi-quantitative analysis, because the precision of quantitative determination is not high as desirable [3]. The arc is an electrical discharge between two or more conducting electrodes, which common material is graphite. Spark discharge is similar to the arc discharge. The difference is that the spark is an intermittent high-voltage discharge rather than a continuous discharge like the arc. Even though the spark discharge is an extremely energetic source with high peak currents and high power densities, limits of detection are usually higher than with arc discharge, and the extent of ionization is higher, resulting in high spectrum background. Also, very little sample is ordinarily consumed during sparking.

In place of the conventional discharge method, nowadays, the inductively coupled plasmas (ICP) is very aggressive light source for spectrochemical analysis. In ICP spectroscopy, the plasma is produced in a quartz tube surrounded by an induction coil that is connected to a high-frequency generator, which plays important role in inducing the plasma. In the quartz tube, a noble gas is flowed during the analysis to act as the support gas for the plasma and as the coolant for the quartz tube. To initiate the plasma, a spark from the induction coil is applied to produce electrons and ions in the quartz tube. The electrons then collide with the noble gas, resulting in plasma consisting of electrons, and ions. Using this method, the high temperature around 9,000 to 10,000 K and very stable plasma has been produced; therefore, the ICP has been known as high sensitive analytical methods [3]. However, ICP has several weaknesses; namely, sample must be prepared in the form of aerosol, the equipment is very big and expensive, and the results have spectral overlap interference.

2.2 Laser Atomic Emission Spectrochemical Analysis

Laser atomic emission spectrochemical analysis (LAESA) is one of atomic emission techniques, in which a high-power pulsed laser is employed as an energy source. Compared to other analytical techniques, LAESA is much easier to widely spread and significantly develop due to the fact that the vaporization, atomization, and excitation processes take place at the same time by a single treatment of laser irradiation [4]. Thus, this method enables one to carry out rapid and direct analysis without significant time consuming. Also, the technique

is highly possible to perform *in-situ* analysis due to its simplicity, flexibility, and freedom from sample pretreatment and is capable of conducting remote analysis because the technique requires only optical access to the sample being tested [5]. Using this technique, various kinds of sample including solids, liquids, and gases can readily be analyzed.

Spectrochemical analysis using laser, Laser Atomic Emission Spectrochemical Analysis (LAESA), was started in 1962 by Brech and Cross [6]. During the time, LAESA become the most typical application of laser. A Q-switched ruby laser or Nd glass laser is focused on the sample in air at atmosphere pressure and photograph plate is used for spectrum recording. The advantages of this method compared to the conventional spectrochemical methods such as spark and arc discharge are that analysis can be realized without pretreatment of the samples, and micro-area analysis as well as *in-situ* analysis can be performed. Furthermore, it is not only applicable to metal sample but also can be applied to non-metals samples. On the other hand, the disadvantages of this method are that the background of this emission spectrum is very strong due to the high density, high temperature plasma, and that self-absorption effect takes place. These disadvantages become the major obstacles in yielding the linearity and sensitivity required for accurate spectroscopy calibration.

To solve these problems at that time, excitation process was separated from laser ablation process; namely, cross excitation was made using auxiliary spark discharge for excitation, and normal oscillation laser for the vaporizing the sample was used as shown in Fig.2.1.[7, 8]. Other methods were excitation in electrode-less high-frequency-discharge such as induction-couple radio frequency (RF) discharge [9] and microwave discharge [10]; and excitation using electron beam as shown in Fig.2.1. However, the problem of non-linearity of the calibration curve and insufficient accuracy involved in this processes were not solved. Also, this technique is no efficient in data collection because the spectrum was recorded on a film using spectrograph, which took time. This cause LAESA method was only used for qualitative or semi quantitative analysis and the research on LAESA had become inactive in the end of 1970.

After 1980, the interest of LAESA method started again due to development of the good quality of laser system such as the Nd:YAG laser. The laser system has been offering good shot to shot power stability and good beam quality which bring high focusibility of laser light. The development of optical multi-channel analyzer (OMA) had also contributed to the study of laser spectroscopy. Supported by these new instruments, the study of LAESA has

entered the new era which was known as Laser-induced Plasma Spectroscopy (LIPS) or Laser-induced Breakdown Spectroscopy (LIBS).

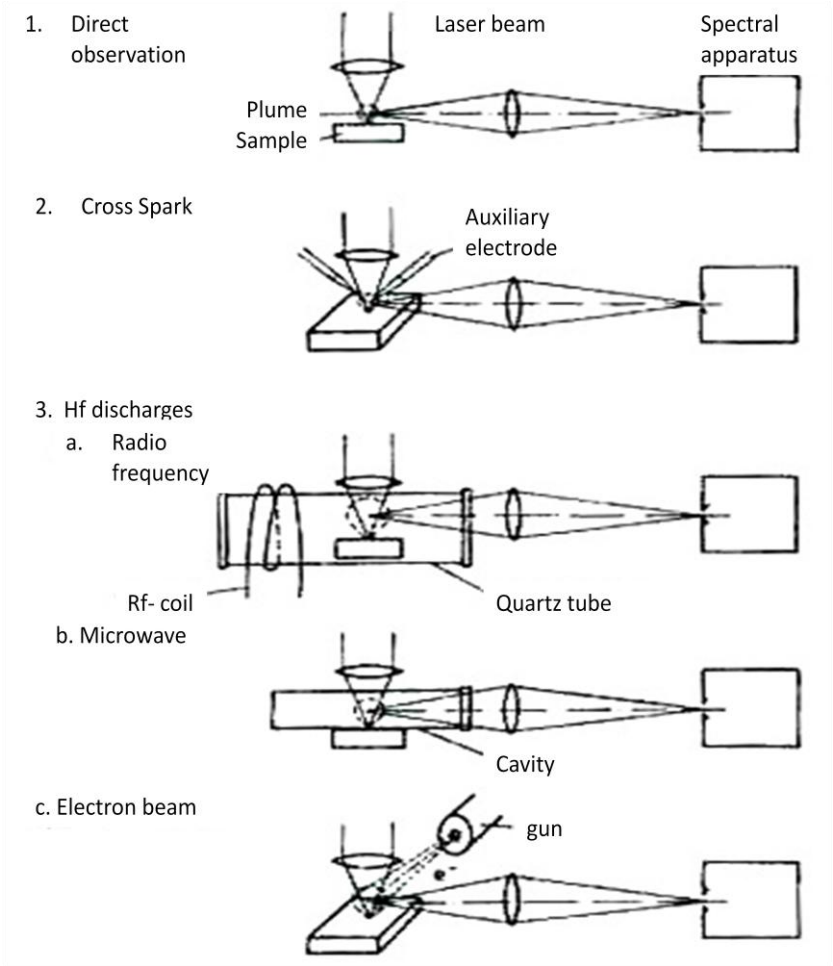

Fig.2.1. Possibilities of optical emission spectroscopy with laser atomizers [7]

Nowadays, in general, LIPS is divided into two main categories differing by the pressure of the surrounding gas; one is using atmospheric pressure and the other is using low pressure. In case of LIPS at atmospheric pressure, a Q-switched Nd:YAG laser with pulsed energy of about several tens of millijoules is focused on the sample, resulting in high-temperature and high-density plasma which cause the strong continuous optical emission. In order to remove this strong continuous optical emission spectrum which exhibited in the initial stage of plasma generation, a gated optical multichannel analyzer (OMA) system must be employed. This kind of method is commonly referred to as Laser-induced Breakdown Spectroscopy (LIBS) and was first developed by Radziemski and coworkers [11, 12].

Another one is LIPS at low gas pressure was developed by Kagawa and coworkers [13-15]. The low-pressure plasma shows favorable characteristics to spectrochemical

analysis; in particular, the low background emission intensity and a good linear relationship between the analytical emissions line intensity and the content. In this method, an analytical spectrum using an OMA system without a gating function can be obtained. Based on many experiment, Kagawa et al. have successfully proved that shock wave played an important role in the excitation of the ablated atoms in the low pressure plasma [16-19].

2.3 Laser-Induced Shock Wave Plasma Spectroscopy

Just after the invention of the pulsed high power laser, there are many reports on the shock wave produced by laser irradiation in gas or solid target in certain ambient gas. The study of this mechanism was started by Ramsden et al [20] and Daiber et al. [21] Streak and framing camera was applied to record the expansion of the luminous plasma front as a function of time when a high peak power Nd:YAG laser was focused into the gas. In their experiment, it was found that the gas breakdown appeared just before the arrival of peak intensity of the laser pulse, and after the occurrence of the gas breakdown, the bright spark developed asymmetrically, moving towards the lens. The rapid expansion of the gas breakdown generated a shock wave propagating in the surrounding gas, while further absorption of the laser energy took place behind the shock front traveling towards lens, in a manner of detonation wave. The heated gas continued to expand in the form of blast wave after the laser pulse lasted.

To record the expansion of the shock-wave when pulse laser was focused on the target, Basov et al [22-23] used a shadowgraph technique in which a high peak power Nd glass laser (6J, 15ns) was focused onto a carbon target at 2 torr of air surrounding gas. They found that the plasma front consist of thin shell structure moving towards the lens agreement with the theoretical shock wave equation formulated by Sedov [24] and the high electron density was observed just behind the shock wave front which means the high temperature plasma occurs only just behind the shock wave front.

It should be emphasized that all of the above experiments were conducted using high energy laser of the order of few joules, while no report ever mentioned the use of low energy laser (in the order of mJ) for the generation of shock wave. Much less was known in the literatures on the relation between the shock wave formation and excitation mechanism of the ablated atoms and its application for spectrochemical analysis.

On the contrary to the technique described above, namely by using low energy laser, Kagawa et al. successfully produced a laser plasma at low pressure surrounding gas of around 1 Torr on a solid material by using many kinds of low energy lasers such as pulsed N_2 laser,

pulsed transversely excited atmospheric (TEA) CO_2 laser, and excimer laser [25, 26]. The result showed that laser plasma consists of two distinct regions. The first region (the primary plasma) is a small area of high temperature plasma which gives off an intense, continuous emission spectrum for a short time just above the surface of the target. The second area (the secondary plasma) expands with time around the primary plasma, emitting sharp atomic spectral lines with negligibly low background signals. Based on the experimental observation, the secondary plasma has a hemispherical shape with the emission front moving at a speed given by Sedov's equation and the emission intensity was found to decrease abruptly below 1 torr. Kagawa and coworkers concluded that the secondary plasma emission was ascribable to shock wave excitation of the ablated atoms.

In the study of the plasma expansion process, a special technique was developed to detect the time-resolved spatial distribution of the emission intensity, yielding the information regarding to the movement of the emission front [19, 27-28]. By employing the Abel conversion methods [29, 30], the intensity distribution of the neutral and ionic emission were analyzed at different moments after initiation of laser bombardment. It was observed that the emission region featured an outer shell structure expanding at a speed as predicted by Sedov's equation for the point explosion to make a blast wave. Further experiment by using confined plasma [31] showed a plane wave structure of the secondary plasma which is similar to the shock wave in a mechanical shock tube generated by a very high speed shock.

In the laser-induced shock wave plasma study, density jump measurement was provided [32]. A special interferometric technique was devised on the basis of a rainbow refractometer, without using an additional and delicate beam-splitting setup for the probing laser. This technique was used for the characterization of plasma induced by TEA CO_2 laser and Q-switched Nd:YAG laser. An unmistakable signal of the density jump was detected simultaneously with the observation of the emission front signal. It was proved that the emission front and the front of the shock wave coincided and move together with time at the initial stage of the secondary plasma expansion. While at the later stage, the emission front began to fall behind the shock wave front propagating in the surrounding air. The data analysis of the shock front movement along this emission characteristic has led to the conclusion that a shock wave was responsible for the excitation process in the secondary plasma [33, 34]. When laser is focused at the sample, electron, atoms, molecules and fine particles release from the surface. They come out with ultrasonic speed and push the surrounding gas like a piston. By this compression, the kinetic energy of propelling atoms is converted into the thermal energy in the plasma, by which atoms are excited. For convenient,

we call the shock wave plasma as “target plasma” in order to distinguish with “gas plasma” which we will describe in the next session.

2.4 Laser-Induced Gas Plasma

Laser-induced gas plasma is a branch of laser-induced plasma at atmospheric pressure condition. In general, mostly Nd:YAG laser was used in laser-induced plasma spectroscopy and laser was focused on the sample surface to make target plasma. When fundamental Nd:YAG laser was focused in the gas, we also have bright emission of plasma which we called as “gas plasma”. When the Nd:YAG laser is focused into the gas, ions and electrons are produced via multiple-photon ionizations process leading to the strong gas breakdown plasma of filament shape. These ions and electrons recombine soon afterward. Meanwhile, the extremely high temperature is produced at the plasma centre by the tightly focused laser light, which gives rise to a strong explosion, generating a shock wave of cylindrical shape.

In case of TEA CO_2 laser, when the laser was focused on metal sample at atmospheric pressure, different plasma phenomenon takes place due to the unique characteristics of TEA CO_2 laser, which is low frequency (long wavelength of 10.64 μm) and long pulse duration (200 ns) [35]. Figure 2.2 shows the illustration on the mechanism of generation of gas plasma, which is produced by focusing TEA CO_2 laser on metal sample at atmospheric pressure. At initial, electrons are released from the surface of metal owing to a multi-photon absorption process that occurs at the focusing point of the laser light. These electrons are then accelerated to high energy in the low-frequency electric field of the laser light, which induces the cascade ionization of the atoms in the gas and generates initial gas plasma. Once this initial gas plasma has been produced, the laser light is completely absorbed in the gas plasma by inverse Bremsstrahlung via free-free transitions. This absorption is much stronger for the TEA CO_2 laser than that for the Nd:YAG laser because the plasma absorption coefficient is proportional to the inverse square of the frequency of the laser light [36]. Furthermore, the pulse duration of the TEA CO_2 laser is relatively long (200 ns), about 20 times longer than that of the Nd:YAG laser, which means that almost all the energy from the TEA CO_2 laser light is absorbed by the gas plasma, thus the metal itself is neither damaged or ablated during this laser irradiation; these processes is quite different from the case of Nd:YAG laser irradiation.

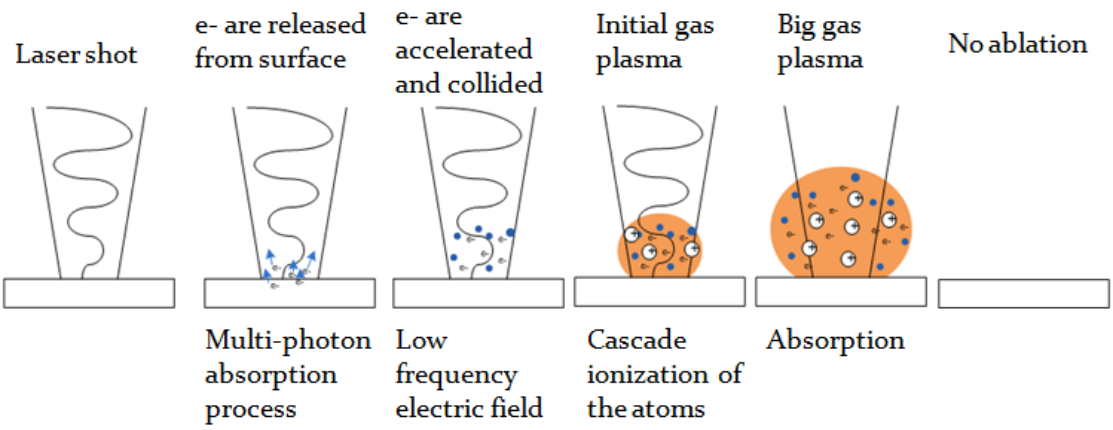

Fig.2.2. The mechanism for plasma generation using a TEA CO2 laser on a metal surface

2.5 Reviews on Hydrogen Analysis

Hydrogen analysis is urgently needed in many fields of investigation covering the field of material sciences as well as in industry. For instance, in light water nuclear power stations, hydrogen analysis in zircaloy tubes is an important issue [15]. During the operation of such power stations, hot water reacts with the zircaloy surface to produce H_2 gas and the gas penetrates and accumulates in the zircaloy tubes (in the form of Zr-H), which causes unacceptable structural damage and seriously reduces the strength of the material. Therefore, the accumulation of hydrogen in the zircaloy tubes must be examined periodically. A commercial method commonly uses a gas detector by melting a portion of a zircaloy tube in a carbon furnace. However, this technique is time-consuming and destructive, and cannot be used *in situ*.

At beginning, our research interest was initiated by observation of hydrogen emission using laser-induced shock wave plasma spectroscopy for the elemental analysis on meteorite samples, which are collected from the Sangiran, Java Island, Indonesia [37]. It is an interesting to note that the detection of a strong H_α emission from the meteorite is an indication that it contains water.

As well known, laser-induced breakdown spectroscopy (LIBS) has become a popular analytical technique for the rapid quantitative analysis of elements in many kinds of samples, including metals. The appealing advantages of LIBS are no sample preparation, the possibility of in-situ analysis under 1 atm, and the capability of micro-area analysis. However, this technique cannot be applied to analysis of hydrogen (H) due to the undesirable effects of line broadening and the "mismatching effect" [5], which will be described as follows;

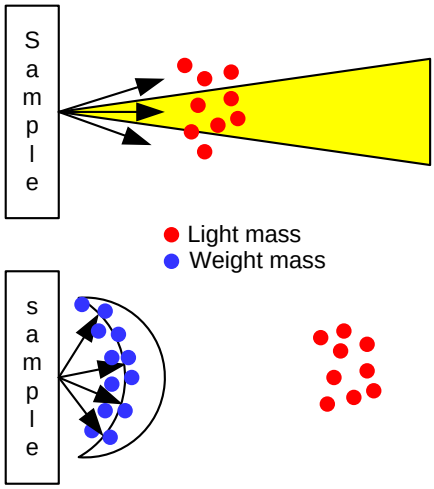

Fig. 2.3 Illustration of mismatching effect

Before we explain the “mismatching effect”, we must describe laser-induced shock-wave generation. Based on the shock wave model, from the primary plasma, atoms gush out with high speed to form a shock wave. Here, it should be recognized that there is a time lag between the laser bombardment and the starting time of the shock wave and that the shock wave is induced by propelling atoms of the host elements which are much heavier than hydrogen. It is assumed that the time lag increases with increasing the pressure. Therefore, at high pressures, hydrogen atoms would gush out earlier with very high speed than other elements because its mass is extremely light than others, and when the shockwave starts the hydrogen already locates at the forward of the shock front as illustrated in Fig 2.3. We call this phenomenon as “mismatching effect”. Thus, only a little part of the early ablated hydrogen atoms can be excited by the shockwave coming later from the behind. Consequently, the hydrogen emission efficiency becomes extremely low at high pressure.

To overcome the undesirable effects of line broadening and the “mismatching effect”, hydrogen analysis in zircaloy sample was successfully made when low-pressure-plasma method was used [4, 38]. However, the weakness of this low-pressure-plasma technique is the inability to perform *in-situ* analysis. To solve this weakness, a new technique was proposed, in which metastable He atoms were produced in helium gas plasma as an excitation source [35, 39]. Namely, helium metastable-excited state is produced in helium gas breakdown plasma using Nd:YAG laser at atmospheric pressure, and the ablated hydrogen atoms from the sample can be excited in the region of the He gas breakdown plasma where the helium metastable-excited states are populated. However, the helium gas breakdown plasma area is rather small. Therefore, it is difficult to fully excite all of the ablated atoms. To

realize highly sensitive H emission, synchronized double pulse lasers, TEA CO_2 laser and Nd:YAG laser was applied. Namely, Q-switched Nd:YAG laser, which is synchronized with TEA CO_2 laser, is focused on the metal sample to be ablated, and the ablated atoms were sent into the region of He gas plasma, which had been produced by the TEA CO_2 laser irradiation. It was assumed that the ablated atoms from the metal sample enter the He gas plasma region and are excited by He metastable atoms, which are produced with very large quantities in the He gas plasma region, due to the facts that He gas plasma has a very long lifetime, and also the detected atomic emission lines are very narrow in spectral widths [40].

References

1. http://www.britannica.com/EBchecked/topic/558901/spectroscopy
2. J. A. C. Broekaert, Analytical atomic spectrometry with flames and plasmas, Wiley-VCH, New York, 2002.
3. J. D. Ingle Jr, S. R. Crouch, Spectrochemical analysis, Prentice-Hall, New York, 1988.
4. D.A Cremers and L.J. Radziemski, Handbook of Laser-Induced Breakdown Spectroscopy John Wiley & Sons Ltd, England, 2006
5. A.W Miziolek, V. Palesschi, and T. Schechter, Eds. Laser-Induced Breakdown Spectroscopy Spectroscopy (LIBS), Fundamental and Application, Cambridge University Press, New York, 2006
6. F. Brech and L. Cross, Optical Microemission Stimulated By a Ruby Laser, Appl. Spectroscopy, **16,** (1962), 59
7. K. Laqua, Analytical Laser Spectroscopy Omenetto N. Ed. ,Wiley, New York, 1979
8. H. Moenke and L. Moenke-Blankerburg, Micro-Spectrochemical Analysis, Adam Hilger, London, 1973
9. U. Mode, Ph.D. Thesis, Munster (1970)
10. F. Leis, Ph.D. Thesis, Dusseldorf (1976)
11. T.R.Loree and L.J. Radziemski, Laser- Induced Breakdown Spectroscopy: Time Integrated Applications, Plasma Chem. Plasma Process, **1**, (1981) p.271-280
12. D.A. Cremers and L.K. Radziemski, Detection of Chlorine and Fluorine in Air by Laser- Induced Breakdown Spectroscopy, Anal. Chem. **55**, (1983) p.1252-1256
13. K. Kagawa, and S. Yokoi, Application of the N_2 Laser Microprobe Spectrochemical Analysis, Spectrochim. Acta Part B: Atom. Spectrom. **37**, (1982) p.789-795
14. K. Kagawa, S. Yokoi, and S. Nakajima, Metal Plasma Induced by the Bombardment of 308 nm Excimer and 585 nm Dye Laser Pulse at Low Pressure, Opt. Com. **45**, (1983) p. 261-265.
15. K. Kagawa and H. Kurniawan, Laser- Induced Shock Wave Plasma Spectroscopy, Appl. Spectrosc. **2**, (1998) pp.1-36
16. K. Kagawa, H. Hattori, M. Ishikane, M. Ueda, and H. Kurniawan, Atomic Emission Spectrometric Analysis of Steel and Glass Using a TEA CO_2 Laser-Induced Shock Wave Plasma, Anal. Chim. Acta **299**, (1995) p.393

17. K. Kagawa, K. Kawai, M. Tani, and T. Kobayashi, XeCl Excimer laser-induced shock wave plasma and its application to emission spectrochemical analysis, Appl. Spectrosc. **48**, (1994) p. 198
18. W. Setia Budi, H. Suyanto, H. Kurniawan, M. O. Tjia, and K. Kagawa, Shock Excitation and Cooling Stage in the Laser Plasma Induced by a Q-switched Nd:YAG Laser at Low Pressures, Appl. Spectrosc. **53**, (1999) p.719.
19. H. Kurniawan, M. O. Tjia, M. Barmawi, S. Yokoi, Y. Kimura, and K. Kagawa, A Time-Resolved Spectroscopic Study on the Shock Wave Plasma Induced by the Bombardment of a TEA CO_2 Laser, J. Phys. D, **28**, (1995) p.879
20. S.A. Ramsden, and P. A Savic, Radiative Detonation Model for the Development of Lase Induced Spark in Air, Nature, **203**, (1964) p.1217.
21. J.W. Daiber, and H.M. Thompson, Laser-Driven Detonation Waves in Gases, The Physics of Fluids, **10**, (1967) p.1162
22. N.G. Basov, O.N. Krokhin, and G.V. Skilzkov, Formation of Shock Wave with the Aid of Powerful Laser Radiation, JEPT. Lett, **6**, (1967) p.168-170.
23. N.G. Basov, V.A.Gibkov, O.N.Krokhin, and V.Sklizkov, High temperature Effects of Intense Laser Emission Focused on a Solid Target, Sov. Phys. JEPT, **27**, (1967) p.575.
24. Sedov, L. I, Similarity and Dimensional Methods in Mechanics Academic Press, New York, 1959.
25. K. Kagawa, T. Manda, H. Kurniawan, T. Kobayashi, S. Yokoi, S. Nakajima, Proceedings of the 18th International symposium on Shock Waves, Springer-Verlag, Tokyo, 1991.
26. K. Kagawa, M. Ohtani, S. Yokoi, S. Nakajima, Characteristics of the plasma induced by the bombardment of N_2 laser pulse at low pressures, Spectrochim. Acta Part B: Atom. Spectrom. **39** (1984) 525-536.
27. Kurniawan, H., Kobayashi, T., and Kagawa, K. The effect of different atmospheres on the excitation process of TEA CO2 laser induced shock wave plasma. Appl. Spectros, **46** (1992) 581-586
28. Kagawa. K, Kawai. K, Tani. M. and Kobayashi. T, XeCl eximer laser-induced shock wave plasma and is application to emission spectrichemical analysis. Appl. Spectros., **48** (1994) 198-205.
29. Bouman, P.W.J.M. excitation phenomena and temperature measurement. In Theory of spectrochemical excitation, plenum presss: newyork, **135** (1966) 19.
30. Bockasten, K. Transformation of observed radiance into radial distribution of the mission of the emission of a plasma J. Optic. Soc. Am., **51** (1961) 943-946
31. K.Kagawa, M.Tani, H.Ueda,M. Sasaki, and K.Mizukami, TEA CO_2 laser induced plasma with a plane shock wave structure, Appl. Spectroscopy, 47 (1993) 1562-1566
32. M. Mangasi, M. Pardede, R. Hedwig, H. Kurniawan, T. J. Lie and K. Kagawa, Coincidence of Density Jump and Plasma Emission Front Induced by Transversely Excited Atmospheric-Pressure CO2 Laser Bombardment at low and High Pressure, Jpn. J. Appl. Phys., **39**, (2000) L601-L603
33. Kurniawan, K.H., Lie, T.J., Idris, N., Tjia, M.O., and Kagawa, K. (2001) Detection of the density jump in the laser induced shock wave plasma using low energy Nd-YAG laser at low pressure of air, J. Spectros. Soc. Jpn., **50** (2001) 13-18
34. Kurniawan, K.H., Lahna, K., Lie, T.J., Kagawa, K., and Tjia, M. O., Detection of density jump in laser-induced shock wave plasma using rainbow refractometer. Apply. Spectros., **55** (2001) 92-97.

35. M. Ramli, N. idris, K. Fukumoto, H.Niki, F. Sakan, T. Maruyama, K. H. Kurniawan, T. J. Lie, K. Kagawa, Hydrogen Analysis in Solid Samples by Utilizing Helium Metastable Atoms Induced by TEA CO2 Laser Plasma in Helium Gas at 1 Atmosphere, Spectrochim, Acta Part B: At. Spectrom. **62**, (2007) 1379-1389.
36. Gibson, A.F., Hughes, T.P., and Ireland, C.L.M. CO_2 laser generation of plasma for spectroscopy and spectrochemical analysis, J Phys D, 4 (1971) 1527-1534
37. T.J. Lie, H. Kurniawan, M. Pardede, H. Suyanto, R. Hedwig, M.O. Tjia, K. Kagawa and T. Maruyama, Hydrogen Emission Spectrochemical Analysis Using Laser Induced Shock Wave Plasma, Phys. J. IPS **A5** (2003) pp. 0220-1 - 0220-4.
38. F. Boué-Bigne, Laser-induced breakdown spectroscopy applications in the steel industry: Rapid analysis of segregation and decarburization, Spectrochim. Acta, Part B **63** (2008) 1122.
39. M. Pardede, K. H. Kurniawan, T. J. Lie, R. Hedwig, N. Idris, T. Kobayashi, T. Maruyama, Y. I. Lie, K. Kagawa, and M. O. Tjia, Hydrogen Analysis in Solid Samples Using Laser-Induced Helium Plasma at Atmospheric Pressure, J. Appl. Phys. **98** , (2005) 043105
40. M. Ramli, N. Idris, H. Niki, K. H. Kurniawan, and K. Kagawa, New Method of Laser Plasma Spectroscopy for Metal Samples Using Metastable He Atoms Induced by Transversely Excited Atmospheric Pressure CO_2 Laser in He Gas at 1 atm, Jpn. J. Appl. Phys., **47**, (2008) 1595 -1601

Chapter 3

Hydrogen Analysis using Nd:YAG Laser-Induced Low Pressure Plasma

3.1 Quantitative Deuterium Analysis of Titanium Samples using Ultraviolet Laser-Induced Low-Pressure Plasma

3.1.1 Introduction

In a recent study [1], the widely adopted practical technique of laser-induced breakdown spectroscopy (LIBS) [2–9] was shown to be applicable to address the urgent need for regular, rapid, and in situ quantitative analysis of detrimental hydrogen impurities penetrated into the zircaloy wall of the fuel vessels of a light-water nuclear power plant. In contrast to the unacceptably broad and weak H emission commonly observed in conventional LIBS operated with ambient air [10,11], the study reported the observation of a remarkable sharp hydrogen emission line when the atmospheric-pressure ambient air used in standard LIBS was replaced by a low-pressure helium gas. Subsequently, the interfering H emission from the ubiquitous surface water and surrounding gas was largely reduced by proper defocusing of the laser irradiation as well as the proper control of ambient air pressure and chamber temperature, which resulted in a linear intensity calibration line [12,13]. In a more recent study [14], doped deuterium impurities in a zircaloy-4 sample were used as a surrogate for H impurities for the investigation of different and distinct characteristics exhibited by the emission of H impurities and that of the dissociated surface water, and the

experimental conditions most favorable for the detection of H impurity emission while suppressing the interfering H emission were thereby determined. The result of using that optimal experimental condition yielded a further suppression of the interfering H emission by a factor of 10, although this was achieved at a cost of reduced linear dynamical range.

Titanium (Ti) and its alloys are also known to suffer from similar problems with the presence of H impurities in the material, and they must therefore be routinely examined to avoid intolerable dysfunction of the material. The metal and its alloys are known to have wide-ranging and sometimes irreplaceable applications as medical materials in the form of pure Ti, as well as industrial materials in the form of its alloys. It is therefore natural to investigate the applicability or the needed modification of the previously developed technique reported in Ref. 14 for hydrogen analysis of Ti samples, in particular the non-alloyed Ti materials used for medical purposes, where the generally low tolerances to H impurity-induced detrimental effects must be strictly observed. Our preliminary experiment has indicated that such an extension requires a study beyond a straightforward adjustment or adaptation of the optimal experimental parameters obtained previously for zircaloy samples [1, 12–14]. In fact, no plasma was observed when the Ti sample was irradiated using the Nd:YAG laser at its fundamental wavelength at various energies up to 30 mJ, while only spattering takes place. This is much like the case of W found in our previous study.

Further increase of the fundamental laser energy is likely to produce unacceptable damage on the small Ti samples, which have a thickness in the range of less than 0.2 mm. Therefore, laser irradiation at a different wavelength must be explored for the desired plasma generation, in conjunction with the need to minimize the produced crater size for nondestructive analysis of small Ti samples. For the different operational laser wavelength, a thorough re-examination of the previous results [14] becomes necessary before its technical implementation for quantitative hydrogen analysis of Ti samples.

This study is firstly aimed at examining the validity of the basic principal adopted in the previous method in which deuterium dopant was introduced in the sample as a surrogate for the H impurity in the study of different effects induced by various experimental parameters on the impurity emission and the interfering H emission. The different effects were employed to explore and determine the most favorable experimental condition for the elimination of the interfering H emission with consistent enhancement of D emission, which may also result in a linear calibration line with a zero intercept.

3.1.2 Experimental Procedures

The experimental setup used in this study is basically the same as the one employed in a previous work [12–14], which is reproduced in Fig. 3.1 for easy reference. The laser system (Nd:YAG, Quanta Ray INDI SERIES, 5 ns, maximum energy of 125 mJ) was employed and operated in the Q-switched mode at 10 Hz repetition rate with the laser output energy fixed at 5 mJ unless otherwise stated. It was found that the laser operating at the third harmonic wavelength of 355 nm succeeded in generating the desired plasma and could be expected to meet one of the important aims of limiting the crater size created by repeated laser pulses as reported previously using a nitrogen laser[16]. The reduction of the crater size, as mentioned earlier, is required for the application of the technique to nondestructive micro-analysis. The He:Ne laser diode is a position marker used to direct the invisible Nd:YAG laser to the spot on the sample surface illuminated by the diode.

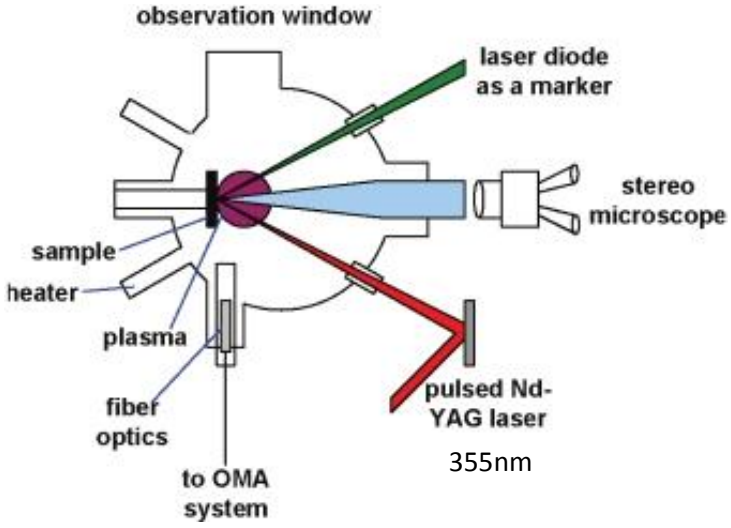

Fig.3.1. Description of experimental setup

The Nd:YAG laser beam was tightly focused by a moveable lens with a focal length of 150 mm and directed at a 45º incident angle onto the sample surface through a quartz window as shown in Fig. 3.1. The power density on the sample surface was estimated to be around 2 GW/cm^2. The shot-to-shot fluctuation of the laser was found to be approximately 3%. The targets employed in this experiment consist of a number of titanium plates separately doped with deuterium at concentrations of 124, 226, 727, and 3000 μg/g. All the samples measure 15 mm x 15 mm in cross-section and 0.4 mm in thickness. After evacuating the sample-containing chamber to a pressure of 0.001 Torr, the helium gas (6N) was introduced into the chamber until a pressure of 10 Torr was reached, which was then

maintained at a constant flow rate of 2 L/min. It should be stressed that in case of low pressure plasma regardless of gas kind, H analysis is possible. Helium surrounding gas was chosen because of the low background.

The plasma emission was detected by an optical multichannel analyzer (OMA system, Andor I*Star intensified charge-coupled device (CCD) 1024 x 256 pixels) attached on one end to a spectrograph (McPherson model 2061 with 1000 mm focal length with Czerny–Turner configuration) and connected to an optical fiber on the other end. The entrance end of the fiber was inserted through a cylindrical quartz tube well into the chamber and fixed at a position 6 mm in front of the sample surface and at a distance of 80 mm side-wise from the plasma center. At this position, the fiber was expected to collect the emitted radiation entering within 27º degrees of solid angle. The spectral window covered by the detector has a width of 20 nm at 500 nm wavelength. The accumulated data of 50 detected spectra from each irradiated spot were monitored on a screen and were recorded to yield the averaged results presented here. Throughout the experiment, the gate delay and gate width of the OMA system were set at 1 μs and 50 μs, respectively. The spectral resolution of this detection system is 0.009 nm at 500 nm. The sample surface condition was constantly monitored during the repeated laser irradiation and data acquisition process using a stereo microscope (Mini Dia Stereo MDS-40, Nissho Optical Co. Ltd.) through a 50 mm quartz window installed parallel to the sample surface. The working distance between the objective lens and the sample surface was kept at 135 mm.

3.1.3 Experimental Results and Discussion

Presented in Fig. 3.2 is the plasma produced by the Nd:YAG laser (355nm) at 5 mJ output energy on the titanium sample containing 3000 μg/g of deuterium in 10 Torr helium surrounding gas. A clear and typically hemispherical shock wave plasma is clearly seen that closely resembles the plasma produced previously by the nitrogen laser [15]. Figure 3.3a shows the emission spectrum from the plasma, which features strong and completely resolved H and D emission lines together with the Ti and He emission lines. The achievement of complete resolution between the D and H emission lines was explained as a result of delayed excitation of H by the metastable helium excited state, which allowed the elimination of the Stark broadening effect [14]. The H emission observed in this spectrum is supposed to have its origin in the surface water and perhaps with some contribution from the H impurity contained in the surrounding gas. The emission spectrum from the same sample at much higher laser energy of 30 mJ is given in Fig. 3.3b, where perceptible intensity

enhancement is observed in all emission lines, including the undesirable background emission. It should be noted, however, that the intensity ratio of D emission against the Ti emission visibly decreases from about 1.3 at laser energy of 5 mJ to about 0.5 at 30 mJ.

Fig. 3.2. Plasma photograph produced by third harmonic (355nm) Nd:YAG laser irradiation of 5 mJ on titanium sample containing 3000 µg/g deuterium impurity with 10 Torr surrounding helium pressure.

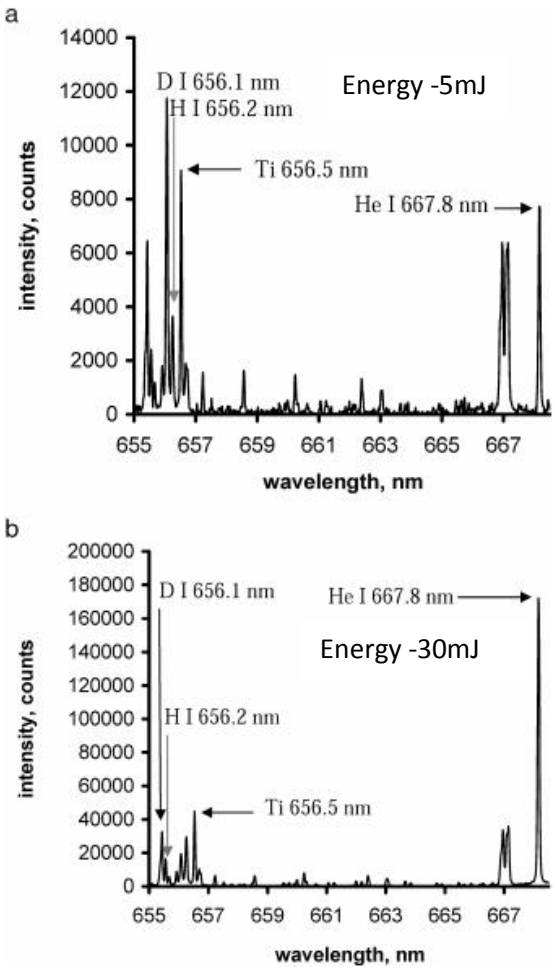

Fig. 3.3. Emission spectra obtained from titanium sample containing 3000 µg/g deuterium with laser energy of (a) 5 mJ and (b) 30 mJ at 10 Torr surrounding helium pressure. The gate delay and gate width of the OMA system were set at 1 µs and 50 µs, respectively

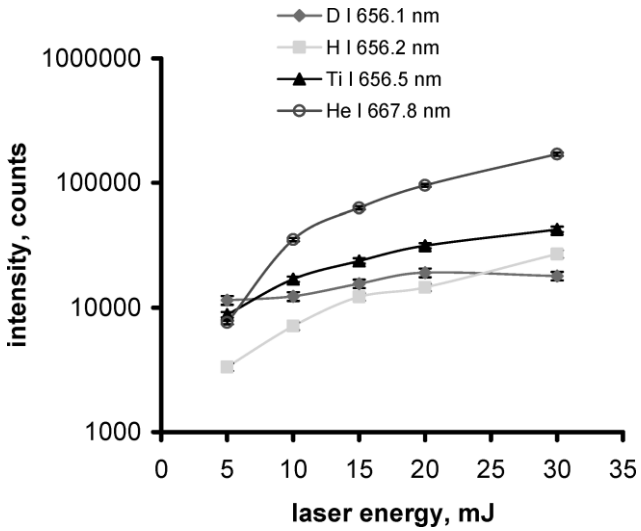

Fig. 3.4. Logarithmic plots of the variations of D I 656.1 nm, H I 656.2 nm, Ti I 656.5 nm, and He I 667.8 nm emission intensities with respect to increasing laser energy obtained from the sample as in Fig. 2 at a fixed surrounding helium pressure of 10 Torr, with 1 μs gate delay and 50 μs gate width of the OMA system.

The measurement of detailed energy-dependent intensity variations was also carried out and the result is presented in Fig. 3.4. It is clearly seen that the He emission experiences by far the largest intensity enhancement in connection with the considerably stronger laser irradiation. This is in clear contrast to the result obtained from the zircaloy-4 sample irradiated with the 1064 nm Nd:YAG laser, in which case the He emission intensity was only moderately enhanced[12,13]. This different energy-dependent effect is related to the lower mass and melting point of Ti, which leads to more effective ablation of the Ti atoms, resulting in more rapid formation of the ionic plasma in front of the sample surface. This ionic shield serves as an efficient energy absorber to the later part of the laser pulse and the fast accumulated laser energy in turn generates the more intense gas breakdown responsible for the stronger He emission. Meanwhile, the increased laser energy is rendered relatively ineffective for the later ablation process as a large part of this energy is already absorbed by the Ti ion shield before reaching the target. These different effects on the He gas and the target atoms readily explain the pronounced difference in the energy-dependent behaviors of the emission intensities shown in Fig. 3.4. It is reasonable to expect that similar relative behaviors will hold when the D impurity is replaced by H impurity. Apart from that, it is important to recall that the D/Ti intensity ratio appears to decline monotonically from about 1.3 to about 0.5 with increasing laser energy in the range considered, and this takes place in conjunction with increasing background emission. We note further that the crater created at 5 mJ laser energy has already reached a diameter of roughly 25 μm. In short, increasing the laser energy appears to induce unnecessary and even unfavorable effects instead of offering

any benefit for the intended micro-analysis of H and D. We have thus chosen to work with 5 mJ laser energy for the ensuing studies on the roles of other experimental parameters.

The result of emission intensity measurements carried out at various surrounding He pressures is presented in Fig. 3.5. It is seen that all emission lines show the general trend of initial rise with increasing helium pressure up to their individual maximum values before reversing the trend beyond that, which is consistent with previous observations carried out on the zircaloy sample.[13] It is obvious from this figure that there is a remarkably large intensity difference between the D and H emission lines due to the large difference between the D and H concentrations. Interestingly, this difference is seen to vary with the gas pressure, reaching its maximum at 10 Torr in favor of the D emission. Therefore, this helium gas pressure was also adopted along with the 5 mJ laser energy for the subsequent experiment. It is worth noting in this connection that the remarkably different pressure-dependent behaviors between the two emission lines may have arisen from the fact that D impurity atoms were bonded inside the target sample while the H atoms were dissociated from water molecules loosely deposited on the sample surface. The same effect is expected to occur when the D impurity are replaced by H impurity.

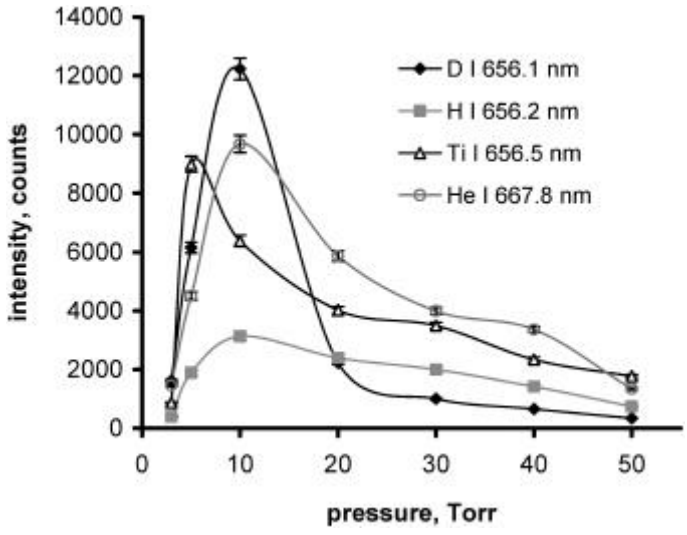

Fig. 3.5. Variations of D I 656.1 nm, H I 656.2 nm, Ti I 656.5 nm, and He I 667.8 nm emission intensities with respect to increasing surrounding helium gas pressure, at fixed laser energy of 5 mJ and 1 μs gate delay and 50 μs gate with of the OMA system

The detailed variations of the emission intensities with respect to the gate delay time measured with 5 mJ laser energy and 10 Torr gas pressure are plotted in Fig. 3.6. It is seen that remarkable rises of all emission lines generally take place about 1 μs after the laser pulse. This is followed by relatively slow decays after reaching their maxima except for the D and H

emission intensities. The general time-dependent behaviors shown in this figure are typical to shockwave-induced emission in low-pressure plasma as reported previously[16]. The sharper initial decays common to D and H emission were also well studied as a consequence of time-mismatch between the extra-fast passage of the very light atoms and the shockwave plasma formation by the much heavier host atoms from the target. This common fast decline of D and H emission intensities is, however, followed by a more extended, relatively slow decaying process indicating the role of the He metastable excited state in sustaining the H and D emission as suggested in a previous work [17]. This observation was the basis of our choice of the large detection window extending from 1 μs to 50 μs for the measurement of the integrated intensities presented in this work.

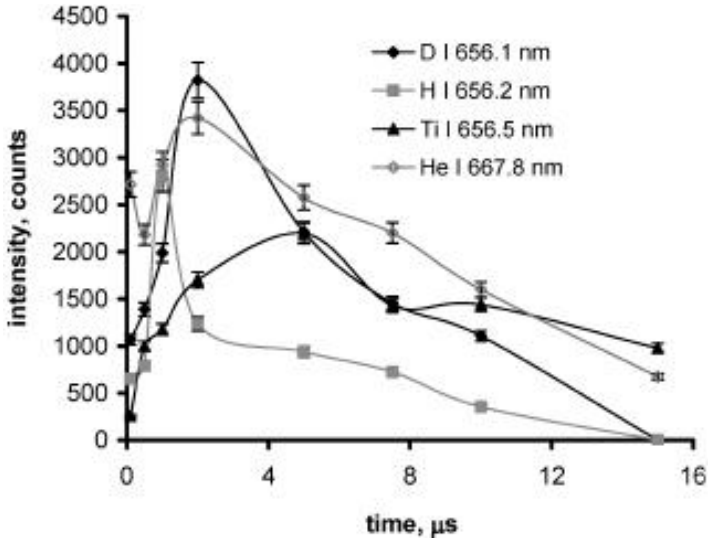

Fig. 3.6. Variations of D I 656.1 nm, H I 656.2 nm, Ti I 656.5 nm, and He I 667.8 nm emission intensities with respect to increasing gate delay of the OMA system at fixed surrounding helium pressure of 10 Torr, fixed laser energy of 5 mJ, and fixed gate width of 50 μs.

Employing the favorable condition ascertained from the experimental results described above, a series of measurements were carried out on a number of titanium samples prepared with different concentrations of doped deuterium. Each data point in the presented experimental result is the average of 50 data produced by 50 successive laser shots on the same sample spot. This measurement was then repeated on five different spots of the same sample surface. The results of these measurements were found to be highly reproducible, implying the uniformity of the impurity D distribution in the sample. The averages of those five measurement results for samples with different impurity concentrations (124, 226, 727, and 3000 μg/g) were then plotted in Fig.3.7(a). It is seen that the relation between the D impurity concentration and its associated emission intensity is clearly short of the linear

character needed for quantitative analysis. Further, a non-zero intercept is also visibly indicated by its extrapolation. However, a separate measurement run on a deuterium-free titanium sample shows the presence of an emission line located exactly at the deuterium emission wavelength as displayed in Fig.3.7(b), although this particular emission is so far unidentified in this study. When this emission component was subtracted from the as-measured emission data, the best fitted result appears as a linear calibration line with near-zero intercept as shown in Fig. 3.7(c), and indicated by the background equivalent concentration of 10 μg/g.

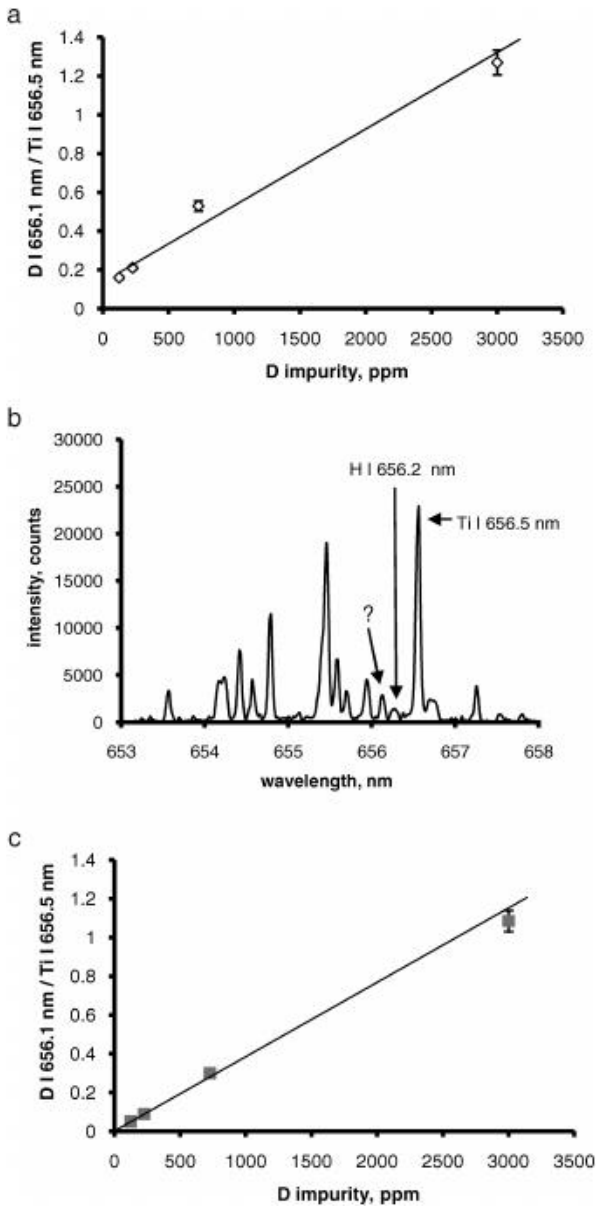

Fig. 3.7. Calibration relations obtained from titanium samples doped with various concentrations of deuterium impurity (124, 226, 727, and 3000 μg/g) (a) before and (c) after correction (see text for details) with error bars indicating ;4.7% deviations. Meanwhile, (b) shows the emission spectrum of the deuterium-free titanium sample.

For an estimation of the detection limit, the emission spectrum of a titanium sample containing 727 μg/g D was measured and the result is presented in Fig. 3.8. Following the conventional criterion for determining the detection limit as a ratio of the signal against three times the noise level, the detection limit of D was estimated to be around 40μg/g, which is well below the tolerated threshold of damaging hydrogen concentration of several hundred μg/g in Ti.

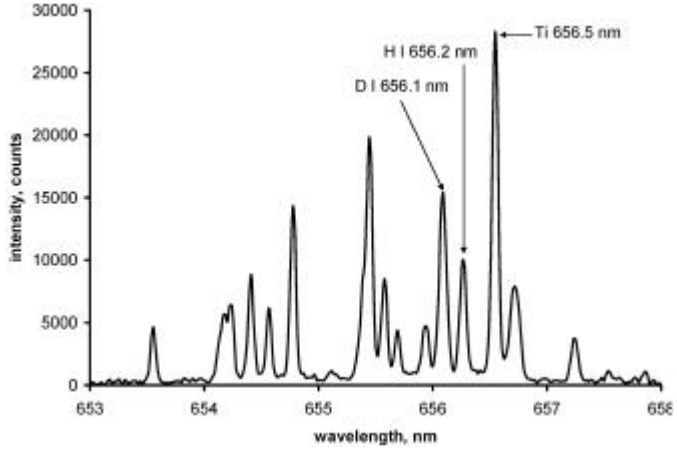

Fig 3.8. Emission spectrum of titanium sample containing 727 μg/g deuterium measured with laser energy of 5 mJ, at 10 Torr surrounding helium pressure, and a detection window (determined by the gate delay and gate width of the OMA system) from 1 μs to 50 μs.

3.1.4 Conclusion

We have demonstrated the possibility of using deuterium atoms doped inside the Ti samples as surrogate hydrogen impurities for the study and determination of the most favorable experimental parameters in UV laser-induced plasma spectroscopy with low-pressure surrounding helium gas. It is found that employing the favorable parameters of 5 mJ laser energy, 10 Torr helium gas pressure, and 1 to 50 μs detection window ascertained from the experiment, an effective enhancement of the D impurity signal and effective elimination of the interfering hydrogen emission from the surface water were achieved with high reproducibility and a linear calibration line with zero intercept was obtained under these experimental conditions. A further measurement also gave a roughly 40 μg/g detection limit for D impurity in Ti. These useful results for quantitative deuterium analysis, while not directly applicable to hydrogen impurity analysis, should provide the basis for a further experiment aiming at the further adjustment of those experimental parameters and its ultimate technical implementation for quantitative micro-analysis of hydrogen impurity in titanium and its alloys.

3.2 Deuterium Analysis in Zircaloy using ps Laser-Induced Low Pressure Plasma

3.2.1 Introduction

Laser-induced breakdown spectroscopy (LIBS) widely employed for practical and rapid spectrochemical analysis has found its way into an ever expanding areas of applications in industries and research laboratories [18–29]. Recognizing its great potential for future applications, a number of experimental studies had been performed early in the 1990s exploring the possibility of enhancing its performance in some particular cases by replacing the commonly used ambient air with helium gas [30-32]. Subsequently, research interest along this line was revived and intensified in response to the need of hydrogen analysis in some important materials, such as zircaloy used for fuel vessels in light water nuclear power plants, the widely used titanium alloys in industry, and the non-alloyed Ti used for medical purposes[12,33]. The excessive penetration of hydrogen into these materials is known to deteriorate the mechanical strength and other useful properties of the materials, thereby jeopardizing their functional reliability. Unfortunately, the usual LIBS method does not deliver its standard excellent performance to the sensitive detection of hydrogen[1]. It is noteworthy, however, that significant improvements have actually been made in recent studies using helium ambient gas, on the reduction of H emission line broadening, the suppression of intensity diminution, and reduction of spectral interfering effect of H from surrounding water molecules[13,34], which are promising for the further development of reliable and sensitive spectrochemical analysis of hydrogen.

Those advances notwithstanding, the practical application of the modified or extended LIBS method to regular H analysis, especially for the regular *in-situ* inspection of zircaloy vessels, is still in need of additional studies addressed to several important practical issues and to demonstrate its relative advantages over the currently adopted destructive method of gas chromatography which requires the sample to be melted prior to its analysis. Among those issues are first, the need of attaining sufficient range of linear calibration for quantitative analysis and, second, the need of depth profiling of the penetrated H distribution inside the sample in order to yield the much desired three-dimensional information of the H impurity distribution in the sample. We recall in this connection that in spite of the achievement in significantly reducing the water interfering effect reported in Ref. 14, the linear calibration line attained was only limited to the small range of 200 μg/g concentration of H impurity. This is known to be well below the threshold value of 800 μg/g for critical

damage evaluation. The need for depth profiling is related to the fact that the detrimental effect of H impurity increases with its penetration depth. So far, experiments on depth profile measurement of H impurity have not been performed in our previous works, and published reports on such experiments by different groups are also rarely found in the literature. It is therefore the purpose of this study to address those two issues and to find their appropriate solutions.

For that purpose, the previously employed nano-second Nd:YAG laser has been replaced by its pico-second model, for reasons to be given later. The experiment is also conducted on deuterium-doped samples where the D dopant serves as the surrogate for H impurity as adopted in a previously study to avoid the water interfering effect[14, 35]. It is shown that we have succeeded in this experiment to obtain the more adequate calibration line applicable to quantitative hydrogen analysis as well as the result demonstrating the feasibility of the development of three-dimensional distribution of the D impurity in zircaloy sample.

3.2.2 Experimental Procedures

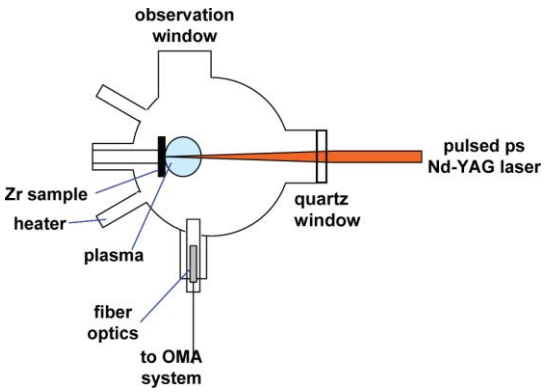

Fig. 3.9. Experimental setup used in this study.

A description of the basic experimental setup used in this study is shown in Fig. 3.9. The chamber used is the same special cylindrical chamber of 115 mm inner diameter employed in our previous experiments [12-14, 33-35]. It was designed with several entry ports to allow the control and monitoring of the specific conditions inside the chamber as needed by the experiment. The major modification of the previous experimental setup is the replacement of the nano-second (ns) laser by a pico-second (ps) laser (Nd:YAG, EKSPLA, model PL 2143, 1064 nm, 20 ps, maximum energy of 30 mJ) which was also operated in the Q-sw mode at 10 Hz repetition rate with the laser output energy fixed at the much lower level of 7 mJ. The reason for the change is based on the suspected unfavorable influences of the relatively long heating by the ns laser pulse with relatively large ablation energy, which may

give rise to some unwanted thermally induced complications in the sample, such as local volume expansion and impurity migration or segregation due to accumulated local heating during the successive ablation process on the same sample spot. These processes will in turn induce changes of local impurity distribution leading to distorted experimental data. The ps laser can, on the other hand, provide the higher power density with much smaller laser output energy in much shorter duration of irradiation. For the purpose of comparative study, however, the ns Nd:YAG laser (QUANTA RAY, model LAB SERIES, 1064 nm, 8 ns, maximum energy of 450 mJ) was also employed in this experiment and operated in the same mode with the laser output energy fixed at 50 mJ. The laser beam was focused by a moveable lens of 120 mm focal length and directed onto the sample surface perpendicularly through a quartz window.

The main targets employed in this experiment consist of a set of zircaloy-4 samples composed of 98.23 wt. % Zr, 1.45 wt. % tin, 0.21 wt. % iron, 0.1 wt. % chromium, and 0.01 wt. % hafnium. These samples were prepared by prolonged high temperature and low pressure doping technique. The resulting concentrations of deuterium impurity (60, 170, 540, 750, 900 and 1700 μg/g) were determined by gas chromatography. All the samples measure 10 mm x10 mm in cross sectional area and 1 mm in thickness. After placing the sample in the chamber, the chamber was evacuated using a vacuum pump to a pressure of 0.1 Pa. Subsequently, the chamber was heated up to 150 ºC for 30 min to remove most of the surface water molecules. The high purity helium gas (Air Liquid, 5 N) was thereafter introduced into the chamber until a pressure of 1.3 kPa was reached at a constant flow of 2 l/min. The chamber temperature chosen for the heating process in this experiment was lower compared to that used previously (200 ºC),[13,34] because the deuterium became completely out gassed when the temperature was raised to 200 ºC due to the weaker bonding energy of Zr-D as compared to Zr-H. The gas pressure of helium 1.3 kPa and the above-mentioned chamber temperature (150 ºC) were henceforth kept constant throughout the experiment.

The plasma emission was detected by an optical multichannel analyzer (OMA system, Andor I*Star intensified CCD 1024 x 256 pixels) attached on one side to a spectrograph (McPherson model 2061 with 1000 mm focal length f/8.6 Czerny Turner configuration) and connected to an optical fiber on the other side. The entrance end of the fiber was inserted through a cylindrical quartz tube well into the chamber and kept at a position 6 mm above the sample surface and at a distance of 80 mm from the center of the plasma. At this position, the fiber was expected to collect the emitted radiation entering within 27º degrees of the solid angle. The spectral window of the detector has a width of 16 nm at 500 nm wavelength. The

accumulated data of 10 detected spectra from each irradiated spot were monitored on a screen, and recorded to yield the averaged results presented here. During the experiment, the gate delay of the OMA system was set at 10 ns for the ps laser and 200 ns for the ns laser unless otherwise stated, while the same gate width of 50 μs was used in both cases. The spectral resolution of the OMA system is 0.012 nm at 500 nm. The sample surface condition was constantly monitored during the repeated laser irradiation and data acquisition process, using a stereo microscope (Mini Dia Stereo MDS-40, Nissho Optical Co. Ltd.) through a 50 mm quartz window installed parallel to the sample surface. The working distance between the objective lens and the sample surface was kept at 135 mm.

For the depth profiling of the penetrated impurity concentration, a preliminary experiment was carried out to determine the total number of laser shots it took to "drill" through the sample of a certain thickness. In the meantime, the crater created by the ablation process was seen to deepen with increasing number of shots, as observed by the stereo microscope. The shot number can thus be used as a reference measure of sample depth probed by each of the successive laser shots.

3.2.3 Experimental Results and Discussion

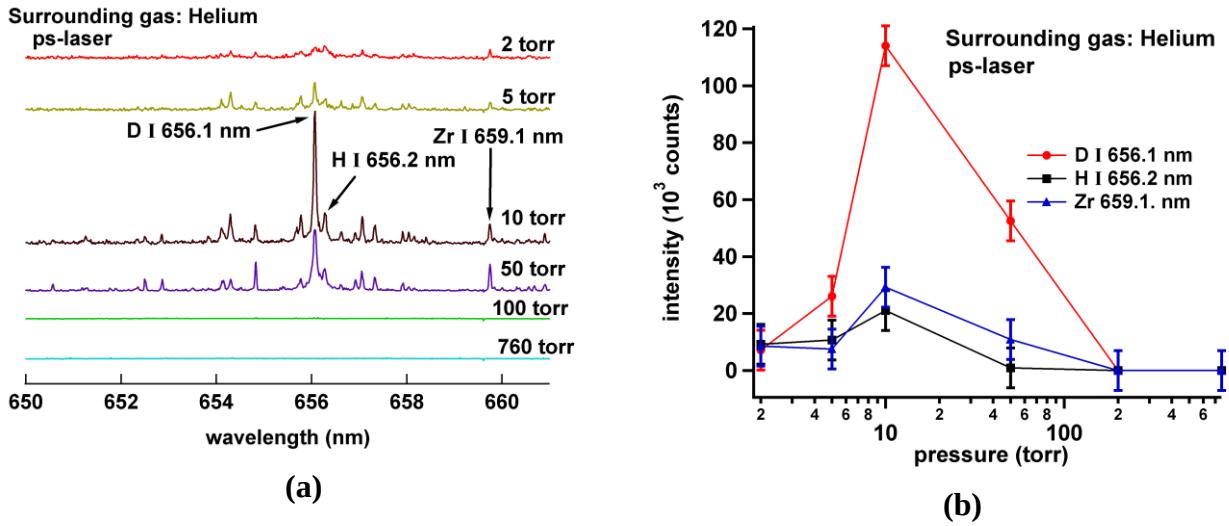

Fig. 3.10 Emission spectra taken from zircaloy-4 sample containing 1700 μg/g of D in different helium gas pressures (a) and (b) complete illustration of pressure dependence for emission lines of D I 656.1 nm, H I 656.2 nm, and Zr I 659.1 nm in helium gas. Picosecond laser of 7 mJ energy was used and the gate delay and width of the OMA system were set at 10 ns and 50 μs, respectively.

It is crucial for this experiment that the D emission line can be clearly distinguished from the H emission. We have learned from a previous study that very sharp and well resolved hydrogen and deuterium emission lines can be indeed readily detected using ns laser

pulses and helium surrounding gas[14]. That observation is verified in the present experiment, prior to the exploration of the possibly more favorable operational parameters with the use of the ps laser. Figure 3.10(a) shows the result obtained from zircaloy-4 sample containing 1700 μg/g of deuterium under different helium gas pressures with relatively small laser energy output of 7 mJ, as chosen previously to obtain a good result for microanalysis with ns laser[33]. It is clear from the figure that the same excellent spectral resolution is achieved in the present experimental condition. One further observes that the D I 656.1 nm emission intensity shows the most sensitive variation with respect to the gas pressure changes, while the H I 656.2 nm and Zr I 659.1 nm emission intensities are clearly less affected by the gas pressure changes. A more complete result exhibiting the present pressure-dependent variations of emission intensities is presented in Fig.3.10 (b). It is seen that all emission lines show the general trend of initial rise with increasing helium pressure up to their individual maximum values before reversing the trend beyond that. This general feature is clearly consistent with the previous observation[33]. The remarkably larger D emission intensity compared to the H emission intensity can be simply attributed to the large difference between the D and H concentrations. Interestingly though, this difference is seen to vary sensitively with the gas pressure as noted earlier, reaching its maximum at 1.3 kPa in favor of the D emission. This helium gas pressure was therefore adopted along with the 7 mJ laser energy for the subsequent experiment.

The relatively insensitive response of Zr emission is readily understood, as Zr atoms are mostly excited by laser generated shock wave induced thermal effect. On the other hand, no detailed explanation is available at the present for those pressure-dependent behaviors, although the difference can be qualitatively explained as follows. Certainly, the increase in helium gas pressure implies a corresponding increase in the helium concentration, and hence the available energy for the He assisted excitation (HAE) process. Assuming that it is this HAE mechanism that plays the major role for H and D emission, as reported previously[1,12-13,33-34]. the different quantities of H and D atoms available in the plasma for the excitation process should naturally account for the observed different intensity variations with respect to the gas pressure, because the D dopant concentration is known to far exceed that of the H atoms from the residual water molecules. It is important to note that this observation is not related to specific different structures or properties of the two atoms; it is therefore reasonable to expect that the same effect will occur when the D impurity is replaced by H impurity.

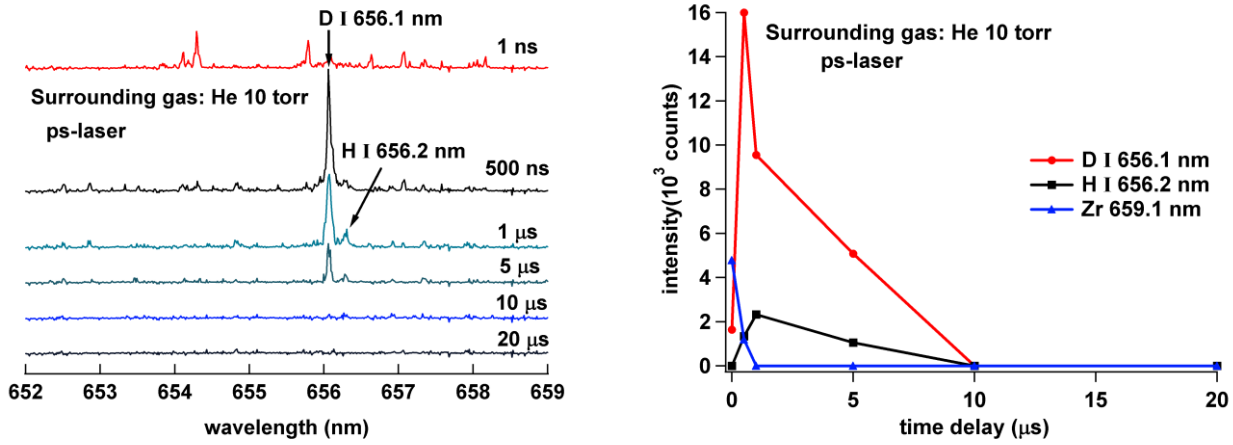

Fig. 3.11. Emission spectra (a) and time profile (b) taken from zircaloy-4 sample containing 1700 μg/g of D in 1.3 kPa helium gas pressure for emission lines of D I 656.1 nm, H I 656.2 nm, and Zr I 659.1 nm. Picosecond laser of 7 mJ energy was used with 200 ns gate width of the OMA system and different gate delays of 1 ns, 500 ns, 1 μs, 5 μs, 10 μs, and 20 μs.

In order to reexamine and verify the dynamics of the plasma emission observed previously using a ns laser, the spatially integrated, time-resolved emission spectra of the same zircaloy sample were measured employing the ps laser, with the same experimental settings except that the OMA delay time in this experiment was varied over a different range, from 1 ns to 20 μs. The detected spectra are presented in Fig. 3.11(a). The detailed variations of the emission intensities with respect to the gate delay time are given in Fig. 3.11(b). It is seen that all three emission lines display similar rapid rises of intensity within the first 1 μs after the laser pulse. After reaching its maximum, the Zr emission intensity variation is followed by an almost equally sharp decline. On the other hand, the D and H emission intensities show significantly slower decline. This phenomenon of sustained emission of H and D has been observed previously and explained as being indicative of the effective role of the helium metastable excited state in sustaining the excitation processes of H and D[12-14, 33-35]. This is in a way corroborated by the concomitant observation of the He I 667.8 nm emission, as shown in Fig. 3.12., which implies the sustained presence of the helium atoms in their metastable excited state.

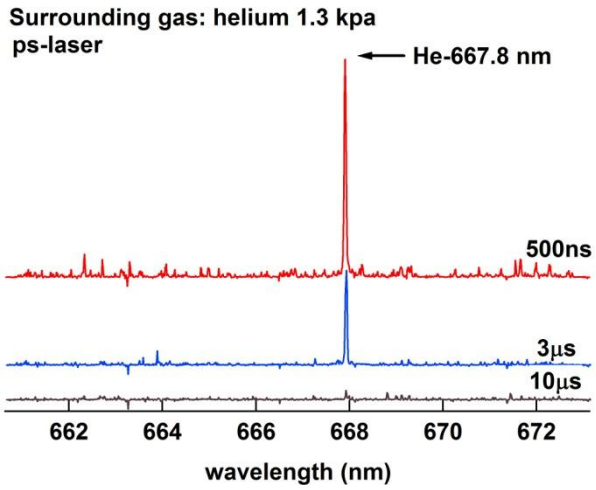

Fig. 3.12. Emission spectra of He I 667.8 nm taken from zircaloy-4 sample containing 1700 μg/g of D in 1.3 kPa helium gas pressure. Picosecond laser of 7 mJ energy was used. The gate width of the OMA system was set at 200 ns with different gate delays of 500 ns, 3 μs, and 10 μs.

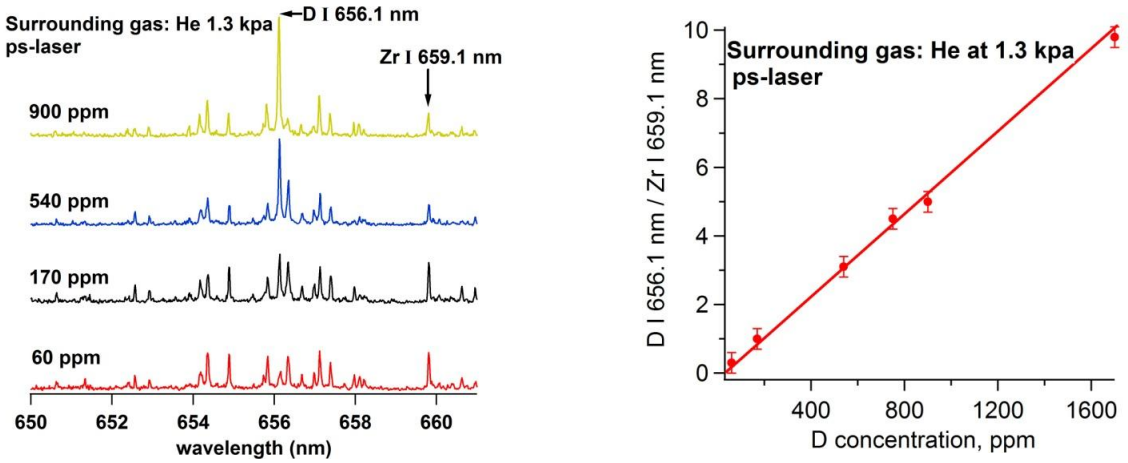

(a) (b)

Fig. 3.13. Emission spectra (a) and calibration curve (b) taken from zircaloy-4 sample containing different concentrations of D in 1.3 kPa helium gas pressure. Picosecond laser of 7 mJ energy was used and the gate delay and width of the OMA system were set at 10 ns and 50 μs, respectively.

Employing the favorable condition ascertained from the experimental results described above, a series of subsequent measurements were carried out on a number of zircaloy-4 samples prepared with different concentrations of doped deuterium. Shown in Fig. 3.13 (a) are the emission spectra measured from zircaloy-4 samples with deuterium concentrations of 60, 170, 540, and 900 μg/g. The associated calibration curve is presented in Fig.3.13(b). Each data point in Fig. 3.13 (b) is the average of 50 data, like one of those shown in Fig. 3.13 (a), produced by 50 successive laser shots on the same sample spot. This measurement was then repeated on five different spots of the same sample surface. The results of these measurements were found to be highly reproducible, implying the uniformity

of the impurity D distribution in the sample. It is seen that the D impurity concentration and its associated emission intensity exhibit a clearly linear relationship over a much broader range than that reported previously[14]. One further observes that a practically zero intercept is also obtained by the extrapolated calibration line. For the estimation of the limit of D detection, the emission spectrum of a zircaloy-4 sample containing 60 µg/g D was measured. The detection limit was estimated following the conventional criterion as a ratio of the signal against three times the noise level. The limit of detection (LOD) was found to be less than 10 µg/g. This value is well below the tolerated threshold of damaging hydrogen concentration of 800 µg/g in a zircaloy vessel used in a nuclear power plant. Taken together the results described above have thus demonstrated the potential application of this technique for useful regular quantitative H analysis of zircaloy vessel. For the study of possible application of the same setup for determining the intensity variation with increasing crater depth, a depth-profile measurement was carried out as explained in the experimental procedure using a sample doped with 900 µg/g D impurity. The emission intensities of H, D, and Zr were measured stepwise, with every step consisting of data detected from 50 successive shots, which were then averaged to produce the result plotted in Fig.3.14(a). As the repeated laser shots directed onto the same spot of the sample were expected to deepen the crater accordingly, the intensity variation with the shot number effectively represents the intensity depth-profile of the associated emission. Plotted in Fig. 3.14 are the variations of Zr emission intensity with increasing shot number, measured separately with the ns and the ps lasers (a), together with the corresponding variations of D emission given in terms of its intensity ratios with respect to the Zr emission intensity (b). It is seen that the Zr I 659.1 nm intensities are more or less flat over the entire process of 600 laser shots in both cases, in good agreement with the well-known homogeneity of the sample. On the other hand, the relative D distribution profiles exhibit a perceptible difference between data obtained in the two measurements. The data obtained with the ns laser show a generally monotonic rise with the shot number, in clear contrast to the roughly constant Zr emission intensity. Whereas the D intensity profile measured with the ps laser resembles rather closely the Zr data, in good agreement with the uniform distribution of the D impurity prepared for the sample. This means that the intensity profile obtained with the ps laser, appears to represent more faithfully the D impurity distribution inside the sample. This result has thus further demonstrated the advantage of the ps laser over the ns laser.

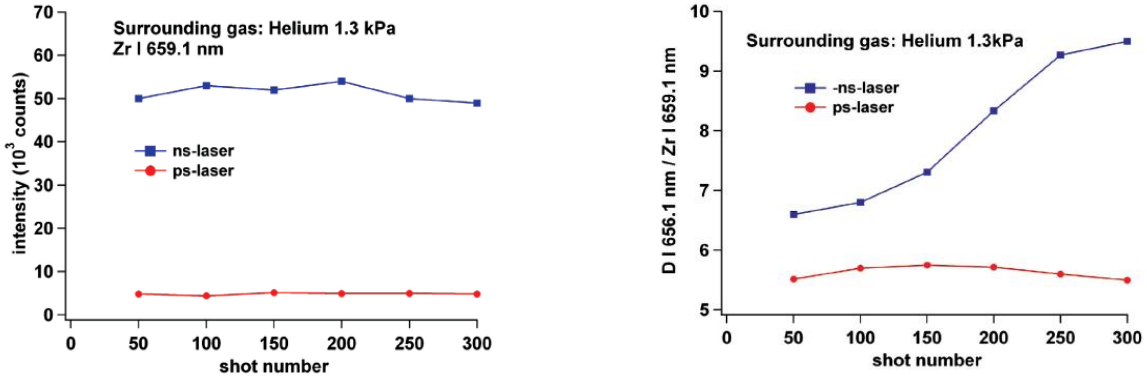

(a) (b)

Fig. 3.14. The variations of Zr emission intensity with increasing shot number, measured separately with the ns and the ps lasers (a), together with the corresponding variations of D emission given in terms of its intensity ratios with respect to the Zr emission intensity(b). Zircaloy-4 sample containing 900 µg/g of D was used as a sample. The helium gas pressure was kept at 1.3 kPa. The gate delay and width of the OMA system were set at 10 ns and 50µ, respectively, for ps laser data and 200 ns and 50 µs, respectively, for ns laser data.

It must be admitted that this experimental result does not at this stage provide sufficient information for the detailed exploration of the more favorable result obtained with the ps laser. Nevertheless, one may envision some possible effect created by the relatively long heating process by the much longer ns laser pulse. As a result, thermally induced segregation or migration of the D impurity may take place inside the sample, resulting in changes in its local distribution. Certainly this rather speculative explanation should be further examined in a separate experiment.

3.2.4 Conclusion

We have demonstrated in this experiment the more consistent and superior quality of the emission spectra of D, H, and Zr from the D-doped zircaloy samples obtained at low pressure He ambient gas by replacing the nano-second Nd- YAG laser with its pico-second version, which was operated at much lower energy of only 7 mJ. It is shown that equally well resolved H I 656.2 nm and D I 656.1 nm was achieved in the present experiment. Further, aside from producing a smaller size crater on the sample surface, a linear intensity versus concentration calibration line was obtained for the D impurity over a much broader range of concentration (1600 µg/g) compared to the previous result of 200 µg/g obtained by using the ns laser. The extrapolated calibration line also exhibits a near zero intercept. These features, together with the below 10 µg/g detection limit, have indicated the feasibility of applying our experimental setup for quantitative micro-analysis of H impurity in the zircaloy vessels used in light water nuclear power plant. It is further shown that the current setup using the ps laser

can be developed for measuring the H impurity concentration inside the sample and thereby produce the much desired three-dimensional information of the impurity distribution in the sample.

References

1. K. H. Kurniawan and K. Kagawa, Hydrogen and Deuterium Analysis Using Laser-induced Plasma Spectroscopy, Appl. Spectrosc. **41**, (2006) 99-130
2. J. L. Gottfried, F. C. D. Lucia, Jr., C. A. Munson, and A. W. Miziolek, Double-pulse standoff laser-induced breakdown spectroscopy for versatile hazardous materials detection, Spectrochim. Acta Part B **62** (2007) 1405–1411.
3. P. Fichet, D. Menut, R. Brennetot, E. Vors, and A. Rivoallan, Analysis by Laser-Induced Breakdown Spectroscopy of Complex Solids, Liquids, and Powders with an Echelle Spectrometer Appl. Opt. **42**, (2003) 6029-6035.
4. A. I. Whitehouse, J. Young, I. M. Botheroyd, S. Lawson, C. P. Evans, and J. Wright, Remote material analysis of nuclear power station steam generator tubes by laser-induced breakdown spectroscopy, Spectrochim. Acta Part B **56** (2001) 821-830.
5. J. M. Vadillo, S. Palanco, M. D. Romero, and J. J. Laserna, Fresenius Applications of laser-induced breakdown spectrometry (LIBS) in surface analysis, J. Anal. Chem. **355**, (1996) 909-912
6. D. G. Papazoglou, V. Papadakis, and D. Anglos, In situ interferometric depth and topography monitoring during LIBS elemental profiling of multi-layer structures, J. Anal. At. Spectrom. **19** (2004) 483.
7. H. Balzer, M. Hohne, R. Noll, and V. Sturm, New approach to monitoring the Al depth profile of hot-dip galvanised sheet steel online using laser-induced breakdown spectroscopy, Anal. Bioanal. Chem. **385**, (2006) 225-233.
8. A. Miziolek, V. Palleschi, and I. Schechter, in Laser-Induced Breakdown Spectroscopy (LIBS) Fundamentals and Applications, Cambridge University Press, New York, 2006.
9. D. A. Cremers and L. J. Radziemski, in Handbook of Laser-Induced Breakdown Spectroscopy, John Wiley and Sons. Ltd., England, 2006.
10. N. Konjevic, Plasma broadening and shifting of non-hydrogenic spectral lines: present status and applications, Phys. Rep. **316**, (1999) 339-401.
11. L. C. Popovic, E. G. Mediavilla, A. Kubicela, and P. Javanovic, Balmer lines emission region in NGC 3516, Kinematics Phys. Properties, A & A **390**, (2002) 473-480.
12. K. H. Kurniawan, M. Pardede, R. Hedwig, Z. S. Lie, T. J. Lie, D. P. Kurniawan, M. Ramli, K. Fukumoto, H. Niki, S. N. Abdulmadjid, N. Idris, T. Maruyama, K. Kagawa, and M. O. Tjia, Quantitative Hydrogen Analysis of Zircaloy-4 Using Low-Pressure Laser Plasma Technique, Anal. Chem. **79** (2007) 2703-2707.
13. M. Pardede, R. Hedwig, M. M. Suliyanti, Z. S. Lie, T. J. Lie, D. P. Kurniawan, K. H. Kurniawan, M. Ramli, K. Fukumoto, H. Niki, S. N. Abdulmadjid, N. Idris, T. Maruyama, K. Kagawa, and M. O. Tjia, Comparative Study of Laser-Induced Plasma Emission of Hydrogen from Zircaloy-2 Samples in

Atmospheric and Low Pressure Ambient Helium Gas, Appl. Phys. B. **89**, 2-3 (2007) 291 – 298

14. M. Munadi, R. Pardede, M. Hedwig, M. Suliyanti, T. J. Lie, Z. S. Lie, K. H. Kurniawan, K. Kagawa, M. Ramli, K. Fukumoto, T. Maruyama, and M. O. Tjia, Study of Hydrogen and Deuterium Emission Characteristics in Laser Induced Low Pressure Helium Plasma for the Suppression of Surface Water Contamination, Anal. Chem. **80**, 4 (2008) 1240-1246.
15. K. Kagawa, M. Ohtani, S. Yokoi, S. Nakajima, Characteristics of the plasma induced by the bombardment of N_2 laser pulse at low pressures, Spectrochim. Acta part B **39** (1984) 525-536
16. W. S. Budi, H. Suyanto, K. H. Kurniawan, M. O. Tjia, and K. Kagawa, Shock Excitation and Cooling Stage in the Laser Plasma Induced by a Q-switched Nd:YAG Laser at Low Pressures, Appl. Spectrosc., **53**, 6 (1999) 719-730
17. K. H. Kurniawan, T. J. Lie, M. M. Suliyanti, R. Hedwig, M. Pardede, M. Ramli, H. Niki, S. N. Abdulmadjid, N. Idris, K. Lahna, Y. Kusumoto, K. Kagawa, and M. O. Tjia, The Role of He in Enhancing the Intensity and Lifetime of H and D Emissions from Laser-Induced Atmospheric-Pressure Plasma, J. Appl. Phys. **105** (2009) 103303-1-6
18. D. Romero and J. J. Laserna, Surface and tomographic distribution of carbon impurities in photonic-grade silicon using laser-induced breakdown spectrometry J. Anal. Atom. Spectrom. **13**, (1998) 557.
19. D. Anglos, Laser-Induced Breakdown Spectroscopy in Art and Archaeology Appl. Spectrosc. **55**, (2001) 186A-205A.
20. M. Kraushaar, R. Noll, and H. U. Schmitz, in International Meeting on Chemical Engineering, Environmental Protection and Biotechnology, ACHEMA2000, Laboratory and Analysis Accreditation, Certification and QM, (Frankfurt, 22-27 May 2000), 117–119, 2000.
21. V. Sturm, L. Peter, and R. Noll, Steel Analysis with Laser-Induced Breakdown Spectrometry in the Vacuum Ultraviolet, Appl. Spectrosc. **54**, (2000) 1275-1278.
22. M. Corsi, A. Tozzi, R. Barale, G. Cristoforetti, M. Hidalgo, D. Iriarte, S. Legnaioli, V. Palleschi, A. Salvetti, and E. Tognoni., LIBS 2002 Technical Digest, Conference on Laser Induced Plasma Spectroscopy and Applications, pp. 172–174, Orlando, FL, 2002.
23. Y. Groisman and M. Gaft, Online analysis of potassium fertilizers by Laser-Induced Breakdown Spectroscopy, Spectrochi. Acta part B **65** (2010) 744–749.
24. R. Sattmann, I. Monch, H. Krause, R. Noll, S. Couris, A. Hatziapostolou, A. Mavromanolakis, C. Fotakis, E. Larrauri, and R. Miguel, Laser-Induced Breakdown Spectroscopy for Polymer Identification, Appl. Spectrosc **52**, (1998) 456-461.
25. J. Gruber, J. Heitz, H. Strasser, D. Bauerle, and N. Ramaseder, Rapid In-Situ Analysis of Liquid Steel by Laser-Induced Breakdown Spectroscopy , Spectrochim. Acta B **56** (2001), 685-693.
26. R. E. Neuhauser, U. Panne, R. Niessner, G. A. Petrucci, P. Cavalli, and N. Omenetto, On-line and in-situ detection of lead aerosols by plasma-spectroscopy and laser-excited atomic fluorescence spectroscopy, Anal. Chim. Acta **346** (1997) 37-48.
27. Samek, D. C. S. Beddows, J. Kaiser, S. Kukhlevsky, M. Liska, H. H. Telle, and J. Young, Application of laser-induced breakdown spec- troscopy to in situ analysis of liquid samples Opt. Eng. **38**, (2000) 2248-2262.
28. Y. Ito, O. Ueki, and S. Nakamura, Determination of colloidal iron in water by laser-induced

breakdown spectroscopy, Anal. Chim. Acta **299**, (1995) 401-405.

29. H. A. Archontaki and S. R. Crouch, Evaluation of an Isolated Droplet Sample Introduction System for Laser-Induced Breakdown Spectroscopy, Appl. Spectrosc. **42**, (1988) 741-746.
30. K. H. Kurniawan, T. Kobayashi, and K. Kagawa, The Effect of Different Atmospheres on the Excitation Process of TEA CO_2 Laser Induced Shock Wave Plasma, Appl. Spectrosc., **46**, 4, (1992) 581-586.
31. M. Kuzuya, H. Matsumoto, H. Takechi, and O. Mikami, Effect of Laser Energy and Atmosphere on the Emission Characteristics of Laser-induced Plasmas, Appl. Spectroscopy, Appl. Spectrosc. **47**, (1993) 1659.
32. M. R. Joseph, N. Xu, and V. Majidi, Time-resolved emission characteristicsand temperature profiles of laser-induced plasmas in helium, Spectrochim. Acta Part B **49** (1994) 89 – 103.
33. S. N. Abdulmadjid, Z. S. Lie, H. Niki, M. Pardede, R. Hedwig, T. J. Lie, E. Jobiliong, K. H. Kurniawan, K. Fukumoto, K. Kagawa, and M. O. Tjia, Quantitative Deuterium Analysis of Titanium Samples in UV Laser-Induced Low-Pressure Helium Plasma, Appl. Spectrosc. **64**, 4 (2010) 365-369.
34. M. Ramli, K. Fukumoto, H. Niki, S. N. Abdulmadjid, N. Idris, T. Maruyama, K. Kagawa, M. O. Tjia, M. Pardede, K. H. Kurniawan, R. Hedwig, Z. S. Lie, T. J. Lie, and D. P. Kurniawan, Quantitative Hydrogen Analysis of Zircaloy-4 in Laser-Induced Breakdown Spectroscopy with Ambient Helium Gas, Appl. Opt. **46** (2007) 8298-8304.
35. R. Hedwig, Z. S. Lie, K. H. Kurniawan, A. N. Chumakov, K. Kagawa, and M. O. Tjia, Toward Quantitative Deuterium Analysis with Laser-Induced Breakdown Spectroscopy Using Atmospheric-Pressure Helium Gas, J. Appl. Phys. **107**, 2 (2010) 023301 1-5.

Chapter 4

Hydrogen Analysis using Nd:YAG Laser-Induced Helium Gas Plasma at Atmospheric Pressure

4.1 Direct Evidence of Mismatching Effect on H Emission in Laser-Induced Atmospheric Plasma

4.1.1 Introduction

Hydrogen analysis is greatly needed in many field of application such as detecting trapped hydrogen in zircaloy pipe in nuclear power plant and in titanium for industrial and medical application[1-2]. As we noted in our previous work [3], the intensity of hydrogen emission is greatly reduced when the surrounding gas pressure was increased to atmospheric-pressure. This unique phenomenon of H emission was interpreted based on shock wave model. Namely, it has been assumed that there is a time lag between the laser bombardment and the starting time of the shock wave and that the shock wave is induced by propelling atoms of the host elements which are much heavier than hydrogen. It is assumed that the time lag increases with increasing the pressure. Therefore, at high pressures hydrogen atoms would gush out earlier with very high speed than other elements because its mass is extremely lighter than others, and when the shock wave starts the hydrogen already locates at the forward of the shock front. We called this phenomenon as “mismatching effect”. We have also proved the atoms are excited just in the limited area behind the shock front. Thus, only a

little part of the early ablated hydrogen atoms can be excited by the shock wave coming later from the behind. Consequently, the hydrogen emission efficiency becomes extremely low at high pressure and this becomes one of the weakness points for *in-situ* laser-induced breakdown spectroscopy (LIBS) technique. For hydrogen analysis in nuclear power station, atmospheric-pressure surrounding gas must be used since the zircaloy tube was submerged in the water. To overcome this problem, we have offered several technique such as by using double-pulse laser irradiation [4-5] and by employing helium metastable excited state to excite the hydrogen atoms at atmospheric pressures [6-13] yielding strong and sharp hydrogen emission. However, direct experimental evidence of the mismatching effect itself has not been reported.

In order to get the direct evidences of mismatching effect, we should have complete figures of spatially and timely distribution of hydrogen and host atoms both in the excited state and in the ground state. To know the population of ground state of atom, laser induced fluorescents (LIF) is usually used, but it is very difficult to get tunable laser for hydrogen which has resonance line of short wavelength (121.5nm). Thus, in this paper, we offer a sophisticate idea to prove the existence of ground state of atoms. Namely, we used the experimental fact reported in our previous work that atoms are effectively excited in the cooled helium gas plasma, which contained a lot of helium metastable excited atoms [6-13]. The second laser irradiation was made on the target surface with suitable delay time against the first laser irradiation when the helium gas plasma has already been cooled down. Thus, when the atoms coming from the target entered the cooled helium gas plasma region, they will be excited through helium metastable atoms. As a result, strong, sharp and low background hydrogen emission spectra were obtained since the hydrogen excitation is not through the thermal excitation process. We have also confirmed that almost all host element atoms used in this study can be excited in this cool helium gas plasma and we have named this technique as “helium metastable atoms probing technique”. Using this technique we have shown the occurrence of the mismatching effect of H atoms in the atmospheric-pressure plasma. It should be noted that this technique is exactly different from ordinary double pulse laser irradiation technique in which the second laser was sent later after the ablation process to improve the spectra quality [14-23].

4.1.2 Experimental Procedures

Fig. 4.1 shows the experimental setup used in this work. A Q-switched Nd:YAG laser

(Quanta Ray, LAB SERIES, 450 mJ, 8 ns) was operated at its fundamental wavelength of 1,064 nm with a repetition rate of 10 Hz. The laser beam at a fixed energy of 110 mJ was focused into the chamber through a quartz window. The chamber is equipped with an inlet and outlet for the helium gas flow and two other quartz windows for the observation of plasma emission. In this set-up, gas plasma which has thin and long in vertical direction was produced by fundamental ns Nd:YAG laser. The plasma exhibits to strong white emission in its center with an outer shell of orange color. The helium gas plasma was produced at 10 μs prior to the target ablation. High purity He gas (6N) was flown to the interaction chamber at a constant flow rate of 2 l/min at 1 atm.

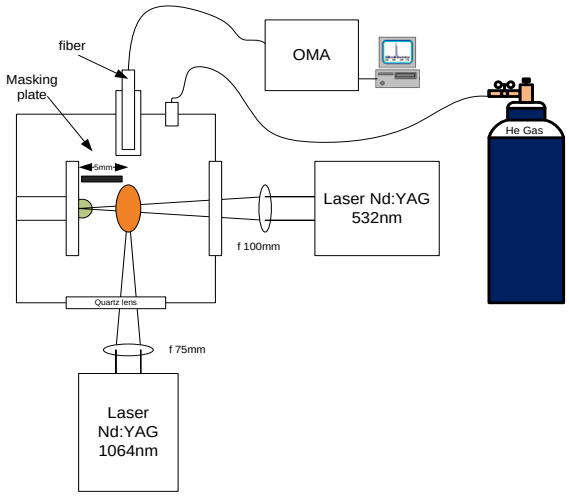

Fig.4.1. Schematic description of experimental setup (top view)

For the experimental study, laser ablation was carried out by focusing the second laser (Nd:YAG, Quanta Ray, LAB SERIES, 532 nm, maximum energy of 225 mJ, 6 ns) onto the solid sample and the ablated atoms were sent onto the helium micro plasma region by diffusion as clearly shown in Fig. 4.1. This laser irradiation was made at two different energies, 37 mJ and 75 mJ. Synchronization of the two lasers system used in this experiment was done by using digital delay generator (Stanford Research System, model DG-535). The resulted emission spectrum of the ablated atoms which was excited by the helium plasma was detected by using an optical fiber inserted into the interaction chamber with a distance of 2 cm from the helium plasma. At this position, the fiber is expected to collect the emitted light entering within 27º degrees of solid angle. The other end of the optical fiber was connected to the entrance slit of the spectrograph. Optical multichannel analyzer (OMA system, Andor I*Star intensified CCD 1,024x256 pixels) was attached to the exit slit of the spectrograph

(McPherson model 2061 with 1,000 mm focal length, 1,800 g/mm grating and f/8.6 Czerny Turner configuration).

The agate sample used in this study was chosen from among the available solid samples for its strongest H emission, which remained practically unchanged after the 100 repeated laser shots on a fixed spot of the sample surface.

4.1.3 Experimental Results and Discussion

Before we made experiment to prove the mismatching effect, we examined the emission spectrum of agate sample by using the ordinary laser method; namely, only one laser used to ablate sample. Also, we studied again how hydrogen emission intensity depends on the pressure of surrounding gas.

Fig. 4.2 shows the emission spectra taken from the agate sample in the wavelength region from 650 nm till 670 nm at laser energy of (a) 75 mJ and (b) 37 mJ. The gate delay and width of the OMA system was set at 100 ns and 50 μs, respectively after the laser-target ablation. It should be noted that only second laser for ablating target was used in this experiment. From this figure, one can clearly see that hydrogen emission line significantly decreased at helium 760Torr as compared to helium 20Torr both for laser energy 37mJ and 75mJ. It should also be noted that other emission lines such as calcium and helium only slightly decreased at helium 760Torr as compared to helium 20Torr.

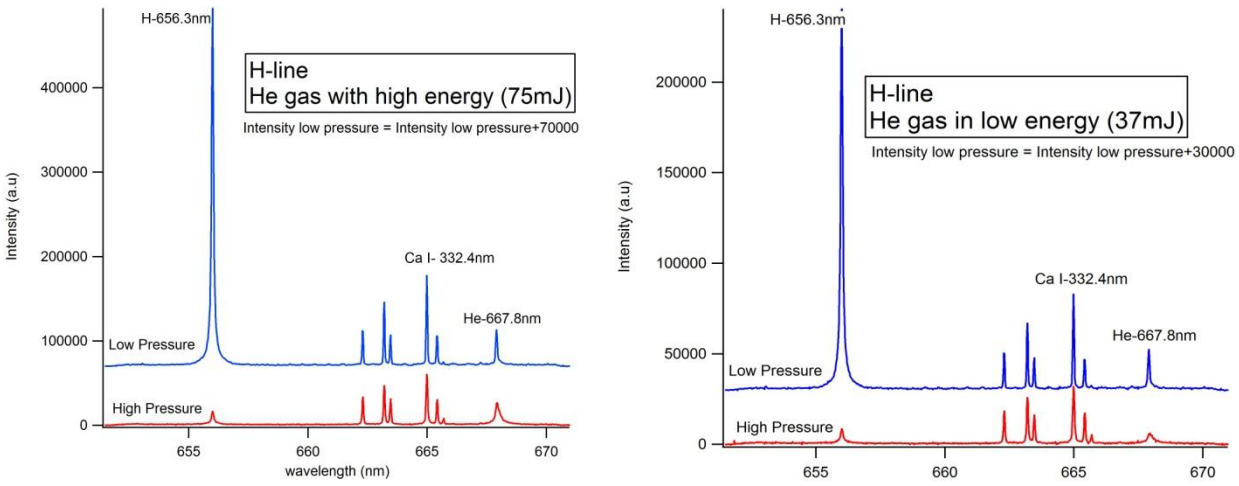

Fig.4.2. Agate spectrum showing H_α, Ca I 332.4 nm and He I 667.8 nm emission lines in the wavelength region from 650nm to 670nm detected in the different surrounding pressure; 20 torr and 760 torr. The laser energy was set at 75mJ (a) and 37 mJ (b) laser ablation energy in He gas. The OMA was operated with 100 ns gate delay and 50 μs gate width right after the laser ablation.

In order to check whether the host elements of silicon and oxygen also suffer from this mismatching effect, spectra of silicon and oxygen was taken and the result is presented in Fig. 4.3, (a) for silicon line and (b) for oxygen lines at laser energy of 37mJ. It is clearly seen from Fig. 4.3(a) that the emission intensity of silicon line was almost the same for both helium 760 Torr and helium 20 Torr. Same result was also obtained for oxygen which has nearly the same excitation energy (10.25 eV) with hydrogen (12.75 eV) as shown in Fig. 4.3(b); only spectrum widths are different because in high pressure plasma serious spectrum broadening takes place.

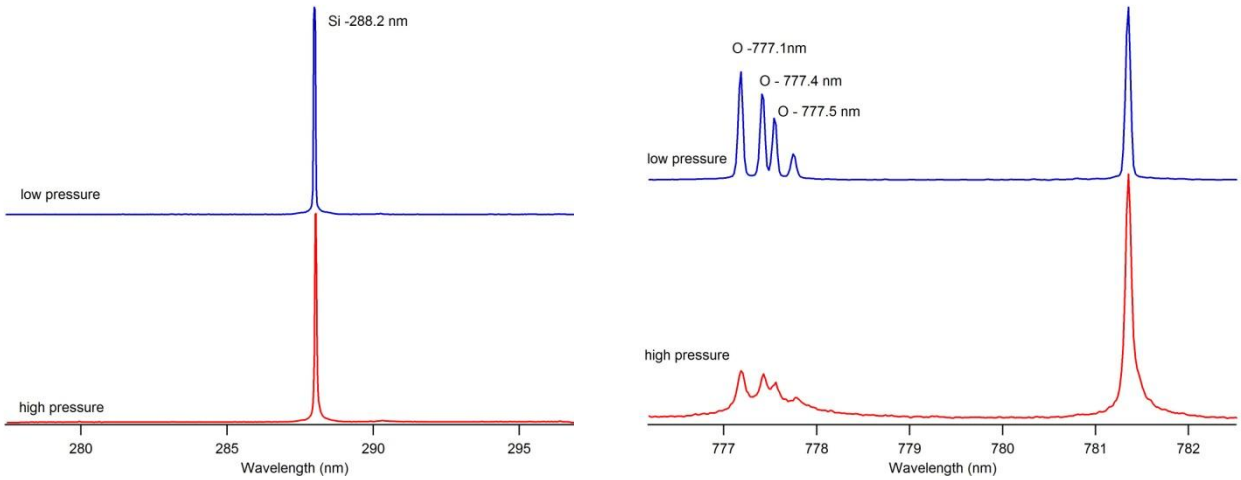

Fig.4.3 Agate spectrum showing Si-288.2nm (a), and O-777nm (b) emission lines at 37mJ laser ablation energy in helium gas with different surrounding pressure; 20 torr and 760 torr. The OMA was operated with 100 ns gate delay and 50 μs gate width right after the laser ablation.

As we have reported in our previous work using slide glass sample [24], hydrogen intensity reduction was much serious in the case of nitrogen surrounding gas. Fig. 4.4 shows the spectra taken from agate sample in the wavelength region from 650 nm to 670 nm in surrounding nitrogen gas at 2 Torr and 760 Torr. It is clearly seen that no hydrogen emission was observed when the nitrogen gas pressure was set at 760 Torr. Meanwhile, the reduction of calcium and silicon emission lines was not pronounced. One should be noted that the strong and sharp hydrogen emission at 2 Torr nitrogen gas was mainly due to the shock excitation as we reported in our previous work [3].

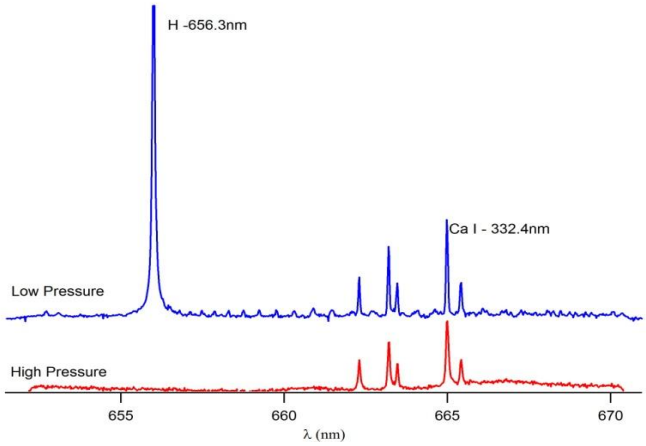

Fig.4.4 Agate spectrum showing hydrogen, calcium and helium lines in the wavelength region from 650 nm till 670 nm at laser energy of 37 mJ. Nitrogen surrounding gas was used in this experiment. The gate delay and width of the OMA system was set at 100 ns and 50 μs, respectively after the laser-target ablation.

As we have mentioned in the introduction, "helium metastable atoms probing" technique was used to know the occurrence of mismatching effect of hydrogen atoms. Before applying this technique, the characteristics of helium gas plasma was examined. In this experiment, we intentionally put the H_2O vapor in the chamber and only fundamental laser was used. Fig. 4.5 shows the time profile of He I 667.8 nm at laser energy of 110 mJ. The gate width of the OMA system was set at 100 ns, respectively. It is clearly seen that after the laser irradiation, He emission increases very fast till 3 μs and then decay slowly till around 30 μs. This He emission time profile was the same as we have reported in our previous work [7]. In this experiment, hydrogen emission was also observed as seen in Fig. 4.5. The time profile of the hydrogen emission is long following the helium emission time profile. This becomes one of signatures that hydrogen was excited by the helium metastable atoms in the cool helium gas plasma.

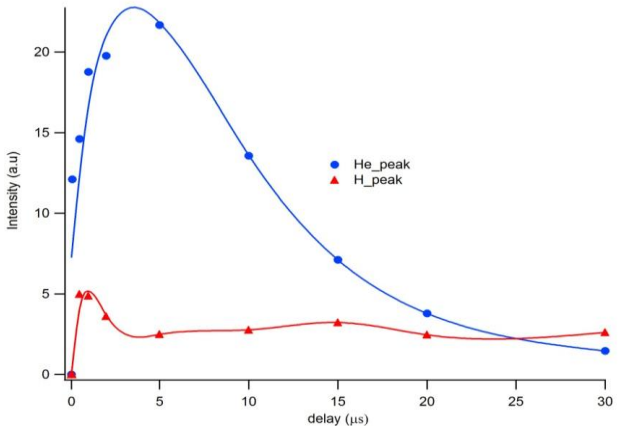

Fig.4.5. The time profile of He I 667.8nm and H I 656.2nm at fundamental laser energy of 110mJ. The gate delay and gate width of the OMA system was set at 20 ns and 100 ns, respectively after the laser irradiation.

In order to prove the "mismatching effect", we examined how the ground states of hydrogen and host elements moved with time. For this purpose, we used a novel technique; namely, He gas plasma was produced in front of the sample surface by focusing fundamental Nd:YAG laser. Then 532nm Nd:YAG laser was irradiated to the sample surface with a delay time of 10 μs to send atoms to the cool helium gas plasma, where metastable existed. When ground state atoms enter the cool plasma, emission takes place by colliding with the metastable helium atom. Figure 4.6 show how H-656.3 nm, O-777.1 nm and Ca-422.6 nm emission intensities, respectively, change with time. In this experiment, the helium gas plasma was formed at 10 μs before the laser target ablation (energy 37 mJ); and the fiber optic was set so that only the emission from the region of helium gas plasma was detected. The gate width of the OMA system was set at 50ns, after the laser target ablation. In Fig. 4.6, it is clearly seen that at 100 ns, H emission has already peaked, this means that the hydrogen atoms have moved at 5 mm within 100 ns, which corresponded to 50 km/s. The decay of the hydrogen emission was also very fast because hydrogen atoms passed through the He gas plasma region within a short time and once they passed the He gas plasma region, they are not excited. As a comparison, we also showed the oxygen and calcium time profile. It is seen that oxygen emission become maximum at 500 ns and calcium emission does at 2 μs. This is consistent with the scenario that depending on the mass, arriving times of the atoms at the probing region are different. It should be noted that, calcium (mass of 40) arrived later as compared to oxygen (mass of 16), which has smaller mass than calcium.

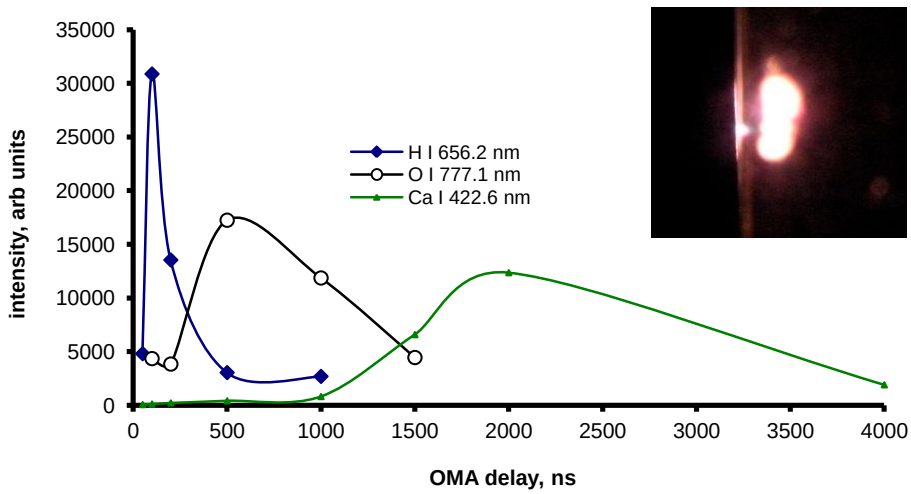

Fig.4.6. The time profile of hydrogen, oxygen and calcium in agate sample. The first laser energy was set at 110 mJ and fired at 10 μs before the second laser. The second laser energy was set at 37 mJ. The gate width of the OMA system was set at 50 ns. He flow rate was set at 2 l/min in atmospheric pressure.

In order to detect the emission time profile of the target plasma (size of plasma around 2mm), we set the fiber optic just near the target surface and the result presented in Fig. 4.7; in this case, no helium gas plasma was generated. It is clearly seen that silicon and oxygen emission have peaks at around 700ns and then slowly decay in cooling stage region. Therefore, according to the shock wave model, we can say that shock excitation stages has maximum around 700ns. It is naturally understood that why H cannot be excited in the target plasma because at 700ns H atoms already pass over 5mm distance from the surface as shown in Fig 4.6. This again proves that hydrogen atoms were not excited by the shock wave and this is in good agreement with our mismatching effect model.

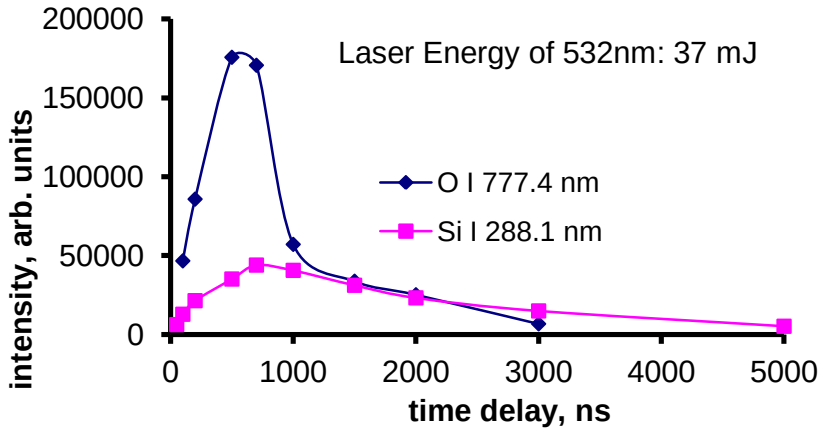

Fig.4.7. Time profile of oxygen and silicon on target plasma was made at laser energy of 37mJ.

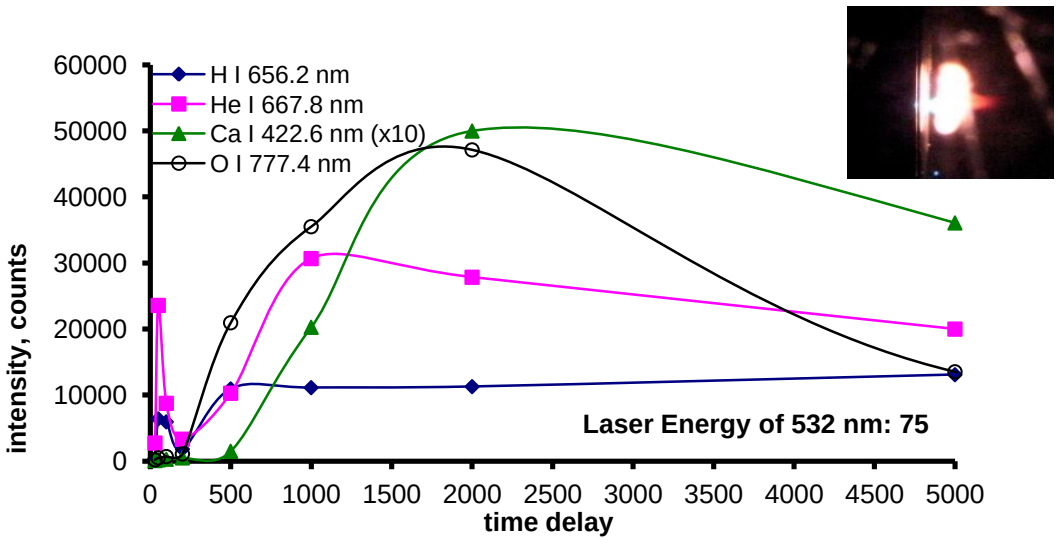

Fig.4.8. The time profile of hydrogen, oxygen, calcium and helium emission in agate sample. The first laser energy was set at 110mJ and fired at 10 μs before the second laser. The second laser energy was set at 75mJ. The gate width of the OMA system was set at 50 ns. He flow rate was set at 2 l/min in atmospheric pressure.

Similar experiment shown in Fig 4.6 was made using high energy of laser 75 mJ which was used to make target plasma; the result is presented in Fig. 4.8. It should be noted that, strong helium emission takes place with two components; one is fast component and another is slow component. While, in the previous experiment shown in Fig 4.6, no helium emission takes place. This fast component of helium emission signal is probably due to the fact that helium metastable atoms are ionized by colliding with high speed hydrogen atoms; namely, high speed hydrogen atoms give energy to helium metastable atoms to be ionized, and He emission takes place through recombination process. The slow component of the helium emission signal is probably due to the fact that helium metastable is re-excited by interacting with the strong shock wave plasma.

Finally it is supposed that such high speed hydrogen atoms will distribute mainly to the forward direction (shape of cone like). To that end, spatial distribution of hydrogen atoms were observed by imaging methods; namely, using a lens, the plasma image was made on the imaging plane and the fiber was moved on the imaging plane in the axis of the vertical helium gas plasma. In this case, the laser energy was fixed at 37 mJ, the gate delay and width of the OMA system was set at 50 ns and 500 ns, respectively. The result is presented in Fig. 4.9. It is clear that the spatial distribution of the hydrogen atoms is shape of cone like. Meanwhile for the host element of calcium, the spatial distribution is quite wider as compared to that of hydrogen

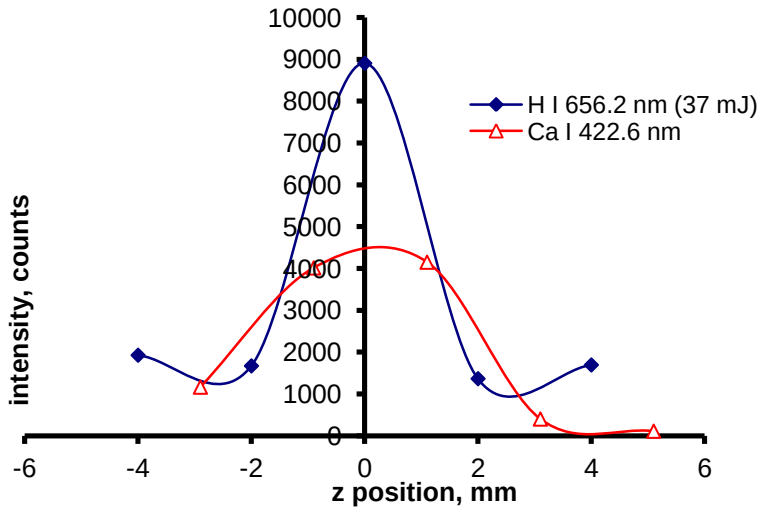

Fig.4.9. Spatial distribution of hydrogen and helium emissions was taken using agate sample. The first laser energy was set at 110mJ and fired 10 μs before the second laser. The second laser energy was set at 37mJ. The gate delay and gate width of the OMA system was set at 50 ns (for initial stage) and 1 μs (for later stage) and 500 ns, respectively after the laser target irradiation. He flow rate was set at 2 l/min in atmospheric pressure.

4.1.4 Conclusion

Experimental study was made in order to understand the specific characteristic of hydrogen emission observed in ordinary LIBS method; namely, H emission intensity decreased with increasing the pressure, and at 1 atmospheric pressure it was extremely weak. It was assumed that the specific phenomenon of hydrogen emission is due to the mismatching between the time when the H atom gushing occurs and the time when the shock wave starts. We called this as “mismatching effect”. It is naturally supposed that the shock wave starting time is slightly delayed with increasing the pressure of the ambient gas, while most of the H atoms will leave from the target with super high speed before the shock wave starting because hydrogen atoms are very light compared to other elements; the H atoms will not be excited because only the atoms located just behind the shock front are effectively excited.

In order to prove this mismatching effect, we must know how the ground states of hydrogen and host elements were populated spatially and timely. For this purpose, we used a novel technique namely “helium metastable atoms probing” technique; namely, helium gas plasma was produced in front of the sample surface by focusing fundamental Nd:YAG laser (110mJ). Then, 532 nm Nd:YAG laser was irradiated to the sample surface with a suitable delay time to send the atoms to the cooled helium gas plasma, where metastable helium atoms existed. When ground state atoms enter the cooled helium gas plasma, emission takes place by colliding with the metastable helium atoms. By this method, we proved that H atoms come out much faster than other elements. Also, we proved that the high speed H atoms distribute mainly to the forward direction with cone shape.

4.2 Highly Sensitive Deuterium Analysis Using ns Nd:YAG Laser Induced Helium Gas Plasma by Combining with ps Nd:YAG Laser for Ablation

4.2.1 Introduction

The worldwide demand for energy has continued to grow at an increasing pace. Meanwhile, the world is confronted with the problems of dwindling supply and increasing cost of fossil fuels, as well as the growing threat that their continued consumption is expected to pose to the global climate. The challenges to cope with those problems, among others, in the past, have led to a renaissance in the development of the nuclear power industry. Unfortunately, the nuclear reactor disaster induced by the devastating tsunami at the Fukushima Nuclear Power Station in Japan is making a significant dent in the further deployment of nuclear power plants worldwide. Nevertheless, this is likely to be temporary in nature, as the initial socio-political reaction is bound to subside with time, especially when the continued improvement of reactor technology can be demonstrated to offer much safer operation of the new generation nuclear power plants. Besides, the large and unique advantages offered by nuclear energy, which are (at least until the end of this decade) unmatched by the other alternative new energy sources, is difficult to ignore, in the face of pressing demand for large-scale and high-efficiency energy supplies [25]. It is also highly improbable that the existing nuclear power plants responsible for a large share of energy supply in some developed countries will be abandoned abruptly. It should also be noted that most of the more recently built reactors are of the improved versions, employing the heavy-water moderator instead of the older version of light-water reactors adopted in the Fukushima Nuclear Power Station. However, there is one important common problem that must be tackled for improving the efficiency of their operations, as described below.

In a light-water nuclear power station, the enriched uranium fuel is contained in zircaloy pipes immersed in a water tank. During the operation of the reactor, hot water reacts with the zircaloy surface to form zirconium oxide and hydrogen gas, which readily penetrates into and accumulates in the zircaloy pipe. The excessive presence of this trapped hydrogen is known to cause a certain type of structural damage, leading to reduced mechanical strength of the material and potentially endangering the operation of the power plants. Therefore, the hydrogen concentration in the zircaloy pipes must be examined periodically. A standard

technique for detecting hydrogen in such a case involves the use of a gas detector and requires the melting of a portion of the zircaloy pipe in a carbon furnace after the special handling for the removal of the remaining fuel in the pipe. Thus, it is highly desirable to replace the existing time-consuming and destructive method by a more-practical and less-destructive one. A similar demand for improved deuterium (D) detection technique is to be expected for the heavy-water nuclear power plants.

As reported previously [3], it is indeed possible to improve the hydrogen (H) detection method by means of some modification of the laser-induced plasma spectroscopy (LIPS), which was first introduced by Brech and Cross in 1962 [26]. This method was later developed into the celebrated technique of laser-induced breakdown spectroscopy (LIBS) by Radziemski et al. [27], which has become a widely adopted modern tool for rapid spectrochemical analysis in industry and research laboratories [21]. Using low-pressure (5 Torr) ambient helium gas [28], we have demonstrated the detection of the sharp H I 656.28 nm and D I 656.10 nm emission lines from the zircaloy sample, overcoming the long-standing problems of the Stark broadening effect and intensity diminution due to the time mismatch effects, which are commonly encountered in the standard operation of LIBS conducted with ambient air at atmospheric pressure. It is worth recalling that the time mismatch effect refers to the premature passage of the ablated atoms before the shock wave formation, thereby missing out on the shock-wave-induced thermal excitation process. This was suggested to be responsible for the weak intensity observed in the emission of very light and fast-moving atoms such as H and D [3]. Taking advantage of the previous result, suggesting the role of the metastable excited state of He in the low-pressure plasma [3], those disturbing effects were effectively eliminated by the appropriately delayed and prolonged detection of the H atomic emission. It was proposed that, during this delayed detection period, the measured H emission, instead of arising from the conventional hot plasma excitation, was mainly the result of the so-called helium-assisted excitation (HAE) process in the sufficiently cooled plasma via the Penning-like ionization process proposed previously [13]. This suggested excitation mechanism was further expanded with detailed energy-level diagram of He and the energy transfer processes in a most recent study of other atomic emission enhancements [29]. However, those results were all achieved with low-pressure (5−10 Torr) ambient helium gas. This implies the need for a vacuum pump for the preparation of the sample chamber, which is unwieldy for the need of rapid and frequent inspections. In a most recent experiment, the need for a low-pressure environment was

circumvented by employing atmospheric-pressure helium gas and an additional surface water precleaning procedure [30], which also succeeded in producing the nice linear calibration line that was needed for quantitative analysis. Nevertheless, the use of a bulky sample chamber in this and all previous cases has virtually prevented its application to in-situ D detection of zircaloy vessel immersed in the water tank. Therefore, further improvement of the experimental method specifically addressed to overcoming this hurdle is badly needed to support the efficient operation and maintenance of the heavy-water nuclear reactor.

It should be added that the importance of developing a practical, in-situ, rapid detection of D can hardly be overemphasized. The benefits of its realization goes beyond just meeting the urgent needs of the existing as well as other heavy-water nuclear power plants to be launched in the immediate future. No less importantly, it will also fulfill the anticipated crucial needs when the current nuclear fission power technology will be replaced eventually by the fusion power technology, which offers safer, cleaner, and more-efficient power production process with long-term sustainability and much smaller amounts of long-lived nuclear wastes, compared to nuclear fission processes. In the thermonuclear fusion reactor, one of the two fuel components used is the deuterium, which is chemically bonded in the solid LiD compound. Therefore, the deuterium analysis of this material is a matter of necessity. Furthermore, deuterium in its gas phase is readily adsorbed by certain metals and can be subsequently released via a simple heating process when needed for use. These metal pieces can be easily transported in disguise for concealed purposes. A practical and reliable D detection method can play an important role in deterring and preventing nuclear terrorism, as well as other illegal abuses of the potentially dangerous and lethal material.

In this work, we have developed a modified version of the conventional double-pulse (DP) LIBS technique employing two laser systems in an orthogonal configuration, which has been widely used for the studies of increasing the emission intensity. The results of those studies have generally demonstrated intensity enhancements with various degrees of enhancement, depending on the sample and ambient gas used [14-19, 22-23, 31-36], as well as the chosen gas pressure [37-38]. Specifically, in the preablation DP experiments, the observed intensity enhancement effect was commonly attributed to the rarefied gas condition created by the preablation laser pulse, which led to a more-effective ablation process [31,32]. In the present experiment, a major technical modification is introduced by employing flowing helium gas at atmospheric pressure. In this setup, the He atoms in their relatively long-lived metastable excited state are produced in the helium gas breakdown plasma generated in front

of the sample, while the sample is separately ablated to release the D atoms into the region of the helium plasma where they are excited by the HAE process. It is found that this method has produced a D emission line of very narrow spectral width, practically free from the interfering emission of H dissociated from the water molecule. It also eliminates the need for a vacuum chamber, hence promising its potential application for in situ analysis. Finally, our result further shows that the excellent D emission spectrum can be obtained by avoiding the use of a large ablation energy, hence preventing the formation of undesirably large crater sizes on the sample surface.

4.2.2 Experimental Procedures

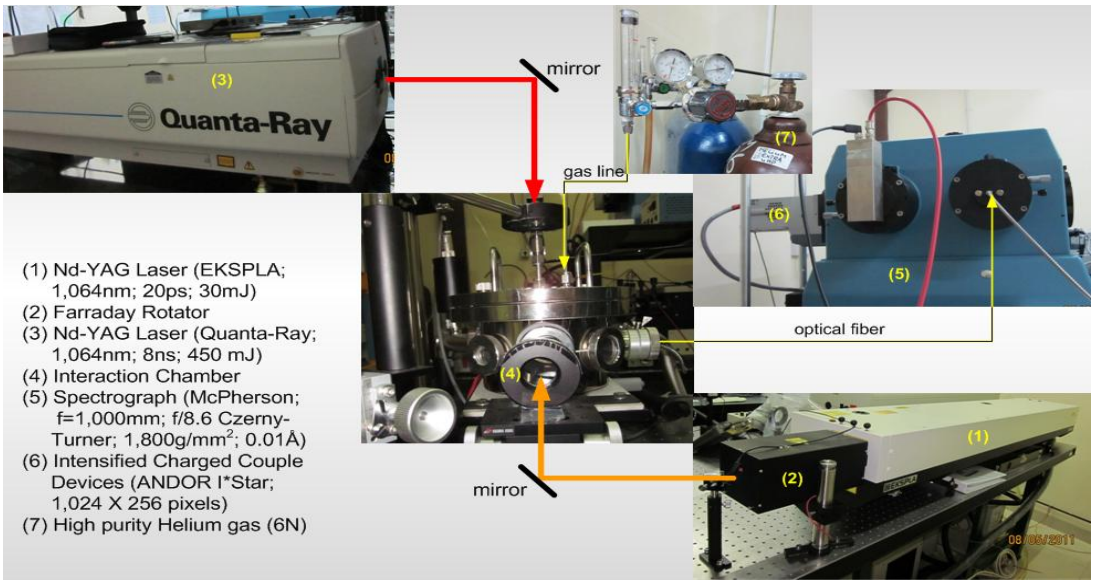

Fig.4.10. Photographic display of the experimental setup used in this study

Figure 4.10 gives the schematic description of the experimental setup consisting of two orthogonally ns and ps Nd:YAG laser system, both were operated in the Q-switched mode with a repetition rate of 10 Hz, and configured to produce the laser beams at mutually perpendicular directions. One of the lasers operating at its fundamental wavelength of 1,064 nm and fixed energy of 80 mJ was focused onto a spot within the ambient He gas in the chamber to generate the He plasma at a point 3 mm in front of the target. A constant flow of helium gas at atmospheric pressure (Air Liquid, 6N) was maintained with a constant flow rate of 3 l/min. The second laser was a Nd:YAG laser in its fundamental wavelength of 1,064 nm with 20 picoseconds (ps) pulse width and a fixed energy of 26 mJ for the ablation of the solid target unless otherwise stated. This second laser irradiation was started at a various time with the generation of He plasma by the first laser, thereby allowing the He plasma sufficient time

to cool itself down. The emission spectra of the ablated atoms were collected by an optical fiber with its entrance end fixed inside the chamber at the distance of 2 cm sidewise from the He plasma. The other end of the optical fiber was connected to the detection system consisted of a spectrograph (McPherson, model 2061, f= 100cm, Czerny Turner configuration) and an Optical Multichannel Analyzer (OMA) (Andor ICCD, 256 x 1024 pixels). The emission of ablated atoms outside the detection area was effectively blocked off by a slit placed in front of the entrance end of the fiber. The OMA system was set at fix gate delay of 4 μs and gate width of 50 μs after the formation of the He gas plasma which gives the maximum emission intensity of D emission.

The main targets employed in this experiment consist of a set of zircaloy-4 samples composed of 98.23 weight % Zr, 1.45 % tin, 0.21 % iron, 0.1 % chromium and 0.01% hafnium. These samples were prepared by prolonged high temperature and low pressure doping technique. The resulted concentration of deuterium impurity (60, 179, 540, 700, 900 and 1,700 μg/g) were determined by Gas Chromatography. All the samples measure 10 mm x 10 mm in cross sectional area and 1 mm in thickness.

4.2.3 Experimental Result and Discussion

Although the possible contribution of the He metastable-excited state in laser-induced plasma was suggested in works dating back to early 1990, no conclusive data and detailed discussion have so far been reported on the possible physical origin of those interesting and important effects. However, we believed that D analysis can only be performed by utilizing the cooled plasma in which He metastable excited state are still populated due to its long life. In the cooled plasma, D will be excited with very narrow spectral width thus enabling to distinguish with H emission with hair splitting wavelength different of 1.8 Å. To prove the excitation process through helium metastable-excited state, first we used copper plate as a target. Figure 4.11(a) shows the He gas plasma generated by focusing a first Nd:YAG laser (wavelength of 1,064 nm, pulse width of 8 ns and energy 80 mJ). A cylinder-like shape diameter of 5 mm and high of 12 mm plasma was formed. The color is orange which is attributed to the He I 587.6 nm emission. The lifetime of the He I 587.6 nm was measured to be around 20 μs. The white and bright color displayed by the rest of plasma is the results of its overexposure due to the strong continuing emission. Figure 4.11(b) show the copper plasma generated by focusing a second Nd:YAG laser (wavelength of 1,064 nm, pulse width of 20ps and energy of 26mJ) onto the copper plate sample under

helium surrounding gas of 1 atm. Faint green color corresponding to Cu I 510.5 nm, Cu I 515.3nm, and Cu I 521.8 nm was found in the outer most layer of the plasma. Figure 4.11(c) shows the plasma when the copper plasma was generated after 3 μs to the helium gas plasma formation. It is clearly seen from the figure that strong green color of Cu emission was observed just in front of the He gas plasma region. It means that the Cu atoms ejected from the target, push helium metastable atoms to outside of the helium emission region and then helium metastable atoms collide with Cu atoms to give Cu emission. It should also be noted that the He gas plasma becomes smaller as compared to Fig. 4.11(a). This is an indication that part of the He metastable-excited state was used to excite the copper atom. From this figure, it is clear to say that there is an optimal time for the ablated atoms to enter the He gas plasma in order to get the maximum emission enhancement and it is naturally to assume that this optimal time depend on the atomic weight of the ablated atoms.

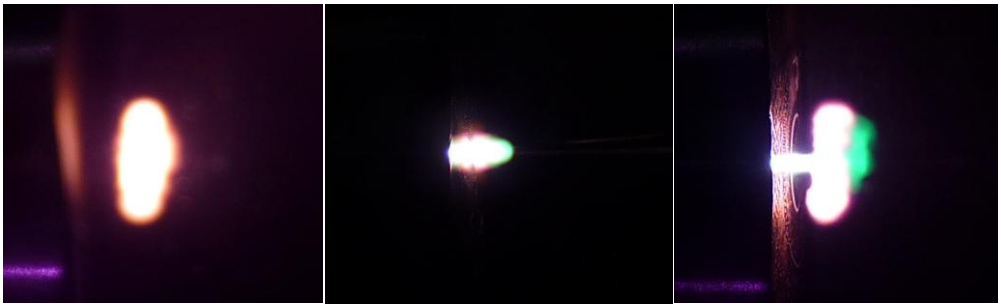

(a) (b) (c)

Fig.4.11 (a) Photograph of the plasma generated in flowing helium at 1 atm by the ns Nd:YAG laser with 8 ns and 80 mJ energy; (b) the much-smaller copper plasma generated by the ps Nd:YAG laser with much narrower pulse of 20ps and lower energy of 26 mJ without irradiation of the helium gas with ns laser; and (c) the result obtain when both laser were interactive with delay 3 μs for he ps laser.

Deuterium which has much smaller atomic weight than Cu was investigated. In order to get highly sensitive of deuterium, we must avoid the disturbance of H_2O from surrounding gas. In conventional method to reduce H_2O, vacuum was used but this technique cannot be used when we apply for *in-situ* analysis. Therefore, double pulse technique was used. Figure 4.12 shows the emission intensity of H I 656.28 nm, D I 656.1 nm, and Zr I 654.9 nm taken at different time between the target plasma formation and He gas plasma formation in zircaloy sample containing 1,700 μg/g with OMA delay of 4μs and gate width of 50μs after the formation of the He gas plasma. For the simplicity, sign "+" indicates that the target plasma was formed after the he gas plasma formation and sign "-" donates the opposite order of laser irradiation. It is clearly seen that the maximum enhancement of D emission was observed

when the ps laser were focused at 1 μs prior to the He gas plasma formation as shown in the inset of Fig.4.12. Therefore, in following experiment, we always send ps laser with 1 μs earlier than ns laser for He plasma generation.

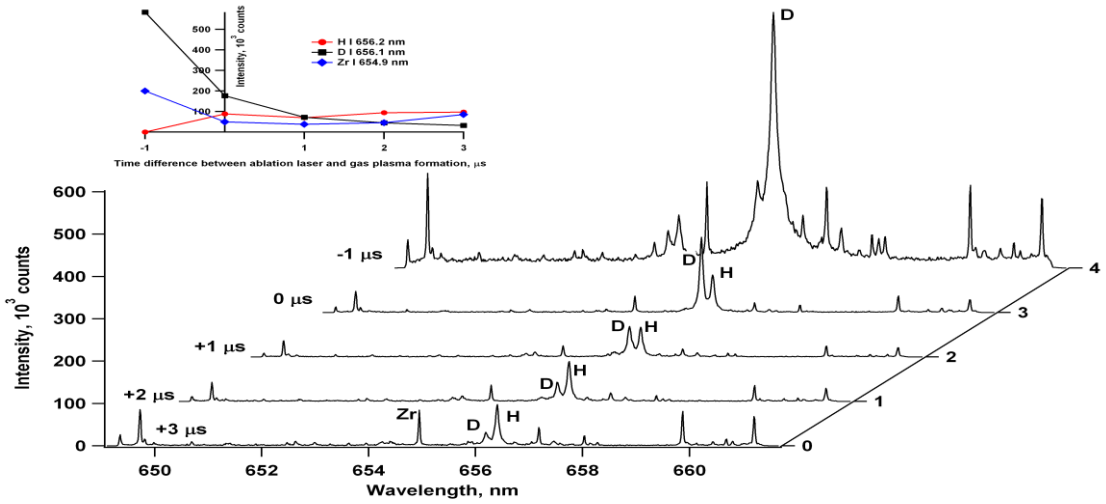

Fig.4.12. Emission spectra of a zircaloy plate containing 1700 μg/g of D impurity measured for synchronize time (τ) = −1, 0, 1, 2, and 3 μs with 26 mJ ablation laser energy. The negative sign (−) indicates the case that the target ablation precedes the helium gas plasma formation, and the positive sign (+) denotes the opposite order of laser irradiations.

It should be mention that when we continued ps laser irradiation at fixed position, penetration takes places after 150 shots, approximately. Figure 4.13 shows the spectra sequences of H emission in Zircaloy free deuterium sample when we make continuing irradiation at fix position with 10 Hz laser operation. This figure shows 3 different conditions; namely, only ns laser irradiation, synchronized irradiation of laser with -1 μs and the spectra when the sample had already been penetrated. In initial spectra when only ns laser was used, H emission appeared. This is due to the dissociated molecules of H_2O by focusing of ns laser in the gas. However, H emission suddenly disappeared when synchronize laser irradiation was made. This is probably due to the fact that ablated atoms by the irradiation of ps laser swept out H_2O molecules located in the region of ns laser focusing point. After the sample is penetrated, H emission increased again because no atom swept out the H_2O molecules. Similar experiment was made using zircaloy sample which is containing 750 μg/g of D and the results was shown in Fig 4.14. It is seen that D emission can be detected clearly without the disturbance of H emission. Namely, the D atoms have already distributed in the region of He gas plasma region. Therefore, when the He gas plasma was generated, most of the D atoms which are already populated in the He gas plasma region were excited.

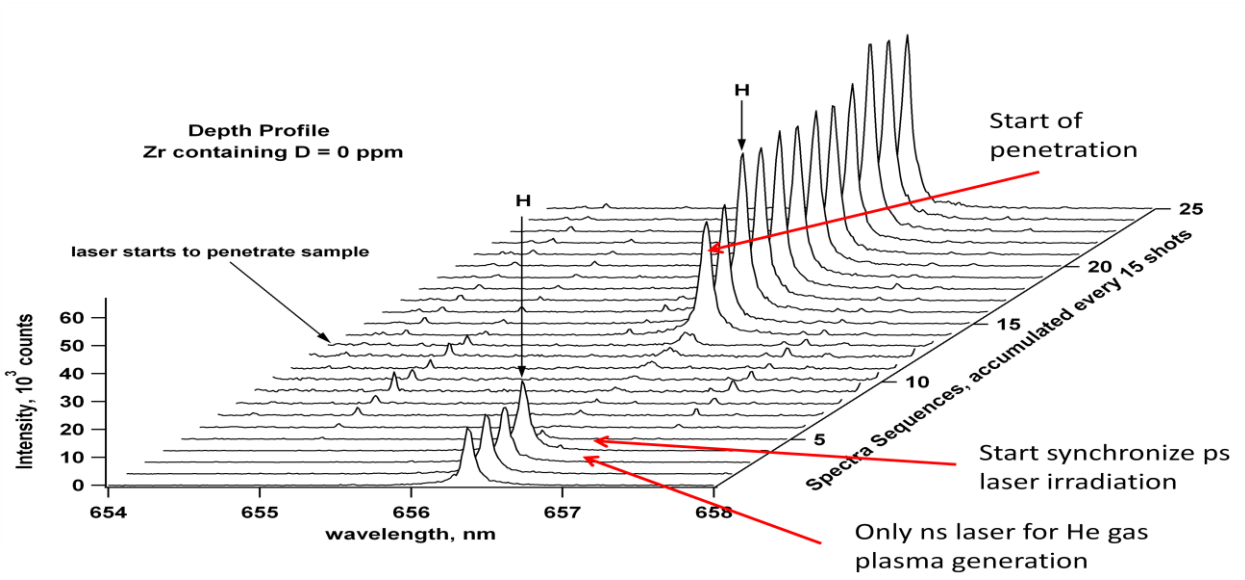

Fig.4.13. Spectra Sequences of a zircaloy plate containing free D measured for synchronize time (τ) = −1 μs with 26 mJ ablation laser energy.

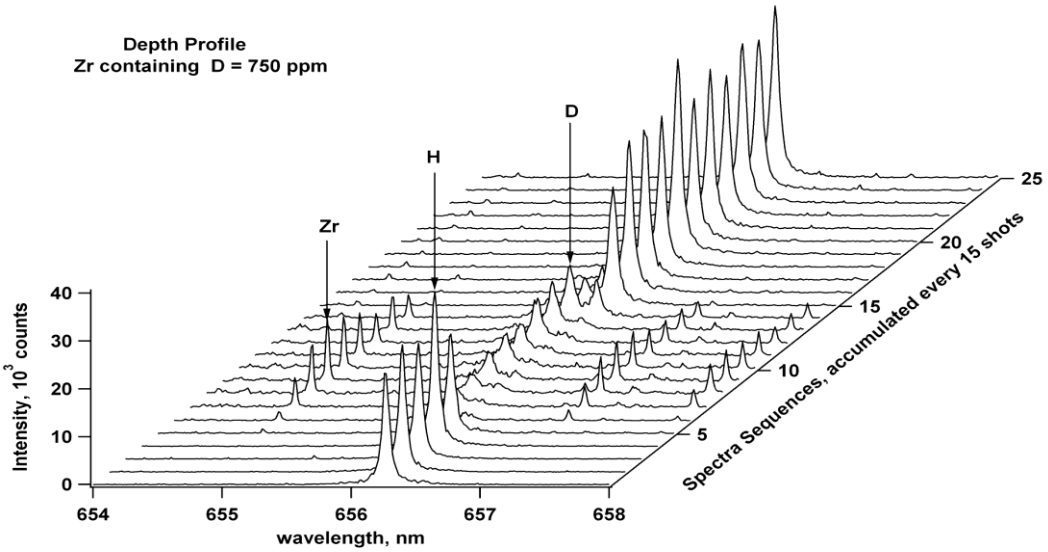

Fig.4.14 Spectra Sequences of a zircaloy plate containing 750 μg/g of D impurity measured for synchronize time (τ) = −1 μs with 26 mJ ablation laser energy.

Figure 4.15 shows the spectra sequences of He-587.6 nm (a) and He-667.8nm (b) in zircaloy sample of free D. In the initial when only ns laser was used, strong He emission appeared. When synchronize irradiation started, He emission decreased significantly. This is probably because helium metastable atoms are used mostly to excite the atom from the sample. After the sample was penetrated, He emission increased again. This emission is

higher than the initial emission. This is probably due to the electrons sent by the sample to the helium gas plasma region, even though the sample had already been penetrated.

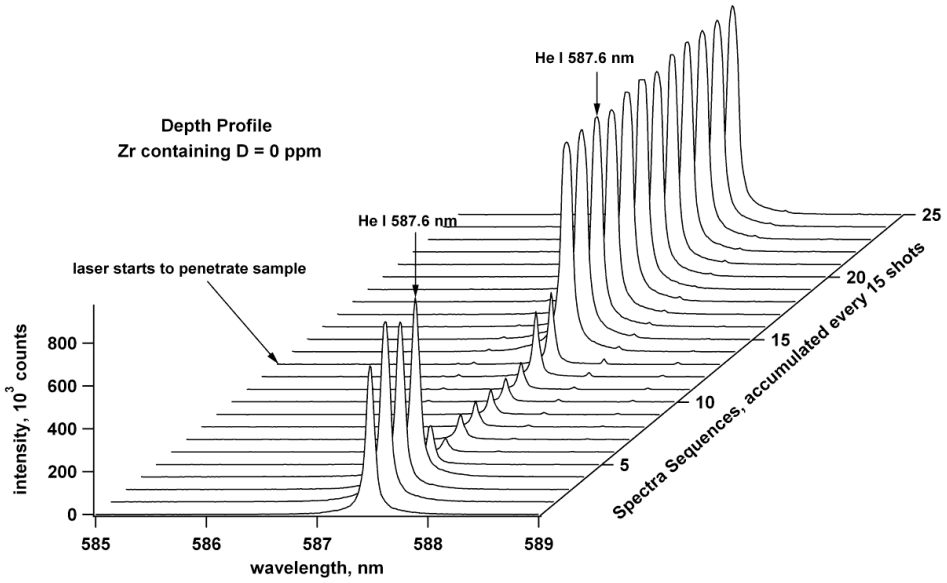

(a)

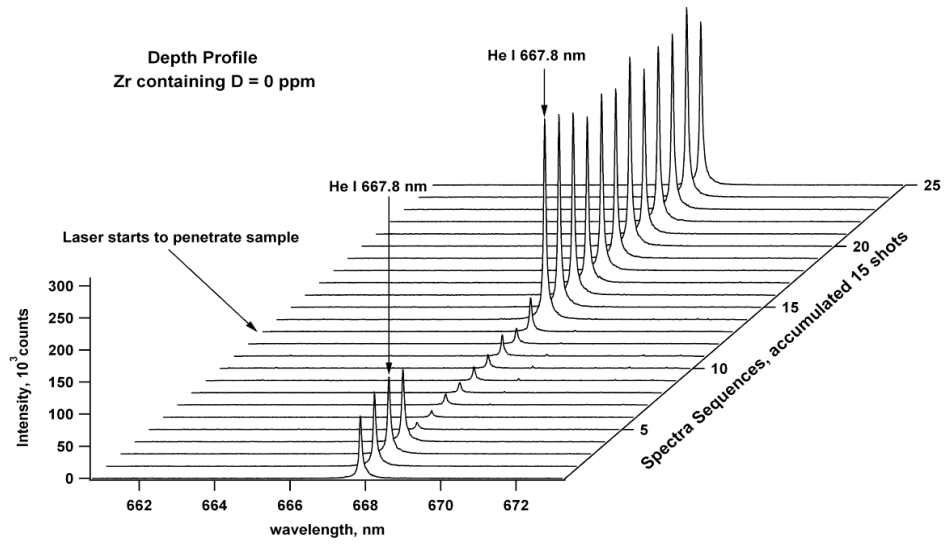

(b)

Fig.4.15. the spectra sequence of He-587.6 nm (a) and He-667.8nm (b) in zircaloy free D in condition synchronize laser -1 μs.

During looking for the best condition to make deuterium analysis, we also tried to understand the mechanism of the excitation of deuterium atom under the conditions when ps laser come earlier or later than ns laser. Figure 4.16 shows the spectra sequences of H emission in zircaloy containing 1700 μg/g of D in synchronized operation system with -1 μs delay (a), -3 μs delay (b) and + 3 μs delay (c). In the best condition as shown in Fig. 4.16(a),

D emission is clearly seen without disturbance of H emission. After laser penetration, H emission increased again because of no ablated atoms which swept out the H_2O molecules in that region. The occurrence of laser light penetration is evident by the absence of Zr and D emission. Figure 4.16(b) shows that the D emission is weaker and H emission stronger than that in Fig. 4.16(a). In Fig 4.16(b), D emission becomes weak because D atoms have already moved out from the ns laser focusing region due to the diffusion process and most of the laser energy which is used for the formation of He plasma. Opposite with D case, the H_2O molecules which were swept out from the area by the ablated atoms were came back to the ns laser focusing region due to the time difference between ps laser and ns laser which cause the H emission become strong. In Fig. 4.16(c), H emission intensity is almost the same as the H emission in the initial, while D emission does not appear. This is because H_2O molecules have already dissociated by the ns laser. The occurrence of no D emission can be interpreted by assuming that due to the high temperature of the hot plasma, D atoms which come from the sample cannot enter to the gas plasma; namely, D atoms which has light mass are repelled by pressure from the hot plasma.

To further endorse our assumption that the ablated atoms swept out the H_2O molecules from the ns laser focusing point region, we intentionally reduced the energy of ps-laser to 12 mJ for ablating the target under the same delay time of – 1 μs. Zircaloy sample containing 700 μg/g of D was used as the sample. Figure 4.17(a) shows that the previous result is exactly reproduced from this sample, displaying the sharp D emission line without the perceptible appearance of the H emission line when the same ablation energy of 26 mJ was used. On the other hand, when the ablation laser energy was reduced to 12 mJ, strong H emission is clearly observable and D emission decreases as compared to that of Fig. 4.17(b). It means that the energy of ablated atom for laser energy of 12 mJ does not enough strong to sweep out the H_2O molecules from the ns focusing point region.

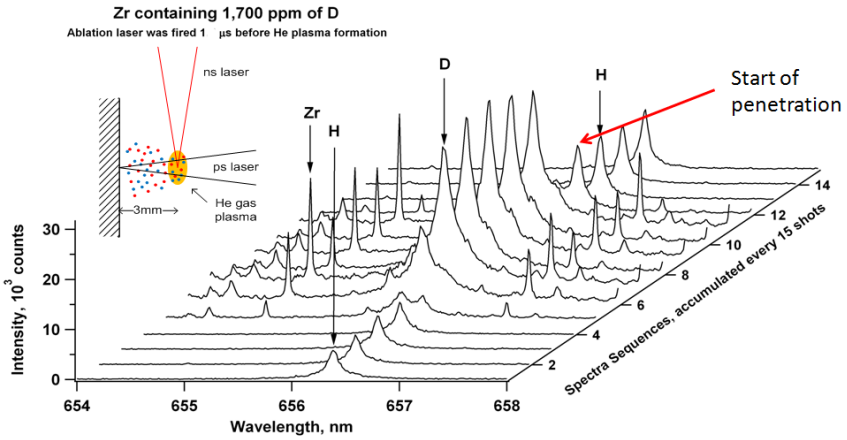

(a)

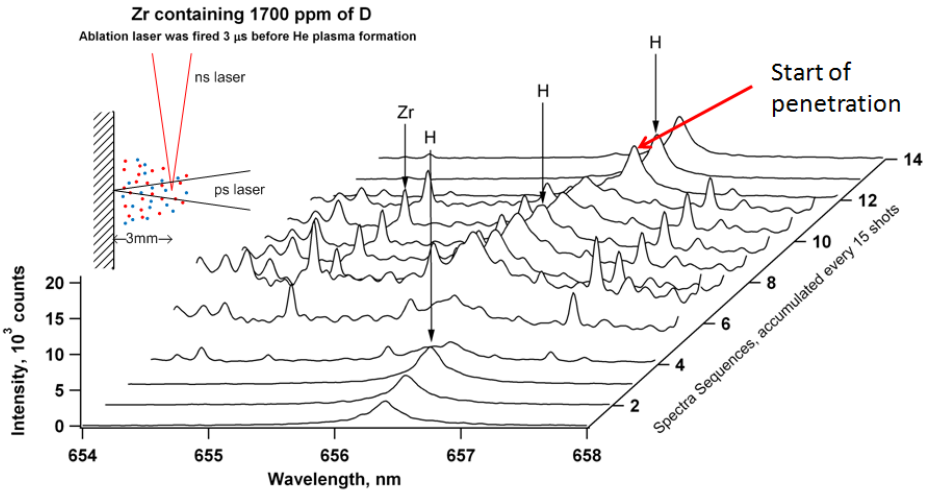

(b)

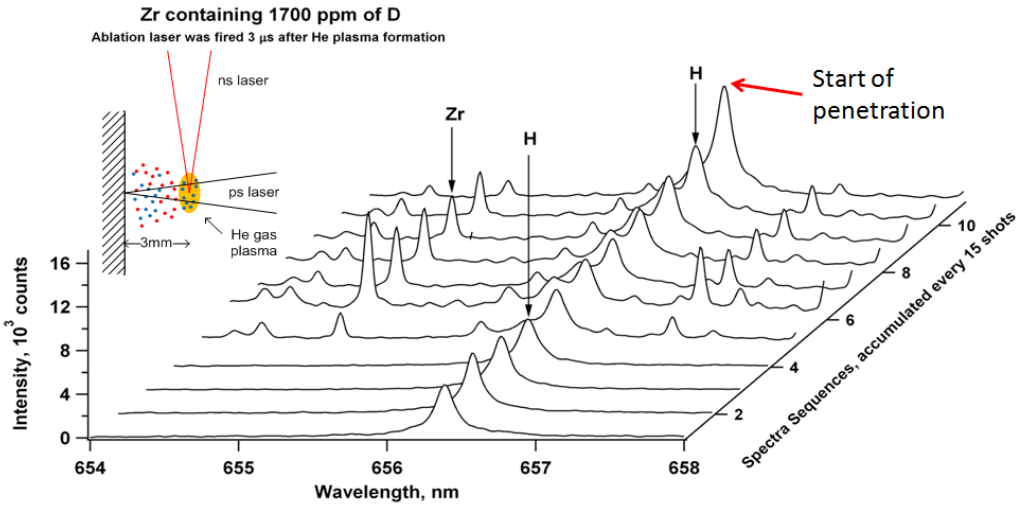

(c)

Fig.4.16. Spectra Sequences of a zircaloy plate containing 1700 μg/g of D impurity measured for synchronized time (τ) of -1 μs (a), -3 μs (b) and + 3 μs (c) with 26 mJ ablation laser energy.

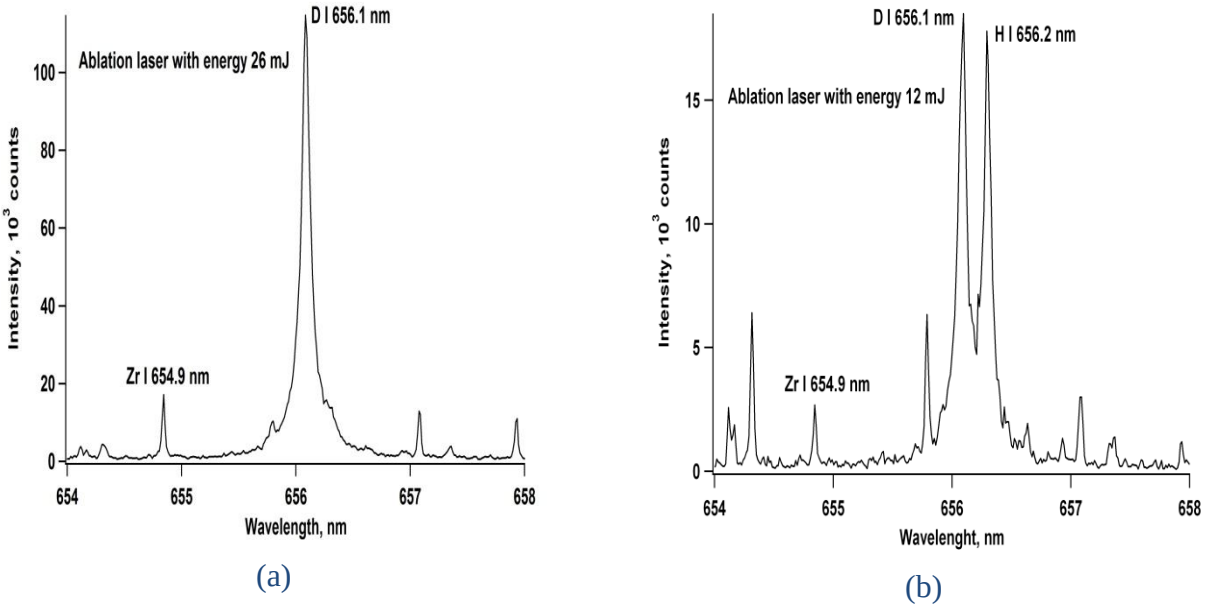

Figure 4.17. Emission spectra of a zircaloy plate containing 700 μg/g of D impurity obtained at different laser ablation energies ((a) 26 mJ, as in the previous case, and (b) 12 mJ, both measured with the same time difference ($\tau = -1$ μs)).

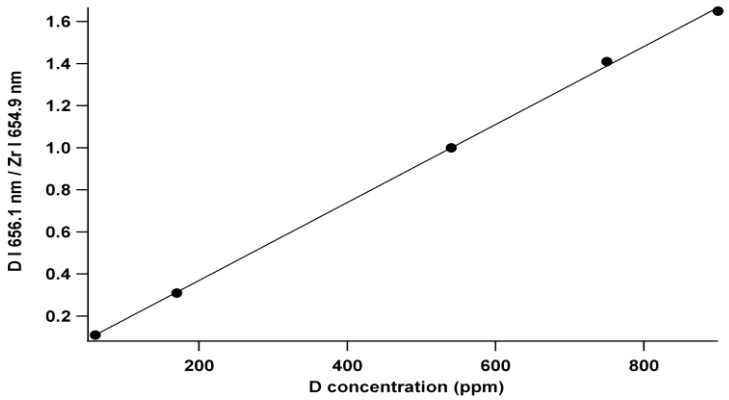

Fig.4.18. Relationship between the ratio of D I 656.1 nm / Zr I 654.9 nm and the D impurity concentration in zircaloy sample.

Finally, employing the favorable condition ascertained from the experimental results described above, a series of subsequent measurements were carried out on a number of zircaloy-4 samples prepared with different concentrations of doped deuterium 60, 170, 540, 700 and 900 μg/g. The associated calibration curve is presented in Fig. 4.18. Each data point in the Fig. 4.18 is the average of 5 data produced by 50 successive laser shots on the same sample spot. These measurements were found to be highly reproducible, implying the uniformity of the impurity D distribution in the sample. It is seen that the D impurity concentration and its associated emission intensity exhibit a clearly linear relationship with a practically zero intercept. For the estimation of the limit of detection, the emission spectrum

of a zircaloy-4 sample containing 540 µg/g of D was used as shown in Fig.4.19. The limit of detection was estimated following the conventional criteria as a ratio of the signal against three times the noise level. The limit of detection (LOD) was found to be less than 20µg/g. This value is more than enough to inspect the H concentration in zircaloy sample to keep safety of the zircaloy pipes which contain uranium fuel. Taken together the results described above have thus demonstrated the potential application of this technique for useful regular quantitative D analysis of zircaloy vessel used in heavy water nuclear power plant. Preliminary application of this new technique to non metal sample was also done. In this case, a concrete sample containing 1 % of D was made and we confirmed that D analysis can be done.

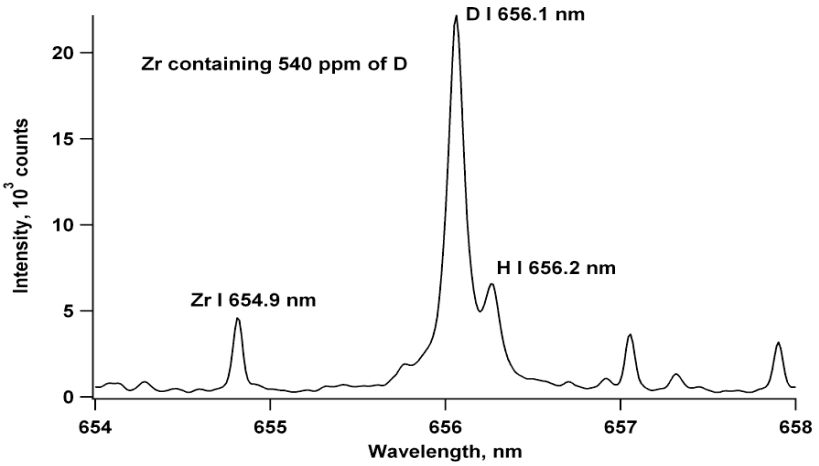

Fig.4.19. The emission spectrum of a zircaoy-4 sample containing 540 µg/g of D

4.2.4 Conclusion

Till now, D analysis with a capability of non-destructive, *in-situ*, micro area analysis and depth profiles analysis is a very difficult issue. However, in this study, we found an exquisite method using unique characteristic of fundamental Nd:YAG laser-induced He gas plasma which can produce a lot of He metastable-excited atoms. By combining with picoseconds laser ablation with suitable energy and with suitable laser synchronize operation timing; we have realized a very sensitive D analysis. We also demonstrated the ability to detect D in zircaloy used in heavy water nuclear power plant with enough sensitivity. Also during this research, we found a good technique to suppress the disturbance from H emission arising from the water molecules which is up to date being a serious obstacle for H analysis. It should be stressed that this D analysis was conducted in ordinary chamber without being heated and under the atmospheric pressure with He flowing of 3l/min. This technique

guarantees an *in-situ* D analysis by just flowing the gas directly onto the sample surface. Further improvement in plasma light collection, OMA sensitivity (suppression of OMA noise), a detection of D at 1 μg/g level can be obtained. In such case a new applied to geological sample can be performed. It is naturally expected that H in rock will change to D by receiving neutron irradiation under deep ground. By measuring the D/H ratio, the age of the geological sample can be estimated.

References

1. K.H. Kurniawan, T.J. Lie, N. Idris, T. Kobayashi, T. Maruyama, H. Suyanto, K. Kagawa, M.O. Tjia, Hydrogen emission by Nd_YAG laser-induced shock wave plasma and its application to the quantitative analysis of zircaloy, J. Appl. Phys. **96** (2004) 1301-1309.
2. K.H. Kurniawan, T.J. Lie, N. Idris, T. Kobayashi, T. Maruyama, H. Suyanto, K. Kagawa, M.O. Tjia, A.N. Chumakov, Hydrogen analysis of zircaloy tube used in nuclear power station using laser plasma technique, J. Appl. Phys. **96** (2004) 6859-6862.
3. K.H. Kurniawan, K. Kagawa, Hydrogen and deuterium analysis using laser-induced plasma spectroscopy, Appl. Spectrosc. Rev. **41** (2006) 99-130.
4. M. Pardede, K.H. Kurniawan, T.J. Lie, R. Hedwig, N. Idris, T. Kobayashi, T. Maruyama, Y.I. Lee, K. Kagawa, M.O. Tjia, Hydrogen analysis in solid samples using laser-induced helium plasma at atmospheric pressure, J. Appl. Phys. **98** (2005) 043105 1-5.
5. S.N. Abdulmadjid, M.M. Suliyanti, K.H. Kurniawan, T.J. Lie, M. Pardede, R. Hedwig, K. Kagawa, M.O. Tjia, An improved approach for hydrogen analysis in metal samples using single laser-induced gas plasma and target plasma at helium atmospheric pressure, Appl. Phys. B. **82** (2006) 161-166.
6. K.H. Kurniawan, T.J. Lie, M.M. Suliyanti, R. Hedwig, S.N. Abdulmadjid, M. Pardede, N. Idris, T. Kobayashi, Y. Kusumoto, K. Kagawa, M.O. Tjia, Detection of deuterium and hydrogen using laser-induced helium gas plasma at atmospheric pressure, J. Appl. Phys. **98** (2005) 093302 1-3.
7. M. Ramli, K. Kagawa, S.N. Abdulmadjid, N. Idris, W.S. Budi, M.A. Marpaung, K.H. Kurniawan, T.J. Lie, M.M. Suliyanti, R. Hedwig, M. Pardede, Z.S. Lie, M.O. Tjia, Some notes on the role of meta-stable excited state of helium atom in laser-induced helium gas breakdown spectroscopy, Appl. Phys. B. **86** (2007) 729-734.
8. M. Ramli, N. Idris, K. Fukumoto, H. Niki, F. Sakan, T. Maruyama, K.H. Kurniawan, T.J. Lie, K. Kagawa, Hydrogen analysis in solid samples by utilizing He metastable atoms induced by TEA CO_2 laser plasma in He gas at 1 atm, Spectrochim. Acta B. **62** (2007) 1379-1389.
9. M. Pardede, R. Hedwig, M.M. Suliyanti, Z.S. Lie, T.J. Lie, D.P. Kurniawan, K.H. Kurniawan, M. Ramli, K. Fukumoto, H. Niki, S.N. Abdulmadjid, N. Idris, T. Maruyama, K. Kagawa, M.O. Tjia, Comparative study of laser-induced plasma emission of hydrogen from zircaloy-2 samples in atmospheric and low pressure ambient helium gas, Appl. Phys. B. **89** (2007) 291-298.

10. M. Ramli, K. Fukumoto, H. Niki, S.N. Abdulmadjid, N. Idris, T. Maruyama, K. Kagawa, M.O. Tjia, M. Pardede, K.H. Kurniawan, R. Hedwig, Z.S. Lie, T.J. Lie, D.P. Kurniawan, Quantitative hydrogen analysis of zircaloy-4 in laser-induced breakdown spectroscopy with ambient helium gas, Appl. Opt. **46** (2007) 8298-8304.
11. K.H. Kurniawan, T.J. Lie, M.M. Suliyanti, M. Pardede, S.N. Abdulmadjid, K. Kagawa, M.O. Tjia, Quenching of He-induced intensity enhancement effect in H and D emission produced by Nd-doped yttrium aluminum garnet laser irradiation on solid targets in low pressure helium gas, J. Appl. Phys. **105** (2009) 013301 1-7.
12. K.H. Kurniawan, T.J. Lie, M.M. Suliyanti, R. Hedwig, M. Pardede, M. Ramli, H. Niki, S.N. Abdulmadjid, N. Idris, K. Lahna, Y. Kusumoto, K. Kagawa, M.O. Tjia, The role of He in enhancing the intensity and lifetime of H and D emissions from laser-induced atmospheric-pressure plasma, J. Appl. Phys. **105** (2009) 103303 1-6.
13. Z.S. Lie, M. Pardede, R. Hedwig, M.M. Suliyanti, E. Steven, Maliki, K.H. Kurniawan, M. Ramli, S.N. Abdulmadjid, N. Idris, K. Lahna, K. Kagawa, M.O. Tjia, Intensity distributions of enhanced H emission from laser-induced low-pressure He plasma and a suggested He-assisted excitation mechanism, J. Appl. Phys. **106** (2009) 043303 1-6.
14. F. Colao, V. Lazic, R. Fantoni, S. Pershin, A comparison of single and double pulse laser-induced breakdown spectroscopy of aluminum samples, Spectrochim. Acta B. **57**, (2002) 1167-1179.
15. M. Corsi, G. Christoforetti, M. Giuffrida, M. Hidalgo, S. Legnaioli, V. Palleschi, A. Salvetti, E. Tognoni, C. Vallebona, Three-dimensional analysis of laser induced plasmas in single and double pulse configuration, Spectrochim. Acta B. **59** (2004) 723-735.
16. J.L. Gottfried, F.C.D. Lucia, C.A. Munson, A.W. Miziolek, Double-pulse standoff laser-induced breakdown spectroscopy for versatile hazardous materials detection, Spectrochim. Acta B. **62** (2007) 1405-1411.
17. C.S. Ake, M. Bolanos, C.Z. Ramirez, Emission enhancement using two orthogonal targets in double pulse laser-induced breakdown spectroscopy, Spectrochim. Acta B. **64** (2009) 857-862.
18. M.V. Belkov, V.S. Burakov, A.D. Giacomo, V.V. Kiris, S.N. Raikov, N.V. Tarasenko, Comparison of two laser-induced breakdown spectroscopy techniques for total carbon measurement in soils, Spectrochim. Acta B. **64** (2009) 899-904.
19. G. Cristoforetti, S. Legnaioli, L. Pardini, V. Palleschi, A. Salvetti, E. Tognoni, Spectroscopic and shadowgraphic analysis of laser induced plasmas in the orthogonal double pulse pre-ablation configuration, Spectrochim. Acta B. **61** (2006) 340-350.
20. D.A. Cremers, L.J. Radziemski, T.R. Loree, Spectrochemical analysis of liquids using the laser spark, Appl. Spectrosc. **38** (1984) 721-729.
21. A. Miziolek, V. Palleschi, I. Schechrer (Eds), Laser-Induced Breakdown Spectroscopy, Cambridge University Press, Cambridge, 2006.
22. L.St-Onge, V. Detalle, M. Sabsabi, Enhanced laser-induced breakdown spectroscopy using the combination of fourth-harmonic and fundamental Nd:YAG laser pulses, Spectrochim. Acta B. **57** (2002) 121-135.
23. D.N. Stratis, K.L. Eland, S.M. Angel, Effect of pulse delay time on a pre-ablation dual-pulse LIBS plasma, Appl. Spectrosc. **55** (2001) 1297-1303.

24. N. Idris, K. H. Kurniawan, T. J. Lie, T. Kobayashi, M. Pardede, H. Syyanto, R. Hedwig, K. Kagawa, and T. Maruyama, Characteristic of Hydrogen Emission in Laser Plasma Induced by Focusing Fundamental Q-switched YAG Laser on Solid Sample, Jpn J. Appl. Phys. **42** (2003) 4221-4228
25. Freidberg, J. P, Kadak, A. C, Fusion-fission hybrids revisited. Nat. Phys. 5 (2009), 370−372
26. F. Brech and L. Cross, Optical Microemission Stimulated By a Ruby Laser, Appl. Spectroscopy, **16,** (1962), 59
27. T.R.Loree and L.J. Radziemski, Laser- Induced Breakdown Spectroscopy: Time Integrated Applications, Plasma Chem. Plasma Process, **1**, (1981) p.271-280
28. Kurniawan. K. H, Lie. T. J, Suliyanti, M. M, Hedwig R,Pardede. M, Kurniawan, D. P, Kusumoto. Y, Kagawa, K. Quantitative Analysis of Deuterium Using Laser-Induced Plasma at Low Pressure of Helium**,** Anal. Chem.**78 (**2006), 5768−5773.
29. Lie. Z. S, Khumaeni. A, Kurihara. A, Kurniawan. K. H, Lee. Y.I, Fukumoto. K, Kagawa. K, Niki. H. Excitation Mechanism of H, He, C, and F Atoms in Metal-Assisted Atmospheric Helium Gas Plasma Induced by Transversely Excited Atmospheric - Pressure CO_2 Laser Bombardment, Jpn. J. Appl. Phys., **50** (2011) 122701 1-7.
30. R. Hedwig, Z.S. Lie, K.H. Kurniawan, A.N. Chumakov, K. Kagawa, M.O. Tjia, Toward Quantitative Deuterium Analysis with Laser-Induced Breakdown Spectroscopy Using Atmospheric-Pressure Helium Gas, J. Appl. Phys. **107**, 2 (2010) pp. 023301 1-5.
31. Stratis D. N, Eland K. L, Angel S. M, Dual-pulse LIBS: why are two lasers better than one?, SPIE−Int. Soc. Opt. Eng. **3853** (1999), 385.
32. Stratis D. N, Eland. K. L, Angel S. M. Dual-Pulse LIBS Using a Pre-ablation Spark for Enhanced Ablation and Emission Appl. Spectrosc. **54** (2000) 1270−1274.
33. Stratis D. N, Eland K. L, Angel S. M. Enhancement of Aluminum, Titanium, and Iron in Glass Using Pre-ablation Spark Dual-Pulse LIBS, Appl. Spectrosc. **54** (2000) 1719-1726.
34. Angel S. M, Stratis D. N, Eland K. L, et al. Fresenius', LIBS using dual- and ultra-short pulses J. Anal. Chem. **369** (2001) 320-327.
35. Sattmann R, Sturm V, Noll, R. Laser-induced breakdown spectroscopy of steel samples using multiple Q-switch Nd:YAG laser pulses, J. Phys. D: Appl. Phys. **28** (1995) 2181-2187.
36. Gautier. C, Fichet. P, Menut. D, Lacour J. L, Hermite D. L, Dubessy. J, Quantification of the intensity enhancements for the double-pulse laser-induced breakdown spectroscopy in the orthogonal beam geometry, Spectrochim. Acta B **60** (2005) 265−276.
37. Cristoforetti. C, Legnaioli. S, Palleschi. V, Salvetti. A, Tognoni. E, nfluence of ambient gas pressure on laser-induced breakdown spectroscopy technique in the parallel double-pulse configuration, Spectrochim. Acta B **59** (2004) 1907−1917.
38. Sdorra. W, Niemax. K, Basic investigations for laser microanalysis: III. Application of different buffer gases for laser-produced sample plumes, Mikrochim. Acta **107** (1992) 319−327.

Chapter 5

Hydrogen Analysis using TEA CO_2 Laser-Induced He Gas Plasma at Atmospheric Pressure

5.1 Hydrogen Analysis in Metal Samples by Selective Detection Method Utilizing TEA CO_2 Laser–Induced He Gas Plasma

5.1.1 Introduction

Laser-induced breakdown spectroscopy (LIBS) has become a popular analytical technique for the rapid quantitative analysis of elements in many kinds of samples, including metals. The appealing advantages of LIBS are no need of sample preparation, the possibility of in-situ analysis under 1 atm, and the capability of micro-area analysis [1]. However, this technique cannot be applied to analysis of hydrogen (H) due to the undesirable effects of line broadening and the "mismatching effect", which generally occurs for light elements in the shock wave generation stage [2]. On the other hand, we have demonstrated that H analysis in a zircaloy sample can successfully be made when we use a low-pressure-plasma method [3, 4]. The weakness of this low-pressure-plasma technique is the inability to perform an *in-situ* analysis. In order to overcome this problem, we have proposed a new technique, in which metastable He atoms produced in helium gas plasma work as an excitation source [5, 6]. However, a highly sensitive and reliable analysis of H cannot be realized via that method because of the disturbance of host emission lines, such as Zr line of 656.9 nm in the case of

Zr metal samples, located near the emission line of H I 656.2 nm (H_α) and the disturbance of ubiquitous water molecules (H_2O) deposited on the sample surface and also populated in the surrounding gas.

The analysis of hydrogen is essentially required for studies related to the application technology of hydrogen fuel cell and nuclear power station [2]. In light water nuclear power stations, a zircaloy tube is used as a vessel of uranium fuel. During the operation, hydrogen from hot water accumulates in the zircaloy tube, which causes unacceptable structural damage and seriously reduces the strength of the material. Therefore, the inspection of hydrogen in zircaloy tubes must be carried out periodically. A commercial method for detecting hydrogen in such a case generally uses a gas detector by means of melting a portion of the zircaloy tube in a carbon furnace. This method is time consuming and is not an *in-situ* analysis.

In this study, we present a novel and sophisticated method on hydrogen analysis in metal samples by utilizing the specific characteristics of a pulsed CO_2 laser (TEA CO_2 laser).

5.1.2 Experimental Procedures

In this experiment, the TEA CO_2 laser (energy of 1.5 J, pulse duration of 200 ns, and beam cross section of 20 mm x 20 mm) was focused directly on the sample surface placed in a cylindrical metal chamber. The spot size on the sample surface was 2 mm x 2 mm when we focused the TEA CO_2 laser beam using a ZnSe lens with a focal length of 200 mm. Prior to the analysis, the chamber was evacuated using a vacuum pump at a pressure of around 3 Pa and heated up to 150^o C, and held for 30 minute to remove H_2O attached on the chamber wall and the sample surface. High-purity helium gas (99.9999 %) was introduced with the gas flow rate of 4 liter per minute (Lpm) into the chamber, and finally the gas pressure was kept constant at 1.04 x 10^5 Pa during the experiment. It should be mentioned that the helium gas used in this experiment had not included H_2O because no H emission could be detected when we induced He gas plasma by focusing the Nd:YAG laser (140 mJ) just at the exit of the metal tube from which helium gas flowed into the metal chamber and that was filled with helium gas at 1 atm.

The plasma emission was collected by an optical fiber, which was set at 50 mm from the helium gas plasma, and the other end of the optical fiber was connected to an optical multi-channel analyzer (OMA) system (ATAGO Macs-320) which has a spectral resolution of 0.2 nm, and another OMA system with high resolution of 0.02 nm was also used. The gate

delay and gate width of the OMA system was set at 10 μs and 100 μs, respectively. Before data acquisition, the laser pre-irradiation was also made to remove the H_2O attached on the sample surface. The samples used in this experiment were pure zircaloy-4, zircaloy-4 doped with deuterium (D) of 2050 μg/g, and zircaloy-2 samples doped with various concentrations of hydrogen (0, 100, 200, 400, and 600 μg/g).

5.1.3 Experimental Results and Discussion

As reported in our previous research [6, 7], when a TEA CO_2 laser was focused on a metal sample surface in He surrounding gas at 1 atm, a large and strong helium gas breakdown plasma was induced without ablating the sample. However, we found in this research that by conscientiously performing the experiment, in which we suppress the amount of the ubiquitous water molecules (H_2O) deposited on the sample surface and also populated in the surrounding gas, the H_α emission is still clearly detected from the zircaloy sample containing several hundreds μg/g of H. Namely, this result indicates that zircaloy sample is faintly melted and only H atoms come out from the sample surface and subsequently move into the helium gas plasma to be excited through He metastable atoms, as illustrated in Fig.5.1. The excellent orange color of the plasma shown in Fig.5.1 is mostly due to the emission of He I 587.5 nm. The plasma features the typical hemispherical shape with a radius of approximately 10 mm for laser energy of 1.5 J. It should be mentioned that when we use Nd:YAG laser, which is commonly employed in conventional LIBS method, such a phenomenon never occurs because all elements, including host elements and impurities, are simultaneously ablated from the metal sample.

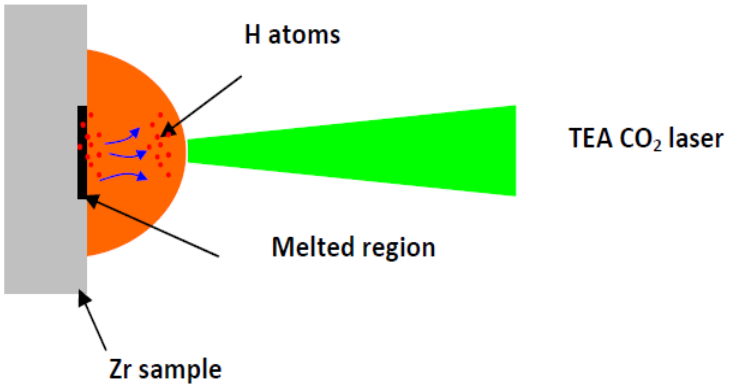

Fig. 5.1 Illustration of the principle on the selective hydrogen analysis method in zircaloy sample by utilizing a TEA CO2 laser in He gas at 1 atm

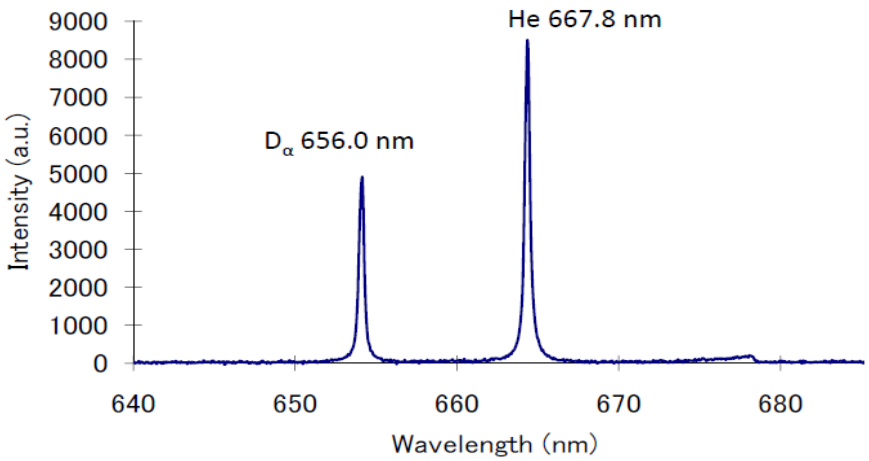

Fig. 5.2 Emission spectrum of D_α taken from zircaloy-4 sample containing 2050 μg/g of D when a TEA CO_2 laser was focused on the sample in He gas at 1 atm

In order to confirm that H emission really came from hydrogen in the sample, we intentionally used the sample which contains D in place of H. Figure 5.2 shows the emission spectrum taken from the zircaloy-4 sample containing 2050 μg/g of D. It can be clearly seen that only D_α 656.0 nm and He I 667.8 nm emission lines appear clearly, and no other lines are detected. Also, the emission lines are very sharp and narrow. It is noticed that the signal-to-noise ratio (S/N) in the emission spectra is considerably high and the detection limit is estimated to be around 30 μg/g. However, the spectrum resolution of the OMA used in this experiment is not enough to distinguish between H_α and D_α (wavelength shift only 0.179 nm). Therefore, we used another OMA with higher resolution (0.02 nm). Figure 5.3 shows the spectrum taken from the same sample used in Fig. 5.2 in the wavelength region of around 486 nm, where emission spectrum of H_β and D_β appears; the reason why we used the wavelength region of H_β and D_β is that the OMA could not work in that wavelength region of H_α and D_α. In Fig. 5.3, we confirmed that the emission mostly comes from deuterium inside the sample because D_β is predominant in the emission spectrum. The weak H_β emission is probably due to the hydrogen from H_2O existing in the surrounding gas and on the sample surface.

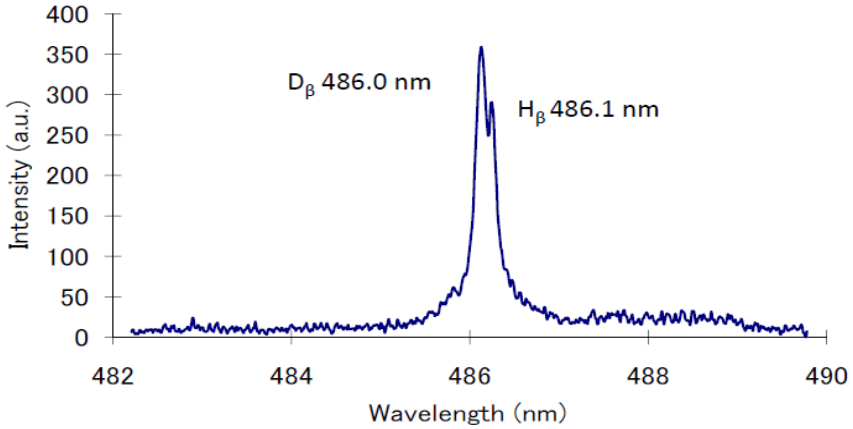

Fig. 5.3 Emission spectrum of D_β taken from zircaloy-4 sample containing 2050 μg/g of D when a TEA CO_2 laser was focused on the sample in He gas at 1 atm

It should be mentioned that in an ordinary experiment, H_α emission faintly takes place even if we use a zircaloy sample containing 0 μg/g of H. This is due to the contribution of unwanted H_2O attached on the sample surface and populated in the ambient gas. In order to take into account such a problem for quantitative analysis, we can employ a compensation method using an emission line of O I 777.1 nm, which is also given by the H_2O. However, if oxygen (O) ablates from the inside of the sample, this compensation method cannot be used. Therefore, we confirmed using two samples, namely pure zirconium (99.999%) and zircaloy-2 containing 0.1 % of O. The result shows that the O emission intensity is the same, which indicates the fact that ablation of O from the sample never occurs. In order to determine the ratio between H and O which is contributed by the H_2O, we employed a zircaloy-2 sample containing 0 μg/g of H and varied intentionally the amount of H_2O in the chamber. As a result, it was proved that the intensity ratio of O and H is always constant, namely one-fourth in our OMA system.

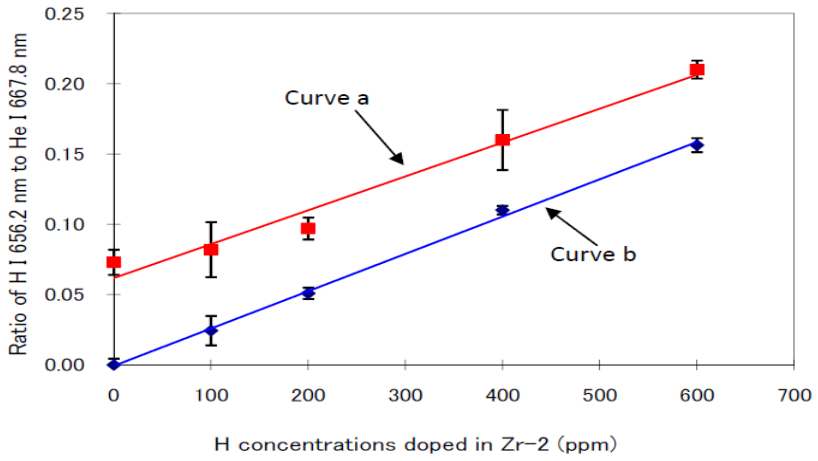

Fig. 5.4 Calibration curve taken from zircaloy-2 samples containing various concentrations of H (0, 100, 200, 400, and 600 μg/g) using selective detection method; (curve a) before and (curve b) after being compensated by emission intensity of O I 777.1 nm

Figure 5.4 curve "a" (red line) displays the calibration curve for H before being compensated by O obtained from the zircaloy-2 samples doped with various concentrations of hydrogen (0, 100, 200, 400, and 600 μg/g). A standardization method was employed using the emission intensity of He I 667.8 nm. Each of the data plotted in the calibration curve is the average of 4 spectra. The curve “a” (red line) shows a good linear relationship between hydrogen emission intensity and H concentration in zircaloy-2 samples. The non-zero intercept of the linear calibration curve is due to the fact that the H contributed by the H_2O in the sample surface or in the gas is also excited in the gas plasma. By using the compensation method described above, an excellent linear calibration curve with a zero y-axis (vertical axis) intercept was obtained as curve "b" (blue line) in Fig. 5.4. This curve indicated that this method can successfully be employed for quantitative analysis of H in metal samples.

It is well known that the presence of H in many kinds of materials such as metals and alloys causes a reduction in the strength of the materials [8-10]. Therefore, hydrogen analysis is very important in many fields. In the case of steel, hydrogen analysis in μg/g order is particularly required. It is naturally expected that the sensitivity of H analysis using this method can be highly increased when we employ a photomultiplier combined with an interference filter to pass H_α emission in place of the OMA system. Using this method, the S/N ratio is improved at least 10^3 over the OMA system case because the solid angle to collect H_α emission is significantly increased. Thus, the H analysis in μg/g order can be realized.

5.1.4 Conclusions

A novel technique for highly sensitive analysis of H on zircaloy metal samples has successfully been developed by utilizing specific characteristics of a TEA CO_2 laser. Namely, when the TEA CO_2 laser was focused on the zircaloy surface, a strong helium gas plasma was produced and only H atoms came out of the sample. The H atoms then moved into the helium gas plasma to be excited through metastable helium atoms. Using this selective detection technique, a nice linear calibration curve has successfully been made.

The present selective H analysis method will be widely used in many fields because of the potentially high sensitivity of the analysis. When the depth analysis of H is required, another UV laser should be irradiated alternately to dig the metal sample surface. It should be stressed that the present method is a very simple and elegant for highly sensitive analysis of H compared with other methods, such as mass spectrometry. We have also confirmed that H and D analysis, wherein the wavelength of D_α shifts 0.179 nm from H_α, can clearly be realized by this method using a high resolution OMA system. Also, it is assumed that analysis of tritium (^3H) might be carried out by this technique using a high resolution OMA system because the spectrum width is very narrow (less than 0.05 nm) and the sensitivity is very high. The narrow spectrum also proves our hypothesis that the H is really excited by metastable helium atoms.

5.2 Emission Characteristics of Hydrogen in Atmospheric Helium Gas Plasma Induced by TEA CO_2 Laser Bombardment on Zircaloy Sample Containing Hydrogen

5.2.1 Introduction

Hydrogen analysis in metals is essential, especially those used in nuclear power stations[2]. Thus, in light water nuclear power stations, a zircaloy tube is used to contain the uranium fuel. During operation, hot water reacts with the zircaloy surface to produce H_2 gas, which penetrates and accumulates in the zircaloy tube, thereby causing unacceptable structural damage and seriously reducing the strength of the material. The accumulation of hydrogen in zircaloy tubes must therefore be examined periodically. The standard technique for detecting hydrogen involves melting a portion of the zircaloy tube in a carbon furnace and measuring the gas emitted using a gas detector. However, this method is time-consuming, destructive, cannot be used in situ, and does not allow a mapping analysis to be performed.

Laser-induced breakdown spectroscopy (LIBS) has recently been shown to be a highly promising technique for rapid quantitative analysis [1, 11]. In this technique, a high-power pulsed Nd:YAG laser is commonly employed to induce a gas breakdown plasma at atmospheric pressure. The most interesting advantages of standard LIBS are the ability to perform in situ analysis and the lack of sample pretreatment. However, a highly sensitive and reliable analysis of hydrogen in zircaloy samples is very difficult with the standard LIBS technique due to interference from many host lines located near the hydrogen emission lines and the broadening of the hydrogen emission spectrum [12]. The so-called ‘‘mismatching effect’’ [2, 3] and interference from ubiquitous water molecules (H_2O) are also serious obstacles to H analysis using the standard LIBS technique.

In our previous paper [13], we reported a new technique for hydrogen analysis in zircaloy samples. Namely, a strong helium gas plasma was produced by focusing a transversely excited atmospheric (TEA) CO_2 laser (1.5 J, 200 ns) onto a hydrogen containing zircaloy sample in He surrounding gas at atmospheric pressure to ensure that only H atoms were produced by the sample. These H atoms then moved into the helium gas plasma region, where they were excited by metastable helium atoms. No host emission lines were produced by the sample as no ablation of host elements takes place. We call this method ‘‘selective detection of H’’. It should be noted that use of a Nd:YAG laser, which is commonly employed

in the standard LIBS method, was not possible as all elements, including host elements and impurities, are ablated from the metal sample simultaneously. Although this technique appeared to be very promising for the highly sensitive analysis of H due to the absence of host emission lines and the reduced spectral broadening in H emission, the suppression of H emission from H_2O remained difficult. Furthermore, the emission characteristics of H and its excitation mechanism are not completely understood.

In order to realize a highly sensitive analysis of H in a zircaloy sample, herein we report a novel technique to significantly suppress the H emission from H_2O. This technique allows us to clearly detect the H alpha (H_α), H beta (H_β), H gamma (H_γ), and H delta (H_δ) emission lines from the H-containing zircaloy sample because of no disturbance of host emission lines and no broadening in H emission. Based on these emission characteristics, which cannot be found in case of standard LIBS method, we will discuss on the excitation mechanism of H, which is crucial issue for H analysis in metal samples.

5.2.2 Experimental procedures

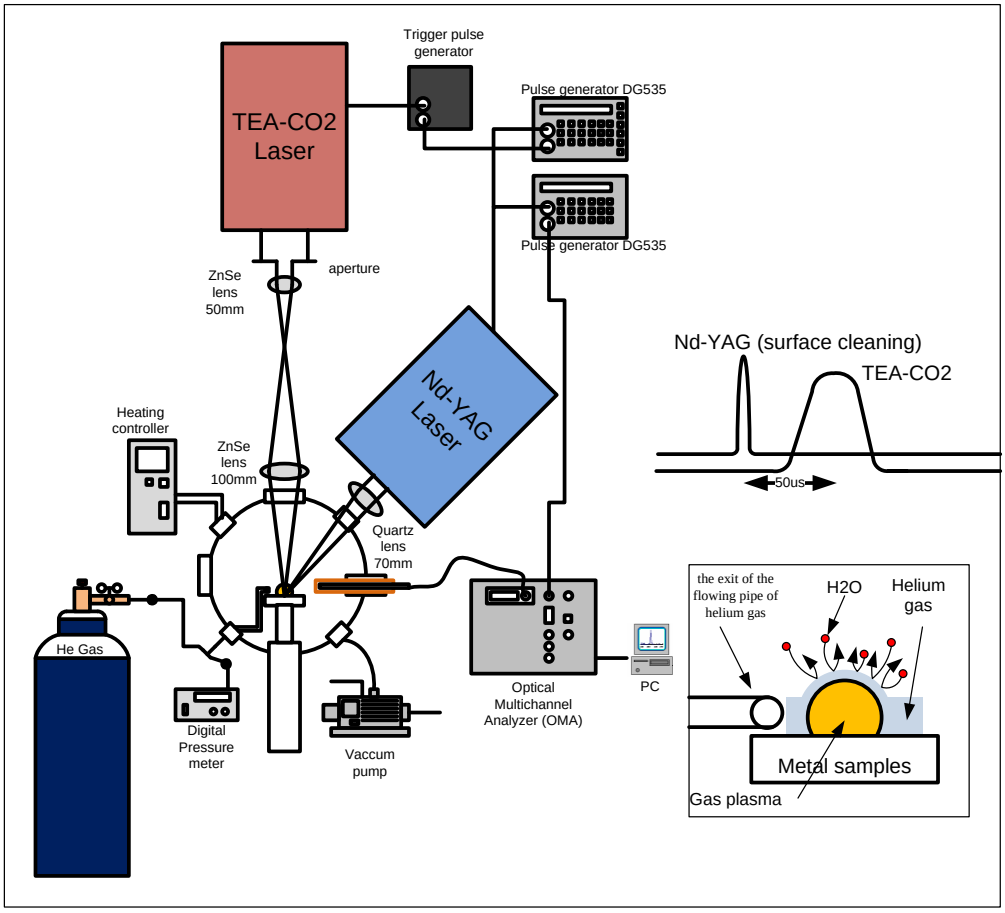

Fig. 5.5 The experimental arrangement used in this study. The Nd:YAG laser was only used during surface cleaning.

The experimental arrangement used in this study is shown in Fig. 5.5. A TEA CO_2 laser (Shibuya SQ–2000, pulse energy of 3 J, wavelength of 10.6 mm, pulse duration of 200 ns, and beam crosssection of 30 x 30 mm^2) was used as an irradiation source. During the experiment, the laser energy was set at 250 mJ by inserting an aperture in front of the focusing lens. The laser beam was focused on the sample surface from the front, through a ZnSe window, using two combinations of ZnSe lenses, one with a focal length of 50 mm and the other with a focal length of 100 mm. The spot size of the laser beam on the zircaloy surface was 0.5 x 0.5 mm^2 for tight focus, thus resulting in a power density of 0.7 GW/cm^2. The laser was operated at 10 Hz.

The samples to be irradiated were attached to a sample holder and placed in a metal chamber with an inner diameter of 115 mm. The chamber was equipped with several windows, a synchronized motor, and a heater. The chamber could be evacuated with a vacuum pump or filled with high-purity He gas (99.99999%). Two kinds of zircaloy sample, one containing hydrogen at 2600 µg/ g and the other free from hydrogen, were used in this experiment. The position of the sample to be irradiated by the TEA CO_2 laser can easily be changed by rotating the holder using a synchronized motor. This treatment was used to ensure that the experimental conditions for the 2600 µg/g sample were the same as those for the hydrogen-free sample. It should be mentioned that special attention was paid to eliminating H_2O deposited on the sample surface and the inner wall of the vacuum chamber, and that present in the surrounding gas, prior to the analysis. Thus, after placing the samples in the chamber, it was evacuated using a vacuum pump to a pressure of around 2 Pa. It should be noted that the oil in the vacuum pump should be new to avoid the presence of H_2O. The chamber was subsequently heated to 150 ºC for 60 min to remove the H_2O. During this process the metal pipes connecting the chamber to both the gas cylinder and the vacuum pump were also heated using a hair dryer to ensure that any H_2O molecules inside the metal pipes were completely removed. High-purity He gas was then introduced into the chamber at a flow rate of 4 L/ min and the pressure inside the chamber was kept constant at 0.11 MPa.

Depending on the experiment, a laser cleaning method was also employed to remove the H emission due to H_2O. In this case, a Q-switched Nd:YAG laser (Systems Polaris III New Wave Research, pulse energy of 160 mJ, pulse duration of 8 ns) operating at its fundamental wavelength of 1064 nm with a repetition rate of 10 Hz was used; its energy was fixed at 40 mJ. The Nd: YAG laser, which is synchronized with the TEA CO_2 laser, irradiates the sample 50 ms earlier than the TEA CO_2 laser from an inclined direction of 45º through a

quartz window by setting a quartz lens with a focal length of 200 mm at a little defocus condition.

The characteristics of the hydrogen emission spectra were also studied using an ordinary low pressure hydrogen discharge lamp (Narika B10–7000, discharge tube length of 205 mm). In case of H emission induced by laser-induced shock wave plasma technique, a water molecular layer (H_2O) deposited on a copper plate was used as the sample. To this end, a copper plate with a dimension of 20 x 20 x 0.1 mm^3 was exposed beforehand to the atmosphere in a room, so that the molecular layer attaches on the copper plate. The plate was then placed into the metal chamber, which was set at low pressure using a vacuum pump to a pressure of 100 Pa. During experiment, nitrogen gas was flowed into the chamber at a flowing rate of 4 L/min. In this experiment, intentionally we did not heat the chamber. The pulse energy of TEA CO_2 laser was set at 1.5 J and the laser light was focused on the sample surface using a lens with a focal length of 200 mm and the sample was slowly rotated with a rotation of 2 rotations per minute (Rpm).

The emission spectrum of the plasma was obtained by detecting laser plasma radiation using an optical multi channel analyzer (OMA) system (ATAGO Macs-320) consisting of a 0.32 m focal-length spectrograph with a grating of 1200 grooves/mm, a 1024-channel photodiode detector array, and a micro-channel plate image intensifier. The spectral resolution of this OMA system is 0.2 nm and the spectral width display is 60 nm. The light emitted from the laser plasma was collected by an optical fiber (27º in solid angle) inserted inside a quartz tube and fed into the OMA system. One end of the fiber was placed at a distance of 3 cm from the focusing point of the TEA CO_2 laser and set perpendicular to the path of the laser beam.

5.2.3 Experimental results and discussion

In our previous work [13], we reported a selective detection technique for H analysis in zircaloy sample. This method has significant potential for the sensitive analysis of H in metal samples as it is not affected by host emission lines, which appear near the H emission line when the ordinary LIBS technique is used.

In this previous experiment, a TEA CO_2 laser (1.5 J, 200 ns) was focused on a zircaloy sample surface in He surrounding gas at 1 atm. This resulted in induction of a large and strong helium gas breakdown plasma when the laser beam impinged on the sample surface without ablating the sample. We concluded that the zircaloy sample was melted to

such a small extent that only H atoms were released from the sample surface. These H atomssubsequently moved into the helium gas plasma region, where they were excited by metastable He atoms. The calibration curve for H obtained from zircaloy samples containing different concentrations of H showed good linearity. However, the line of this calibration curve did not pass through zero as the H emission line still appeared even when the zircaloy sample containing free hydrogen was used as a sample. We noted that the most difficult aspect of H analysis is disturbance of the H emission due to H_2O deposited on the sample surface and present in the surrounding gas.

In order to overcome this serious problem, herein we offer a novel solution in which a small-sized He gas plasma is produced intentionally. Thus, the small helium gas plasma (diameter of around 5 mm) was covered with high-purity helium surrounding gas, as shown in the inset of Fig. 5.5. The gas plasma was produced on the zircaloy sample surface by irradiating with a TEA CO_2 laser with energy of 250 mJ. During the laser bombardment, helium gas was passed over the surface through a metal pipe at a flow rate of 4 L/min. The exit of the pipe was located close to the focusing point of the gas plasma (at a distance of 3 mm). The pressure of He gas close to the exit of the pipe was set to be higher than that of the surrounding gas in the chamber (0.11 MPa) to ensure that H_2O from the surrounding gas could not enter the gas plasma region.

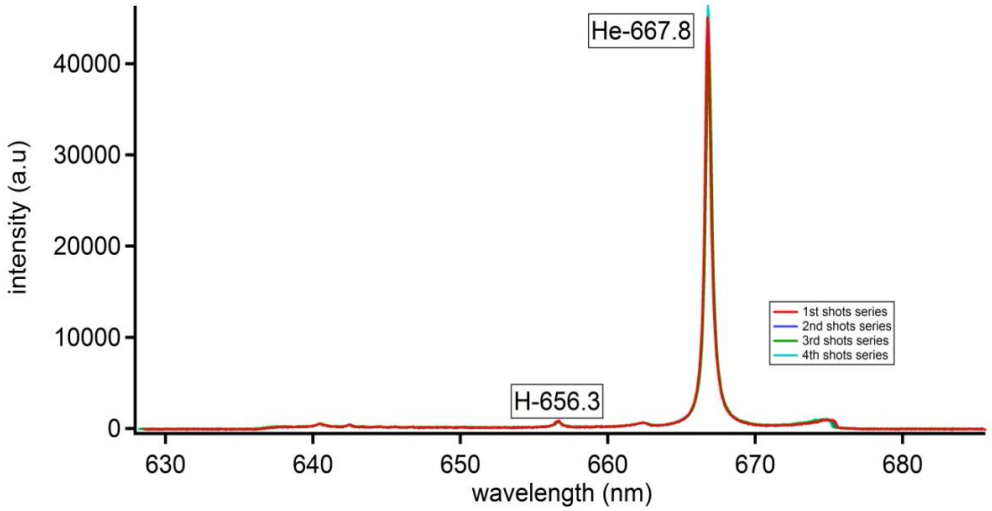

Fig. 5.6. A series of emission spectra taken from the zircaloy sample containing 0 µg/g of H after irradiation with a TEA CO2 laser at a fixed position. Each spectrum was taken after 10 laser shots.

Fig. 5.6 shows a series of emission spectra taken from the zircaloy sample containing 0 µg/g of H obtained using the present technique. Each spectrum was taken under 1 s of TEA

CO_2 laser irradiation, in other words 10 laser shots, and spectral acquisition was repeated four times at the same sample position. The gate delay time and gate width of the OMA system were set 2 μs and 2 μs respectively. It should be noted that the emission lines of H and He are very stable regardless of the number of laser irradiation shots, thus confirming the good reproducibility of the He gas plasma production. It should also be noted that no emission lines other than those for H and He appears, thus supporting our assumption that no ablation takes place upon irradiation of the metal surface with the TEA CO_2 laser. It can also be seen that the ratio between the H emission intensity at 656.3 nm and the He emission at 667.8 nm is much lower than that obtained using our previous technique [13] (0.02 vs. 0.07). This result indicates that the present technique can effectively be used to suppress H emission arising from H_2O. We assume that the small H emission line in Fig. 5.6 is due to H_2O molecules deposited on the sample surface in the time period between the TEA CO_2 laser pulses (100 ms). During this period, H_2O molecules from the surrounding gas can attack and be deposited on the sample surface, therefore the H emission line always appears even when the zircaloy sample containing 0 μg/g of H is used.

Fig. 5.7 shows a series of emission spectra taken from the zircaloy sample containing 2600 μg/g of H. Each spectrum was taken after the first 10-shot accumulation of laser irradiation. It can be seen from spectrum A that the H emission line at 656.3 nm (H_α) clearly appears with a very high intensity and has a narrow spectral width. In the second spectrum (spectrum B), taken with shots 11 to 20, the H emission intensity is only around half of that in spectrum A, whereas the He emission remains almost constant. It can also be seen that after 20 irradiation shots the intensity of the H emission line continues to decrease with an increasing number of laser shots. This reduction in H emission intensity can be explained by the fact that the sample surface is melted under the TEA CO_2 laser irradiation and the H atoms located near the surface are removed. The H emission intensity therefore decreases with the number of laser shots, thus confirming that the H emission comes from the zircaloy sample rather than from H_2O deposited on the metal surface or present in the surrounding gas—if the H emission were due to H_2O, it would not decrease. In our previous paper [13] we used a zircaloy sample containing deuterium in order to distinguish the hydrogen emission coming from the sample and that from H_2O. The result shown in Fig. 5.7 can also be used to confirm the principle underlying this novel ‘‘selective detection method of H’’ technique.

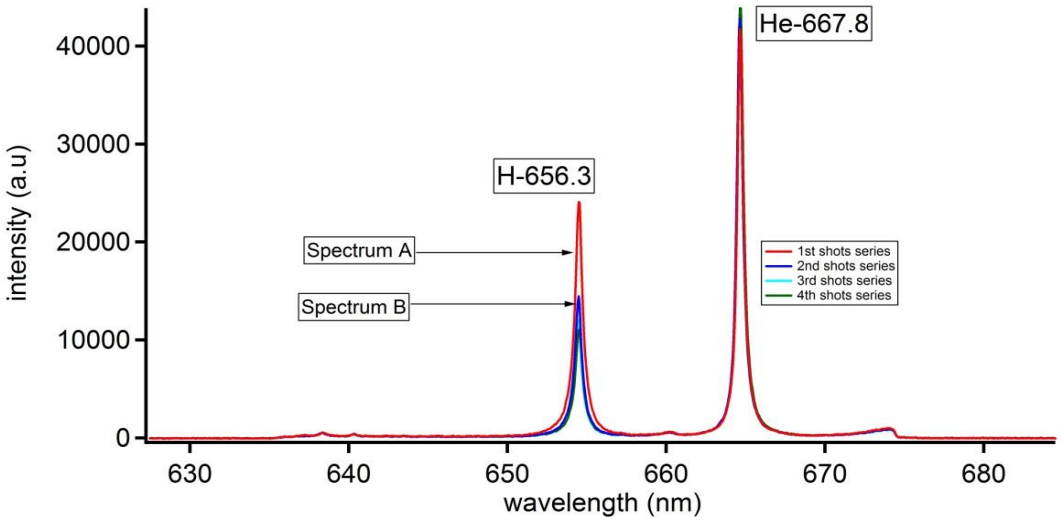

Fig. 5.7 A series of emission spectra taken from the zircaloy sample containing 2600 µg/g of H after irradiation with a TEA CO_2 laser at a fixed position. Each spectrum was taken after 10 laser shots. Spectrum A was taken after shots 1 to 10 and spectrum B after shots 11 to 20.

By comparing the H intensity obtained for the sample containing 2600 µg/ g of H with that for the 0 µg/ g sample, we estimated that the remaining H emission line in Fig. 5.6 (zircaloy sample containing 0 µg/ g of H) corresponds to approximately 65 µg/ g of H. Although we did not perform a calibration curve for H analysis in this study, the linearity between H concentration and the ratio between H and He has already been demonstrated in our previous work [13]. In our previous technique, it proved very difficult to suppress the H emission due to H_2O, therefore a rather strong H emission signal corresponding to 200 µg/ g appeared for the zircaloy sample containing 0 µg/ g of H. The new technique presented herein is therefore far superior to that described in our previous work. The analysis of zircaloy samples used in nuclear power stations requires the H analysis in the concentration-order of 200–300 µg/ g in order to check the degradation due to hydrogen accumulation, therefore the error of 65 µg/ g arising from H_2O interference is not particularly serious. However, this present technique is not suitable for H analysis in steel samples as this requires the concentration-order of only a few µg/ g.

We assume that the remaining H signal in Fig. 5.6 is due to the contribution of H_2O molecules, which attack, and are deposited on the zircaloy surface between the laser pulses, as described above. In order to remove any H_2O from the sample surface we employed a laser cleaning method. Thus, a Nd:YAG laser synchronized with the TEA CO_2 laser was irradiated on the sample surface 50 ms before the TEA CO_2 laser irradiation. Fig. 5.8 shows the emission spectra taken from the zircaloy sample containing 0 µg/ g of H (red line) and 2600

μg/ g of H (blue line). It can be seen from this figure that no H emission line appears for the zircaloy sample containing 0 μg/ g of H, whereas a very high H emission intensity, with a very low background intensity, can clearly be seen for the sample containing 2600 μg/ g of H. This result confirms that this laser cleaning technique can be applied to completely remove the H contribution from H_2O. It should be noted that the Nd:YAG laser irradiation was performed in defocus mode to ensure that very little plasma was generated. We therefore assumed that, after 50 ms, the plasma induced by the Nd:YAG laser had already decomposed and that the Nd:YAG laser irradiation functions only to remove the H_2O from the sample surface. However, we also found that the helium intensities differ depending on the sample (0 and 2600 μg/ g; see Fig. 5.8), thereby suggesting that irradiation with the Nd:YAG laser may affect the helium gas plasma generation. Further studies are therefore required to clarify the effect of this Nd:YAG laser cleaning process.

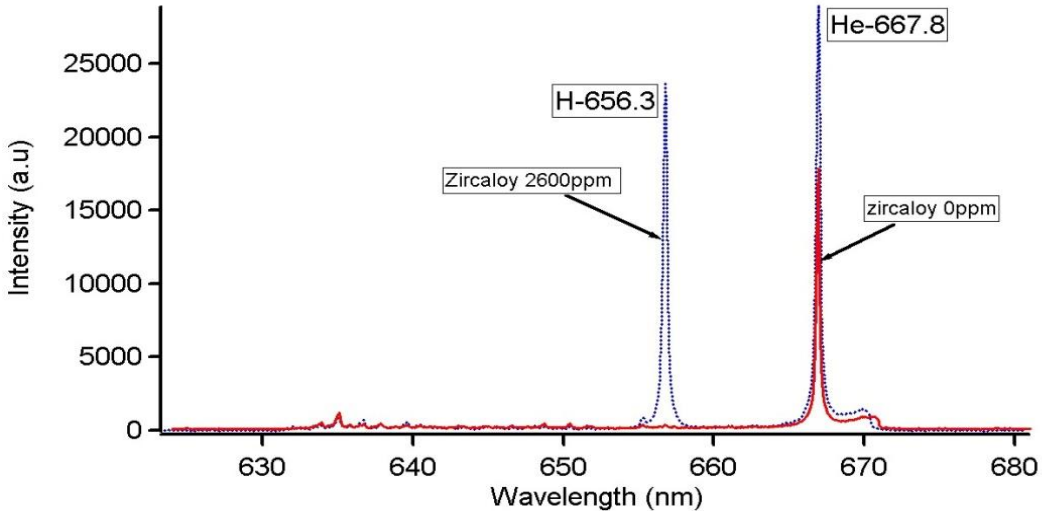

Fig. 5.8 Emission spectra taken from the zircaloy sample containing 0 (red line) and 2600 μg/ g_1 H (blue dotted line) after laser cleaning using a synchronized Nd:YAG laser.

Fig. 5.9 shows how the H and He emission intensities at 656.3 and 667.8 nm, respectively, change with time after the TEA CO_2 laser bombardment. It should be mentioned that we did not use the Nd:YAG laser to clean the sample surface in this experiment as the H emission arising from H_2O is negligibly weak (see Fig. 5.6). The curves in Fig. 5.9 were taken from the zircaloy sample containing 2600 μg/ g of H. Each data point plotted in the curve was obtained using 10 shots of laser irradiation and data acquisition was always made using a new position on the sample surface. It can be seen that the intensity of the He emission at 667.8 nm increases steeply up to 2 μs and then decreases sharply up to 15 μs, whereas the intensity of the H emission at 656.3 nm increases gradually up to 6 μs and then

slowly decays with a rather long lifetime. It should be noted that, in contrast to our previous work[14], where the H emission has both a fast and a slow component, there is no fast rising component in the H emission profile. In our former work, we used a double-pulse technique, namely a TEA CO_2 laser to induce He gas plasma and a Nd:YAG laser to ablate the atoms from the zircaloy sample into the helium gas plasma region. As the fast component of H emission increased very steeply up to 2 μs after the Nd:YAG laser bombardment, we concluded that this fast component is due to the fact that H atoms enter the gas plasma region earlier than the host elements because of their much lower mass. A comparison of the time profiles for H emission (Fig. 5.9) with the data from our previous work [14] indicated that no ablation of H atoms takes place and therefore that the H atoms are released by thermal evaporation from the sample surface. We have assumed that once the TEA CO_2 laser is irradiated on the H-containing zircaloy metal sample, the sample surface is melted due to the heat of the helium gas plasma and only H atoms are released from the sample, thereafter moving into the He gas plasma region to be excited.

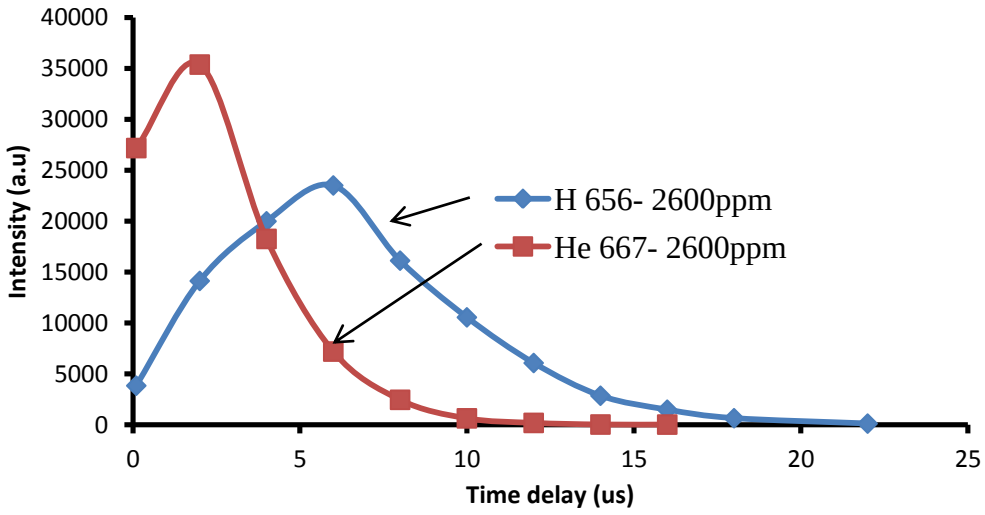

Fig. 5.9 Time profile of the H and He emission intensities (656.3 and 667.8 nm, respectively) after TEA CO_2 laser bombardment of a zircaloy sample containing 2600 μg/ g of H.

The emission characteristics of H alpha (H_α), H beta (H_β), and H gamma (H_γ) offer important information when it comes to understanding the excitation process of H in the plasma as they have different excitation energies (12.0, 12.7, and 13.0 eV, respectively).

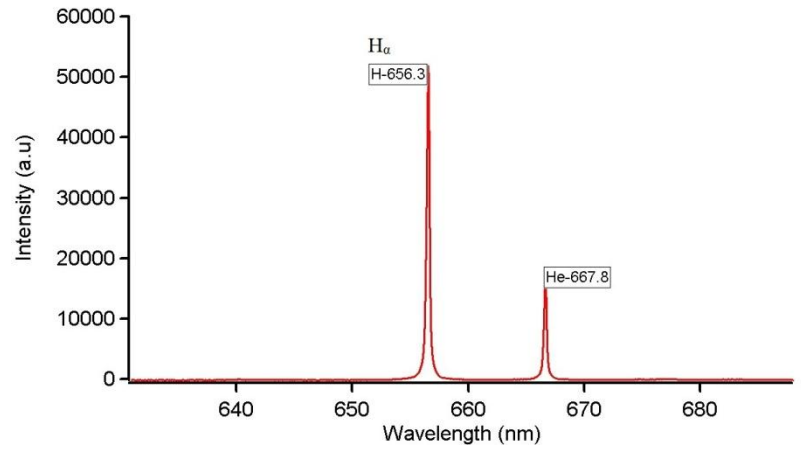

(a)

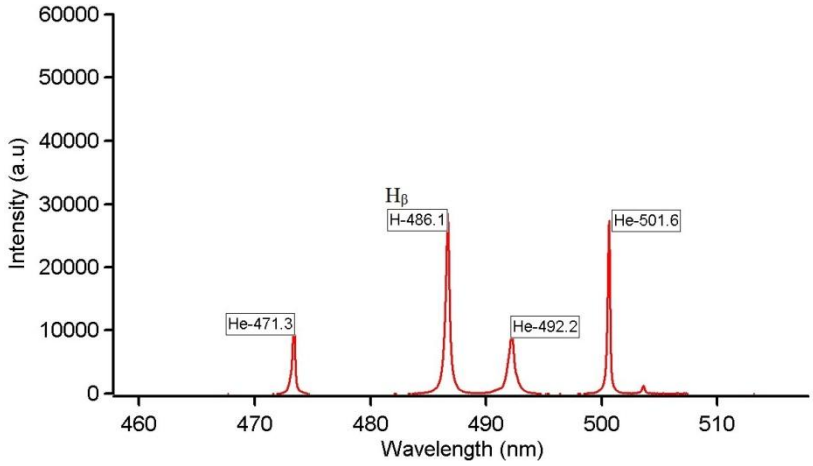

(b)

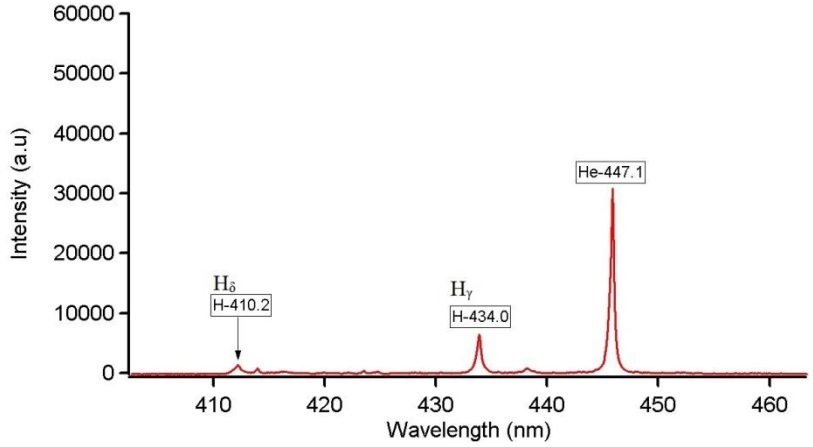

(c)

Fig. 5.10 Hydrogen emission spectra for the zircaloy sample containing 2600 µg/g of H: (a) H_α at 656.3 nm, (b) H_β at 486.1 nm, and (c) H_γ at 434.0 nm and H_δ at 410.2 nm

Fig. 5.10 shows the hydrogen emission spectra taken from the zircaloy sample containing 2600 µg/ g of H with the gate time and gate width of the OMA system both set to

5 ms. In this experiment, we also omitted the Nd:YAG laser cleaning step. Strong and very narrow H_α and H_β emission lines (Fig. 5.11(a) and 5.12(b), respectively) with a very low background and no interference from host emission lines can be seen at 656.3 and 486.1 nm, respectively. Furthermore, the H_γ line at 434.0 nm and the H_δ line at 410.2 nm can also be clearly observed (see Fig. 5.12(c)). It should be stressed that, to date, the LIBS technique has proved unable to provide clear H_α, H_β, H_γ, and H_δ emission lines due to interference from host emission lines and line broadening due to the Stark effect in the high temperature plasma. Thus, nobody discusses about the ratio of emission intensity of H_α, H_β and so on. We were therefore unable to compare the ratio of the H_α, H_β, H_γ, emission intensities with literature findings.

In this study, we found the ratio of H_β and H_α drastically changes depending on the excitation method. In case of helium gas plasma induced by TEA CO_2 laser, emission intensity of H_β is high relative to the H_α, resulting in the ratio of 0.55 as shown in Figs. 5.10a and 5.10b. On the other hand, we have already reported in our previous paper that the emission intensity of H_β is rather low, giving the ratio between H_β and H_α to be around 0.1, in the low pressure plasma where shock wave plays an important role to excite the atoms [3]. In that experiment, the glass sample containing H in the form of OH cluster was used, and the temperature of the plasma induced by the shock wave was estimated to be around 5000-7000 K based on the assumption that the Boltzmann distribution is fulfilled [15]. In this work, we confirmed again the ratio between H_β and H_α for the case of shock wave-induced low pressure plasma using a water molecular layer (H_2O) deposited on a copper plate. The copper plate was irradiated by TEA CO_2 laser in the surrounding gas of nitrogen of 100 Pa. The resulting spectrum was shown in Fig. 5.11, which is taken using compact OMA system as mentioned in the experimental procedure. It should be noted that the intensity of H_β emission is rather low compared to that of H_α, giving the ratio between H_β and H_α to be around 0.14. It should be mentioned that another line appeared in Fig. 5.11 is due to the host copper lines because the ablation happened to some extent in the low pressure plasma from the metal sub-target; it should be again mentioned that the low pressure plasma is different from that produced at 1 atm for the case of TEA CO_2 laser irradiation.

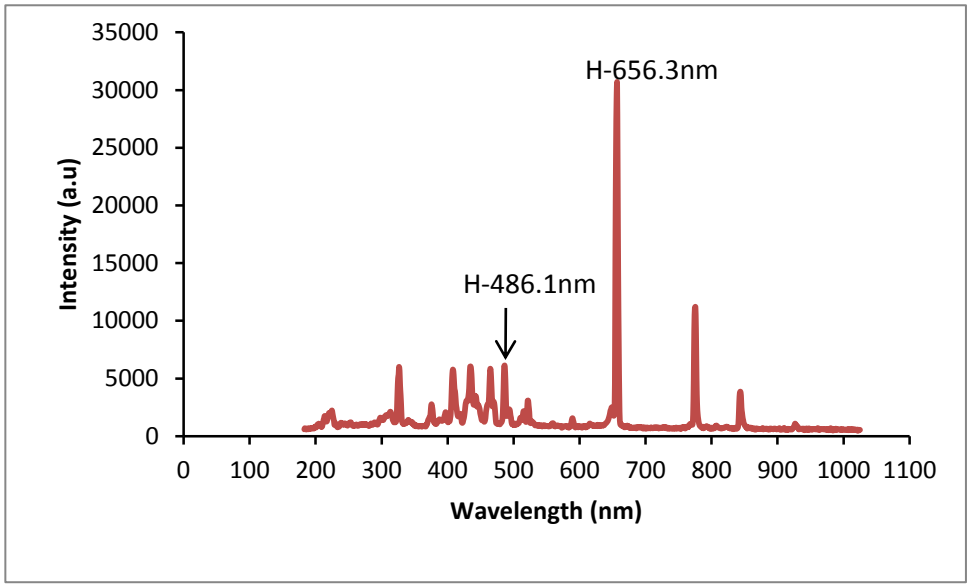

Fig. 5.11 Hydrogen emission spectra taken from the copper plate using the shock wave-induced low pressure plasma technique

If the excitation in helium gas plasma had been followed the Boltzmann distribution (thermal excitation), the plasma temperature would be more than 10.000 K when the ratio between H_β and H_α is 0.55, considering the energy difference between the upper level of H_β and H_α. In such case, the spectrum background would be very high and the H emission would be broadened. However, actually the spectrum background is very low and the hydrogen emission is very narrow as shown in Fig. 5.10. Therefore, we conclude that the excitation taking place in helium gas plasma is not due to the thermal excitation, and offers the following excitation mechanism, in which helium metastable atoms play an important role.

When a TEA CO_2 laser is focused on a zircaloy sample containing H, the sample surface is melted and H atoms come out from the surface. The atoms then move and enter into the strong He gas plasma region. The atom collides with metastable He atom (He*) (excitation energy of 19.8 eV) populated in the He gas plasma region through the Penning effect. The H atom is then readily ionized, resulting in free electron, which has high energy. This free electron collides many times with helium atoms and then recombines with H atom after the electron energy is reduced, resulting in making the higher level of H atoms from which H_α, H_β, H_γ and H_δ emission take place. The unique characteristics of the excitation process through He* are those the emission lifetime of atom is long and the atomic emission line width of H atom is narrow with low background intensity because the hydrogen excitation takes place in the cool plasma where the ions and electrons have already been recombined.

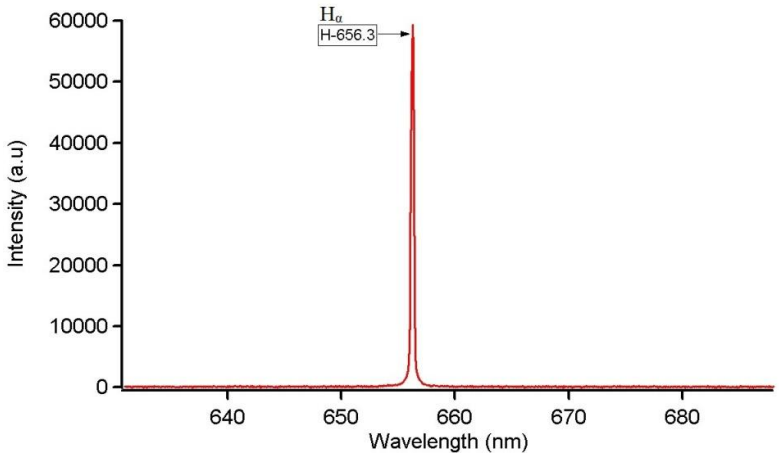

(a)

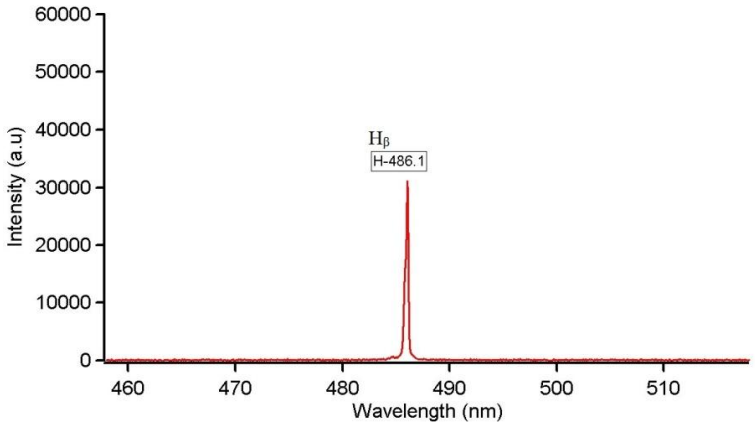

(b)

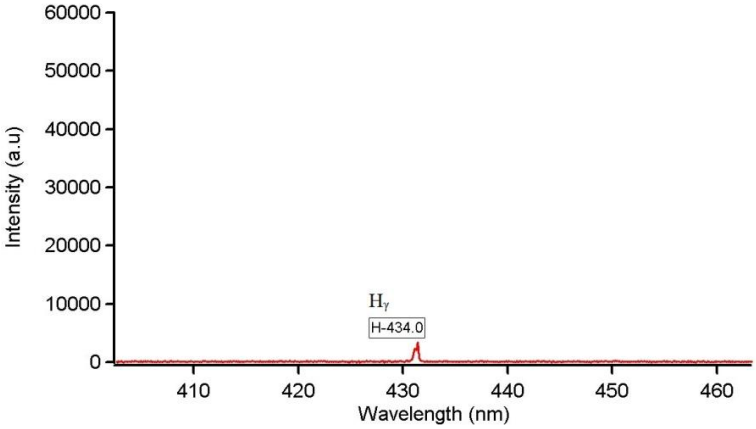

(c)

Fig.5.12 Hydrogen emission spectra for the conventional low pressure hydrogen discharge lamp: (a) H_α at 656.3 nm, (b) H_β at 486.1 nm, and (c) H_γ at 434.0 nm

It is very interesting to compare the H emission spectra taken from the helium gas plasma (Fig. 5.10) with those taken from a low pressure hydrogen discharge lamp (Fig. 5.12). Surprisingly, the ratios of the H emission lines are almost identical. Thus, the ratio H_α : H_β :

H_γ is 1 : 0.52 : 0.06 for the discharge lamp and 1 : 0.55 : 0.12 for the laser-induced helium gas plasma. Furthermore, all lines are very narrow, thus suggesting that the excitation of H atoms takes place in the cooled plasma rather than in the hot plasma. It should be noted that the H_δ is absent from Fig. 5.12(c) whereas it can clearly be seen in Fig. 5.10(c). The similarity between the spectra taken from the laser-induced helium gas plasma and those from the low pressure discharge hydrogen lamp would indicate that the hydrogen excitation process is almost the same. Namely, the excitation process of hydrogen takes place through the recombination process and is not due to the thermal excitation.

5.2.4 Conclusion

In this study, we offer a novel technique for H analysis in zircaloy samples that combines our previously reported ‘‘selective detection method of H’’ with a novel method for suppressing the H emission arising from H_2O. Thus, to suppress the interference from H_2O, a small helium gas plasma was intentionally produced close to the exit of the helium gas pipe and covered with a high purity helium surrounding gas to protect against attack by H_2O molecules. At this stage, the H emission due to H_2O was not completely suppressed but had nevertheless been reduced to a level of about 65 μg/ g. However, on the basis of our results, we expect that if we modify the helium gas flow system by using a larger diameter pipe to ensure that the helium gas plasma is completely covered by fresh helium gas the remaining H emission arising from H_2O should be reduced to around 10 μg/ g or less. Such an error in H analysis for zircaloy samples would pose no practical problems. Thus, the method presented in this paper should be applicable to Hanalysis for the zircaloy used in nuclear power stations. It should be stressed, however, that the greatest advantage of this technique compared with the ordinary method, is that a hydrogen mapping analysis can be performed. Such an analysis is not possible with the ordinary method as the sample
must be completely melted in a furnace.

We have also succeeded in clearly detecting the H_α, H_β, $H_{\gamma,}$ and H_δ emission lines for a hydrogen-containing zircaloy sample with very low background spectra and a very narrow spectral width by using our ‘‘selective detection of H’’ technique. We also compared the H emission spectra taken from the laser-induced helium gas plasma with those taken from a low pressure hydrogen discharge lamp and confirmed the good coincidence between the H_α : H_β : H_γ ratio in both cases, thus implying that the hydrogen excitation mechanism is almost the same. Clarification of the mechanism underlying the excitation process is obviously crucial in

order to establish this ‘‘selective detection method for hydrogen analysis’’ as an analytical technique, therefore further studies will be conducted in this respect. It is well known that the presence of H in many kinds of materials, especially metals and alloys, causes a reduction in their strength [8-10]. Hydrogen analysis is therefore very important in many fields. The novel technique presented in this paper will be developed to perform H analysis at a μg/g level in metal samples.

5.3 Excitation Mechanism of H, He, C and F Atoms in Metal-Assisted Atmospheric Helium Gas Plasma Induced by Transversely Excited Atmospheric-Pressure CO_2 Laser Bombardment

5.3.1 Introduction

It is well known that hydrogen analysis in metal is important in material science and industry technology [1, 16]. For instance, in light water nuclear power station [2], hydrogen analysis in zircaloy tubes is important issue. During the operation, hot water reacts with the zircaloy surface to produce H_2 gas and the gas penetrates and accumulates into the zircaloy tube, which causes unacceptable structural damage and seriously reduces the strength of the material. Therefore, the accumulation of hydrogen in zircaloy tube must be examined periodically. A commercial method commonly uses a gas detector by means of melting a portion of the zircaloy tube in a carbon furnace. However, this technique is time-consuming, destructive, and cannot be *in-situ*.

The technique of laser-induced plasma spectroscopy (LIPS) has spread worldwide due to its high performance in rapid quantitative analysis [1, 11]. The popularity of this subject is indicated by a large number of papers published on this topic even this subject has been reviewed in many times in many journals [17-19]. In LIPS, the plasma generation is made at atmospheric pressure and a fundamental Nd-YAG laser is mostly used as ablating energy source, which people say laser-induced breakdown spectroscopy (LIBS). The most interesting advantages of standard LIBS are the feasibility of *in-situ* analysis and freedom from sample pretreatment. However, a highly sensitive and reliable analysis of hydrogen is very difficult when we employ the standard LIBS technique due to the disturbance by many host lines located near the hydrogen emission line and the occurrence of broadening [12] in the hydrogen emission spectrum. Also, the "mismatching effect" [2-3] and the disturbance by ubiquitous water molecules (H_2O) are serious obstacles in H analysis using the standard LIBS technique.

In our previous paper [13, 20], we have reported a noble technique for hydrogen analysis in metal sample. Namely, when a transversely excited atmospheric (TEA) CO_2 laser was focused on a zircaloy sample containing hydrogen (H) in He surrounding gas at atmospheric

pressure, a strong helium gas plasma was produced and only H atoms came out from the metal sample because the sample surface was faintly melted due to the heat of the gas plasma. The H atoms then moved into the helium gas plasma region to be excited through metastable helium atoms, while no host emission line from the sample appeared due to the fact that no ablation of host elements takes place. It should be mentioned that when we used a Nd:YAG laser, which is commonly employed in standard LIBS method, such phenomenon never occurs because all elements including host elements and impurities are simultaneously ablated from the metal sample. This new technique has high capability to realize a highly sensitive analysis of H in metal. However, the excitation mechanism of hydrogen in helium gas plasma has not been understood yet.

In our previous work [21], we also studied about hydrogen analysis in gas. In this experiment, Nd:YAG laser is focused into atmospheric helium gas which contains H_2O as an impurity. It was proved that H emission takes place with long lifetime and narrow spectrum width. However, when we used nitrogen gas, lifetime of H emission is short and the H emission spectrum is significantly broadened. In order to explain the hydrogen emission characteristic for helium gas, we offered the model, in which helium metastable atoms play an important role.

In order to clarify the excitation mechanism of hydrogen atoms in TEA CO_2 laser-induced helium gas plasma, emission characteristics of hydrogen and also those of helium and other elements should be studied. In this paper, we used Teflon as a sample because it contains carbon and fluorine as host elements and hydrogen as impurity. As is well known, fluorine is difficult element to be detected by ordinary LIBS technique due to the high excitation energy (14.5 eV).

5.3.2 Experimental Procedures

The experimental arrangement used in this study is shown in Fig. 5.13(a). A TEA CO_2 laser (Shibuya SQ 2000 laser, pulse energy of 3 J, wavelength of 10.6 μm, pulse duration of 200 ns in full width at half maximum, beam cross section of 30 mm x 30 mm), which was developed and commercially produced by Shibuya Company for laser marking, was used as an irradiation source. The laser beam was focused by a ZnSe lens (f = 200 mm) on a target sample through a ZnSe window. The laser energy was set up 750 mJ by inserting an aperture in front of the focusing lens. The spot size of laser beam on sample surface for the tight focusing condition was 1 mm x 1 mm, which is shown in Fig. 5.13(b).

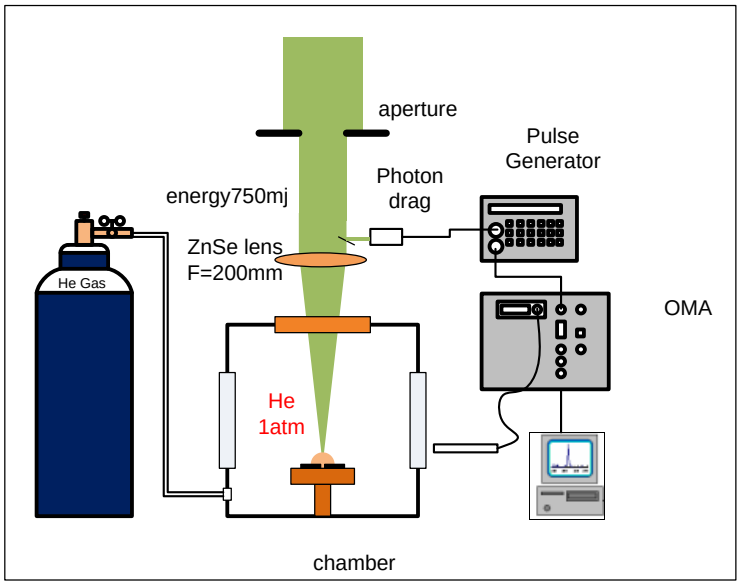

(a)

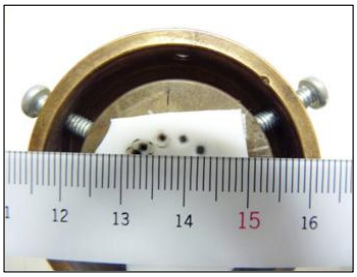

(b)

Fig.5.13 (a) The illustration of experimental arrangement (b) the Teflon sample attached on the metal sub-target. The hole was produced by 100 shots of TEA CO_2 laser bombardment.

The Teflon sample was used in this experiment. The sample, of which dimension is 25 mm x 25 mm x 2 mm, was attached directly on a brass holder, which works as a metal sub-target for gas plasma generation, and the holder was placed in a metal chamber with a dimension of 12 cm x 12 cm x 12 cm. During the experiment, high-purity helium gas (99.999999 %) was flowed into the metal chamber, in which the pressure of the surrounding gas was kept constant at 1 atmosphere. Depending on the experiment, high purity nitrogen gas (99.999%) was also used. The flow rate of the gases was 4 liters per minute.

The emission spectra were obtained by detecting laser plasma radiation using optical multi channel analyzer (OMA) system (ATAGO Macs-320) consisting of a 0.32 m focal-length spectrograph with a grating of 1200 groves/mm, a 1024-channel photodiode detector array, and a micro-channel plate image intensifier. The spectral resolution of the OMA system is 0.2 nm. The light emitted from the laser plasma was collected by an optical fiber (θ= 27° in solid angle) and fed into the OMA system. Gating time of OMA was set

using a pulse generator (Stanford Research System INC, model DG-535), of which trigger was taken from the signal of a photon drag detector. One end of the fiber was placed at a distance of 4 cm from the focusing point of the laser light and set perpendicularly to the path of the laser beam. In order to acquire spectral emission in a time with a wide spectral range of 200-1000 nm, a compact OMA system (Lambda Vision SA-100-HPCB) was also employed. The OMA system was set in time-integrated mode with an exposure time of 2 s. Almost the data of emission spectra and time profile of the emissions, when we used Teflon sample, were taken after 50 shots of laser irradiation because the TEA CO_2 laser-induced gas plasma has already been stable.

5.3.3 Experimental Results

It should be mentioned that the plasma generation aspect for TEA CO_2 laser irradiation is quite different from the case of Nd:YAG laser. Namely, when TEA CO_2 laser was focused on a metal surface at atmospheric pressure, strong gas plasma was produced and no ablation takes place from the metal surface.

In Fig. 5.14, the emission intensity of fluorine (685.3 nm) in Teflon sample is plotted as a function of the number of laser shots for two different gases; namely, helium and nitrogen gases. Gate condition of OMA system was set at 2-100 μs. It is seen that at initial stage, no fluorine emission takes place. However, after 25 shots of laser irradiation, emission of fluorine starts and increases sharply. Then the emission intensity increases slowly until 50 shots, and finally becomes rather stable. On the other hand, for nitrogen surrounding gas, emission starts at the same number of laser shots with the case of He gas, but the emission intensity was totally weak compared to that of helium surrounding gas.

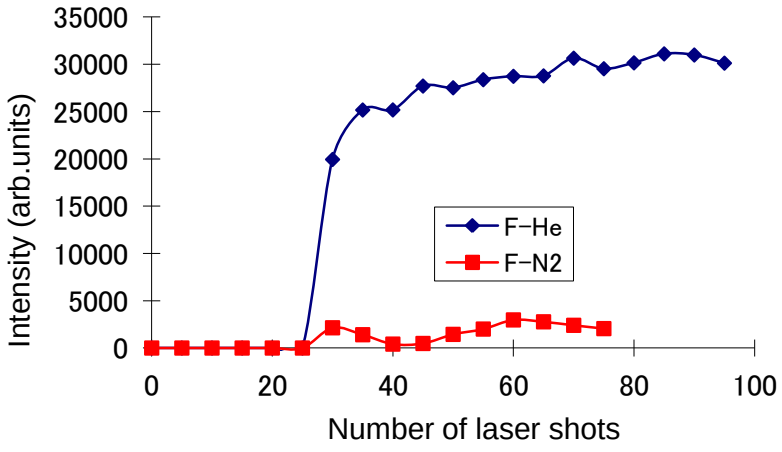

Fig.5.14 Emission intensity of fluorine in Teflon sample as a function of number of laser shots taken from different gas, helium and nitrogen in TEA CO_2 laser induced gas plasma at atmospheric pressure.

It should be stressed that the initial stage before 25 shots and the later stage after 25 shots are different in plasma production. Namely, before 25 shots, no plasma generation takes place, nevertheless evaporation from Teflon sample occurred and crater depth increased with laser shots. After 25 shots, the laser beam directly attacked on the metal sub-target sample, and strong gas plasma was induced. Therefore, we conclude that fluorine is excited in helium gas plasma region. It should be mentioned that during the plasma expansion, the gas plasma interacted with the wall surface of the crater of Teflon and the sample are vaporized to be dissociated and excited in the helium gas plasma region.

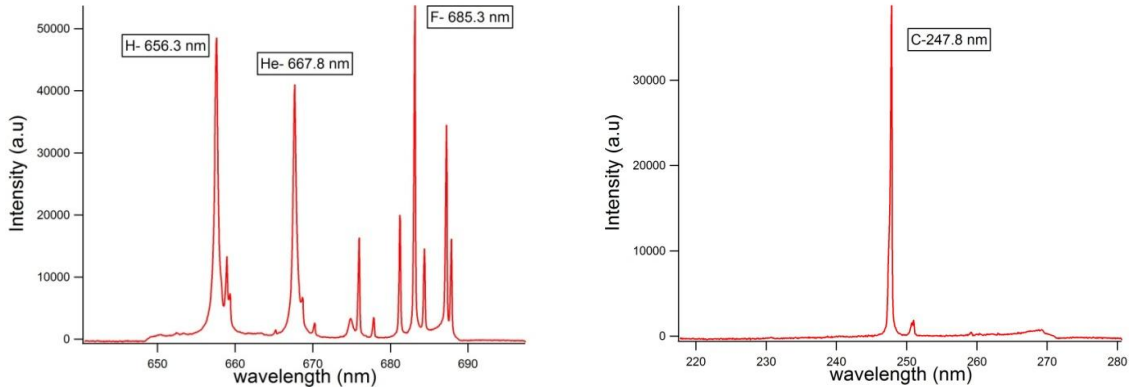

(a) (b)

Fig.5.15 Emission spectra taken from Teflon sample in a TEA CO_2 laser-induced He gas plasma at atmospheric pressure. (a) Emission lines of H, He, and F (b) emission line of C.

Figure 5.15(a) shows the emission spectra of hydrogen, helium and fluorine and Fig. 5.15(b) shows the emission spectra of carbon taken from Teflon sample under helium surrounding gas. The spectra were taken after helium gas plasma becomes stable (after 50 shots) with a gate condition of OMA system to be 2-100 μs. It should be noted that the emission lines of H, He, F and C are strong in intensity, and narrow in spectrum width with low background emission intensity. Also, it should be mentioned that no atomic emissions line due to the atoms of metal sample target appeared because no ablation takes place for TEA CO_2 laser case.

In order to understand the excitation mechanism of atoms taking place in helium gas plasma, it is important to examine the time profile of each emission of hydrogen, helium and fluorine. Figure 4 shows how hydrogen, helium and fluorine intensities at 656.3nm, 667.8 nm and 685.3 nm, respectively, change with time after the TEA CO_2

laser bombardment on Teflon sample in helium surrounding gas. These data were taken after the gas plasma becomes stable (after 50 shots). The gate width of OMA system was set at 2 μs. Each data point plotted in the curve was obtained using 5 shots of laser irradiation. These emission lines, H-656.3 nm, He-667.8 nm and F-685.3 nm were taken in one spectrum frame of OMA system. Thus, the experimental error could be minimized. In order to discuss on the excitation mechanism for nitrogen gas, time profile of fluorine obtained for nitrogen gas was also plotted in this figure.

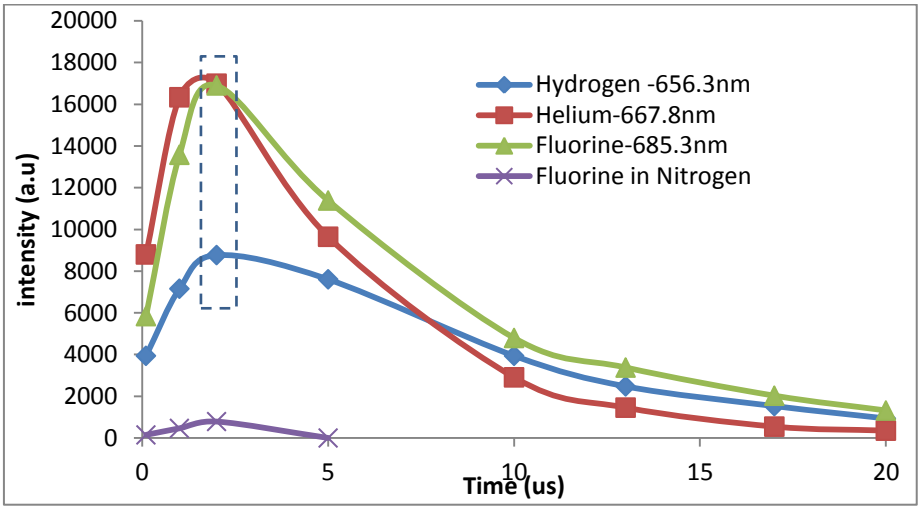

Fig.5.16 Time profile of H, He and F emission intensity (656.3nm, 667.8 nm and 685.3 nm, respectively) after the TEA CO_2 laser bombardment on Teflon sample in helium surrounding gas and F emission in nitrogen surrounding gas.

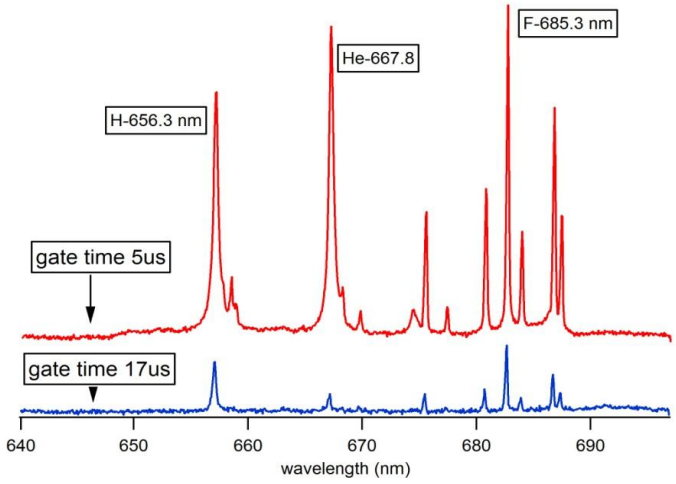

Fig.5.17 Emission spectra taken from Teflon sample with gating time 5μs (red line) and gating time 17 μs (blue line). The gate width of OMA system was set at 2 μs.

It is seen that in helium gas case, the emission of fluorine increases sharply with the peak at 2 μs and decreases slowly until about 30 μs. While for nitrogen gas case, the time of peak emission is almost the same with that of helium gas but decays faster; namely, at 5 μs emission intensity of fluorine is almost zero. The time profile of hydrogen is similar to that of fluorine emission, while the helium emission decays faster in comparison with F and H emission as shown in Fig.5.16. One might think that the emission decay difference between hydrogen and helium, and also fluorine and helium are not so much. However, the decay difference was always clearly observed. Figure 5.17 shows the comparison of emission spectra on hydrogen, helium and fluorine taken at two different times; namely, at early stage of 5 μs (red line) and at later stage of 17 μs (blue line). The gate width of OMA was set at 2 μs. In early stage, helium emission is very strong, while in later stage helium emission become very weak compared to those of hydrogen and fluorine. Namely, helium emission decays faster than hydrogen and fluorine emission. In order to show the difference in the emission decay, we plotted in Fig. 5.18 how the ratio between hydrogen and helium (blue line) and also between fluorine and helium (red line) change with time. These data were taken from those in Fig.5.16. It is seen that the ratio increase with time, which means surely helium emission decay faster than those of hydrogen and fluorine.

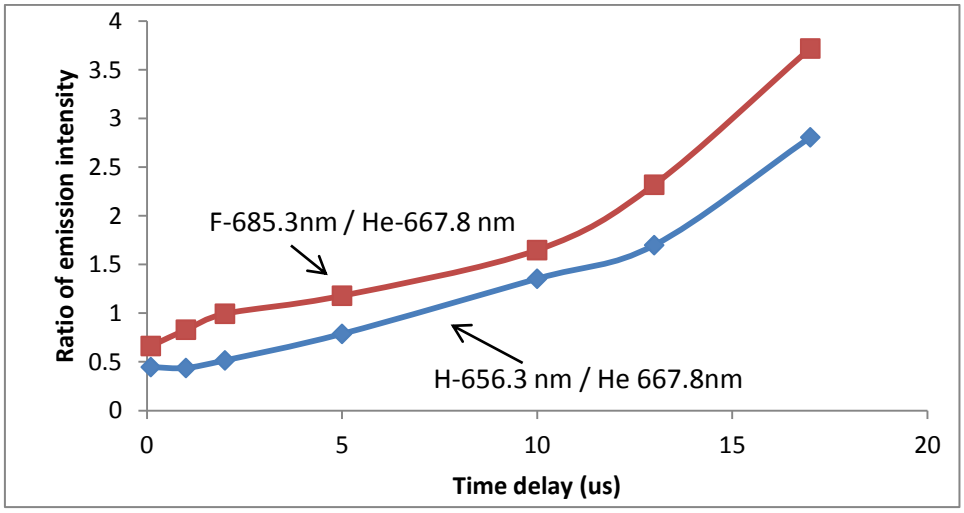

Fig.5.18 Time profile of ratio between fluorine and helium (red line) and ratio between hydrogen and helium (blue line) after the TEA CO_2 laser bombardment on Teflon sample in helium surrounding gas.

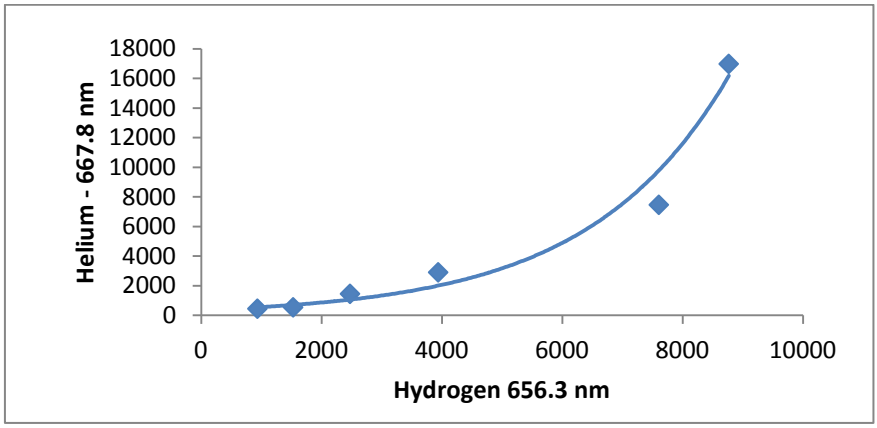

(a)

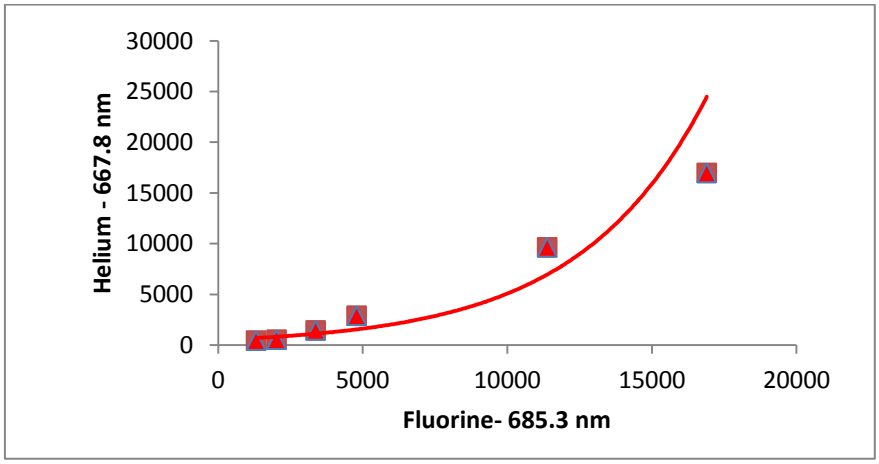

(b)

Fig.5.19 (a) The relationship between H emission intensity and He emission intensity, and (b) the relationship between F emission intensity and He emission intensity. Data were taken from those in Fig. 5.16.

As we described later, helium metastable atoms will contribute not only in hydrogen and fluorine excitation process, but also in helium excitation process to induce helium emission. Therefore, it is meaningful to see the correlation of emission intensities between hydrogen and helium, and also between fluorine and helium. Figure 5.18 shows Time profile of ratio between fluorine and helium (red line) and ratio between hydrogen and helium (blue line) after the TEA CO_2 laser bombardment on Teflon sample in helium surrounding gas. Figure 5.19(a) shows the relationship between hydrogen intensity and helium intensity and Fig. 5.19(b) shows the relationship between fluorine intensity and helium intensity. These data were taken from those shown in Fig. 5.16. It is seen that the curve seems to be a parabolic curve. In Fig. 5.20(a), helium emisson intensity is plotted as a function of square of hydrogen emission intensity and

in Fig. 5.20(b), helium emisson intensity is plotted as a function of square of fluorine emission intensity. These data were taken from those shown in Fig. 5.16. For instance, these data surrounded by dashed boxes shown in Fig. 5.20(a) and Fig. 5.20(b) are derived from the data at 2 μs in Fig. 5.16, which are also surrounded by a dashed box. It is seen that there are approximately linier relationship between them. The data before 2 μs in Fig.5.16 were not included in Fig. 5.20(a) and Fig. 5.20(b) because it is considered that the production of helium metastable atoms is not well completed before 2 μs.

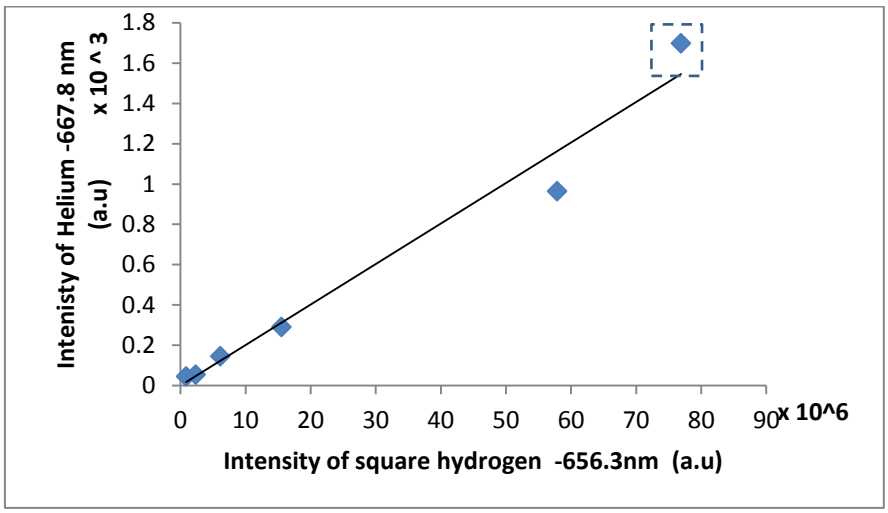

(a)

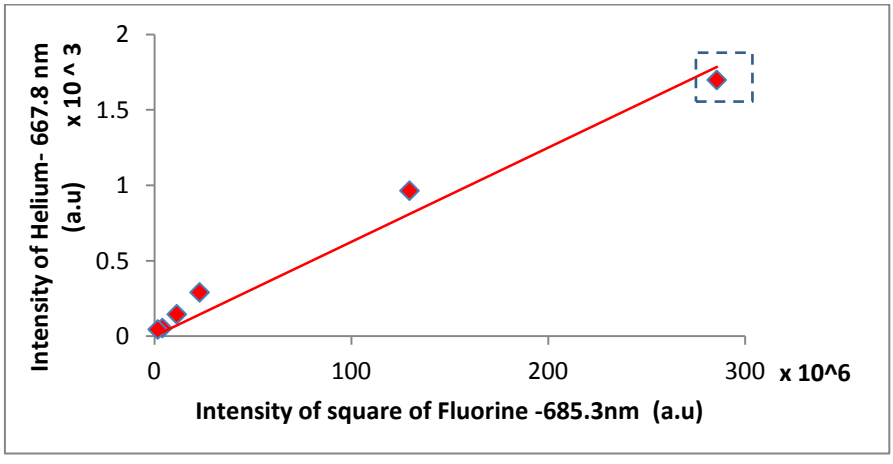

(b)

Fig.5 20 (a) The correlation between He emission intensity and the square of H emission intensity, (b) the correlation between He emission intensity and the square of F emission intensity. The data were derived from Fig. 5.16. For instance, these data in dashed box shown in Fig. 5.20(a) and Fig. 5.20(b) are derived from the data at 2 μs in Fig. 5.16, which are also surrounded by dashed box.

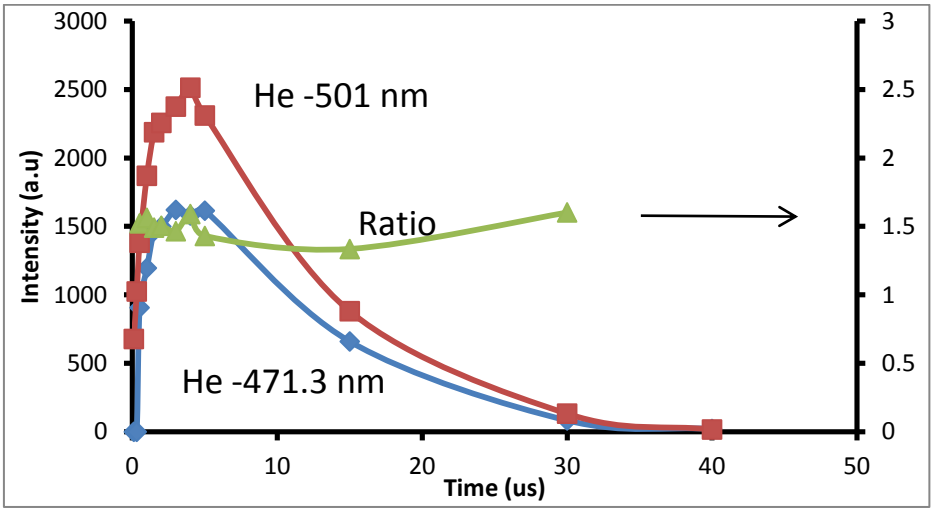

(a)

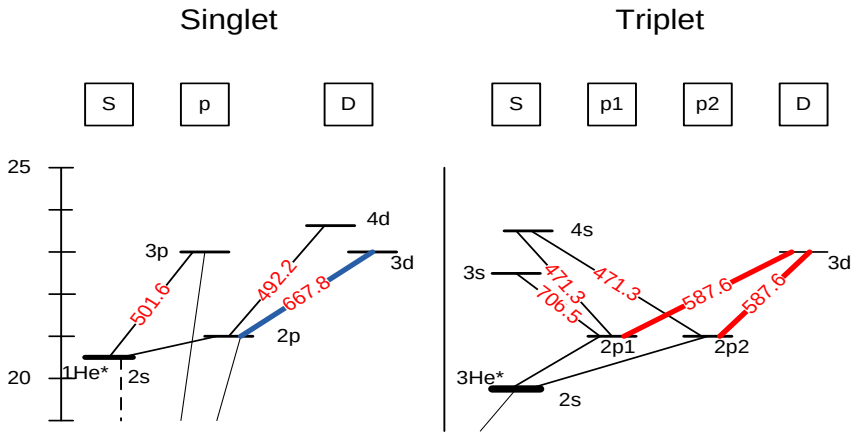

(b)

Fig.5.21 (a) Time profiles of He 501.6 nm intensity and He 471.3 nm intensity; and the ratio of emission intensities between 501.6 nm and 471.3 nm against the time after TEA CO_2 laser bombardment on metal surface. (b) Part of energy level diagram in helium.

In order to discuss about the excitation mechanism of helium in helium gas plasma, it is important to examine the time profiles of helium emissions, which have different excitation energy from metastable states. Figure 5.21(a) shows the time profile of helium 501.6 nm and 471.3 nm and the ratio of emission intensity between 501.6 nm and 471.3 nm were also plotted as a function of time. The gate width of OMA system was set at 2 μs. In this experiment, the Teflon sample was not used, and laser beam was directly focused on the brass sub-target. It should be noted that the helium emission life time in Fig. 5.21(a) is longer than that in Fig. 5.16. This is probably due to the fact that

the quenching effect is negligibly small because of no impurity atoms, while in Fig. 5.16 quenching effect of helium metastable atoms would be very large due to the existence of lot impurity atoms. In this experiment, we chose the helium emission line of 501.6 nm and helium emission line of 471.3 nm because we can take these emission lines simultaneously in one frame of display of the OMA system. Helium -501.6 nm is due to the transition (3p-2s) in singlet state; the energy gap between the upper level of the transition and the singlet metastable state is 2.5 eV. On the other hand, helium-471.3 nm is due to the transition ($4s\text{-}2p_1$, $4s\text{-}2p_2$) in the triplet state; the energy gap between the upper level of the transition and triplet metastable state is 3.8 eV as shown in Fig. 5.21(b). It is seen that the ratio of emission intensities between 501.6 nm and 471.3 nm is almost constant regardless of the time after the TEA CO_2 laser bombardment.

As is well known, there are two kinds of metastable in helium atoms; namely, the singlet metastable and the triplet metastable. To examine which one contributes more in atomic excitation process, wide-range emission spectrum is required. We obtained helium emission spectrum by focusing TEA CO_2 laser on the metal sub-target. In this experiment, a compact OMA system was used with time-integrated mode. The spectrum was shown in Fig. 5.22. It is seen that emission intensity of helium -587.6 nm (triplet), of which transition is from 3d to 2p , is much stronger than that of helium -667.8 nm (singlet), of which transition is the same as the case of 587.6 nm, namely from 3d to 2p .

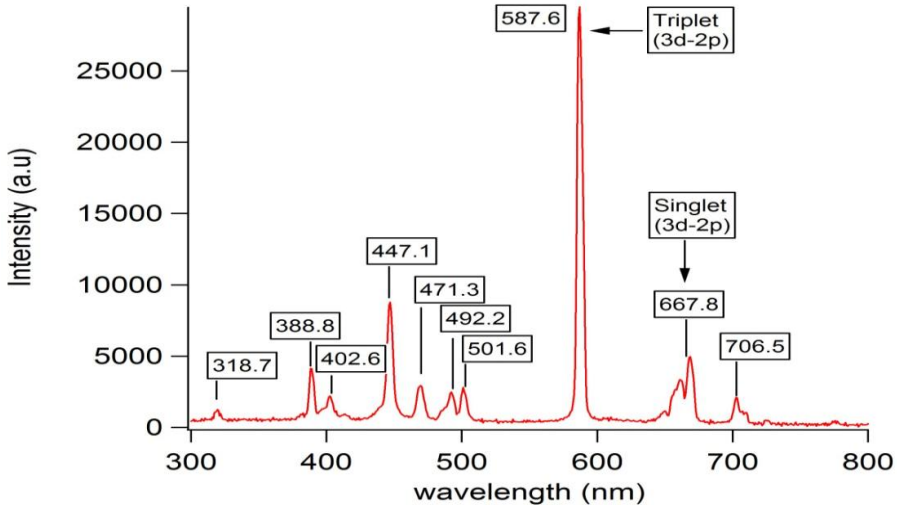

Fig.5.22 Emission spectrum of He taken when TEA CO_2 laser focused on metal sample in helium gas plasma at 1 atm. In this experiment, a compact OMA system was used with time integrated mode.

5.3.4 Discussion

First, we describe about gas plasma generation when a TEA CO_2 laser was focused on a metal surface in atmospheric pressure. The gas plasma generation by TEA CO_2 laser has a unique characteristic owing to its low frequency (long wavelength of 10.64 μm) and long pulse duration (200 ns). [6] When a TEA CO_2 laser is focused onto a metal surface, electrons are released from the surface of the metal owing to a multi-photon absorption process that occurs at the focusing point of the laser light. These electrons are then accelerated to high energy in the low-frequency electric field of the laser light, which induces the cascade ionization of the atoms in the gas and generates initial gas plasma. Once this initial gas plasma has been produced, the laser light is absorbed in the gas plasma by inverse Bremsstrahlung via free-free transitions. This absorption is much stronger for the TEA CO_2 laser than that for the Nd:YAG laser as the plasma absorption coefficient is proportional to the inverse square of the frequency of the laser light [22]. Furthermore, the pulse duration of the TEA CO_2 laser is 200 ns, and about 20 times longer than that of the Nd:YAG laser, which means that almost all the energy from the TEA CO_2 laser light is absorbed by the gas plasma, thus the metal itself is neither damaged or ablated during this laser irradiation; these processes is quite different from the case of Nd:YAG laser irradiation.

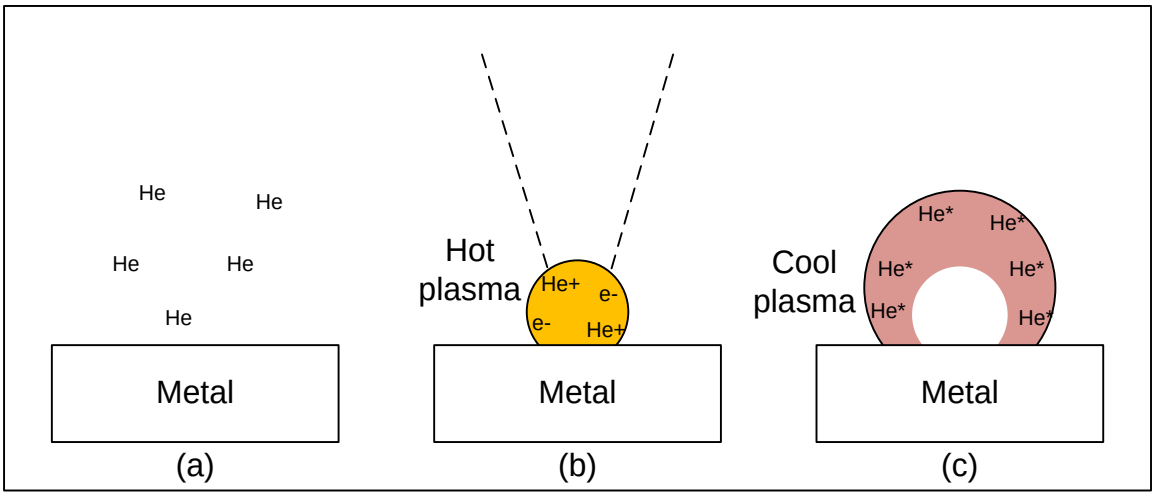

Fig.5.23 The illustration of the helium gas plasma production and expansion process. (a) before laser irradiation, (b) just after the laser irradiation, and (c) later state of the helium gas plasma production. In the hot plasma, a lot helium ion (He^+) and electron exist. In the cool plasma, helium metastable atoms (He*)are populated and expand with time.

In case of helium gas, it is supposed that helium atoms are ionized in hot plasma at the initial stage of the gas plasma production, and soon the helium ions will recombine with electrons to produce a lot helium metastable state [6]. Then, helium metastable atoms move and expand with time as illustrated in Fig. 5.23. Helium metastable atom has high excitation energy of 19.8 eV. Therefore, we assumed that all elements are excited through helium metastable because the excitation energies of other element are lower than that of the helium metastable state.

As shown in Fig. 5.16, fluorine emission, which has high excitation energy of 14.5 eV takes place with a strong emission intensity and long lifetime when we used helium surrounding gas. On the other hand, the different result was observed when nitrogen surrounding gas was used. It is considered that excitation of fluorine takes place only when the temperature of plasma was high. Namely, fluorine is excited by thermal excitation for nitrogen surrounding gas. We must note that the temperature of the plasma in helium gas is actually almost the same or lower than that of nitrogen gas. Thus, we conclude that excitation of fluorine in helium gas is not due to the thermal excitation, but due to another process. Therefore, we assumed that fluorine was excited through helium metastable atoms. As shown in Fig. 5.16, hydrogen emission has similar characteristic with that of fluorine emission. We also confirmed that carbon emission characteristic is almost the same as that of fluorine and hydrogen. Thus, we conclude that the excitation through helium metastable atom takes place in all elements in the helium gas plasma.

It is known that the excitation energy of metastable helium atom is rather high (19.8 eV), whereas the excitation energy of ablated atom is much lower. The difference in the excitation energy between the metastable helium atoms and the ablated atoms is rather high, which means that it is impossible for energy of the metastable helium atoms to be transferred directly to the atoms. We, therefore, propose the following processes to explain the excitation mechanism.

He^*+X (ground state) →	$He + (X^+ + e^-)$	(Penning Effect)	(1)
$X^+ + e^-$ →	X^{***}	(Recombination)	(2)
X^{***} →	X^{**}	(through cascade transition)	
X^{**} →	$X + h\nu$	(Emission)	(3)

The atom will collide with helium metastable atom (He*) to be ionized through the Penning effect. The X atom is then readily ionized, resulting in free electron, which has high energy as shown in Eq. 1. The energy of this free electron corresponds to the energy difference between the excitation energy of He* and the ionization energy of X atoms. This free electron collides many times with helium atoms and then recombines with X ion to produce atom with higher energy level (X***) (as shown in Eq. 2). Through the cascade transition, the excitation state (X**) is produced, from which atomic emission that is used as an analytical line takes place as shown in Eq. 3. This unique excitation process through He* offered the favorable characteristic of emission spectrum because the atom excitation takes place in the cool plasma, where ions and electrons have already been recombined. Thus, spectrum background is very low and emission lines are narrow in spectrum width.

We believe that helium metastable atoms also give contribution in the excitation process of helium itself, because helium emission continues for long time and the excitation energy is much higher than those of other elements including fluorine. It is assumed that there are 2 possible excitation mechanisms, in which helium metastable plays important role, as shown in the following:

Process 1:

He^{*} +thermal energy→ He**

He**→ He *+hv (Emission) (4)

Process 2:

He*+He* → He + (He^{+} +e^{-}) (Penning Effect) (5)

He^{+} +e^{-} → He*** (Recombination) (6)

He*** →He** (through cascade transition)

He**→He*+ hv (Emission) (7)

In the Process 1, helium-excited state, from which emission takes place, is produced from helium metastable atom by absorbing thermal energy in helium gas plasma because energy difference between the excited state and the helium meta–stable state is not large, less than 4 eV. If this process were true, the emission from the excitation level, which has a large energy difference (3.8 eV) from metastable state,

would decay faster than that which has a small energy difference (2.5 eV); it should be remained that the plasma temperature decreases with time, thus the excitation to higher energy level becomes difficult with time. However, as shown in Fig. 5.21(a), the ratio of emission intensities, which have different energy from metastable state, is almost constant regardless of time, namely regardless of the plasma temperature. This fact indicates that the Process 1 is not a major process. Based on the result, we conclude that Process 2 is a major in the helium excitation process. Namely, in the cool helium gas plasma, atom of helium metastable state is ionized by colliding with another atom of helium metastable state through the Penning effect (as shown in Eq. 5). Then, helium ions and electron recombine to produce the higher energy state of helium (He ***) (as shown in Eq. 6) and by cascade transition, helium excitation state (He**) is produced, from which helium emission takes place (as shown in Eq. 7).

It should be mentioned that the number of helium metastable atoms decreases with time due to several processes. Therefore, it is expected that helium emission decays faster than other elements because in order to make helium excited state (He**), two helium metastable atoms are necessary. In fact, as shown in Fig. 5.18 helium emission decays faster compared to those of hydrogen and fluorine. Namely hydrogen and fluorine have different characteristics in the time profile of emission compared to that of helium.

In order to make semi-quantitative discussion, we offer the following equations,

$$[X^{**}] \propto [He^{*}] \qquad (8)$$

$$[He^{**}] \propto [He^{*}][He^{*}] \qquad (9)$$

where the notation of "[ ]" is the number of atoms.

As shown in Eq. 8, the number of excited state of X atoms is proportional to that of helium metastable atoms. This is derived from Eq. 1. As described in Eq. 9, the number of excited state of helium (He**) is proportional to the square of the number of helium metastable state (He*). By combining Eq. 8 and 9, the following Eq. 10 can be derived,

$$[He^{**}] \propto [X^{**}]^2 \qquad (10)$$

Namely, the number of helium excited state [He**] is proportional to the square of the number of excited state of X atoms (X**). In fact as shown in Fig. 5.20 (a), helium emission intensity is approximately proportional to the square of the emission intensity of hydrogen. Also as shown in Fig. 5.20(b), helium emission intensity is approximately proportional to the square of the emission intensity of fluorine.

Finally, we discuss about which helium metastable state works as a major in this excitation process; namely, triplet helium metastable state or singlet helium metastable state. As shown in Fig. 5.22, the helium emission at 587.6 nm is much stronger than helium 667.8 nm. It should be stress that these emissions take place in the same electronic transition, namely 3d to 2p. Also, it should be noted that the difference in the emission intensities are not due to the wavelength dependence of OMA sensitivity because the OMA has wide wavelength range sensitivity (200 nm-100 nm). This fact seems to indicate that during the recombination process between helium ions and electrons, mostly triplet helium metastable are produced and the production of singlet metastable is a minor process. Thus, we assume that triplet metastable atoms play important role in the excitation process of atoms in TEA CO_2 laser-induced helium gas plasma. However, further studies are required to get more evidence to clarify which metastable, singlet or triplet, is a major to excite atoms in helium gas plasma.

5.3.5 Conclusion

With a motivation to clarify the excitation mechanism of hydrogen in TEA CO_2 laser induced helium gas plasma, emission characteristics were studied on hydrogen, carbon, fluorine and helium using Teflon sample. It was proved that hydrogen, carbon, fluorine and helium takes place with strong emission intensities, narrow spectrum width and also with low background emission intensities. Time profiles of the emission of these elements were studied, and it was proved that emission life time is rather long. However, when we used nitrogen gas, the emission of fluorine, which has excitation energy of 14.5 eV is very weak and lifetime is short.

We offered the excitation model, in which helium metastable atoms play important role. Based on our model, we explained the characteristics of emission on H, F and He. As the result, we concluded that not only impurity atoms but also helium atoms are excited through helium metastable atoms. This helium metastable atom is

produced at initial stage of the helium gas plasma production through recombination process between ions and electrons. Based on our experimental results, we assumed that not singlet helium metastable atom but triplet helium metastable atom is a major contributor in the excitation process.

Finally, it should be stressed that our technique is quite different from ordinary LIBS. Namely, in LIBS atoms was excited thermally in hot plasma, while in our method, atoms are excited through helium metastable atoms in the cool plasma, where ions and electrons have already disappeared. Thus, spectrum background is very low, which offered a good condition to realize high sensitive analysis. Therefore, this new method of LIPS-He* (laser-induced plasma spectroscopy using helium metastable state) has a potential for realizing high sensitivity analysis on H analysis and also on any elements.

5.4 Effective Techniques to Suppress H Emission from H_2O in TEA CO_2 laser-Induced Helium Gas Plasma for Highly Sensitive and In-situ Hydrogen Analysis in Metal Sample

5.4.1 Introduction

Laser-induced breakdown spectroscopy (LIBS) was recently shown to be a promising technique for rapid quantitative analysis of elements in many kinds of samples, including metals [1, 11, 23-24]. The most interesting advantages of standard LIBS are the ability to perform *in-situ* analysis and fewer sample pretreatments. However, highly sensitive and reliable analysis of hydrogen in metal samples is very difficult with the standard LIBS technique due to a broadening of the H emission spectrum [12, 25], a mismatching effect [2-3, 26], the disturbance from ubiquitous water molecules (H_2O) [2], and interference from host lines near the hydrogen emission (656.3 nm) line.

Alternatively, hydrogen analysis is essential for studies related to the application technology in nuclear power stations [2]. In light water nuclear power stations, a zircaloy tube is used as a vessel for uranium fuel. During operation, hot water reacts with the zircaloy surface to produce H_2 gas, which then penetrates and accumulates in the zircaloy tube, causing unacceptable structural damage and critically reducing the strength of the material. Therefore, hydrogen inspection in zircaloy tubes must be performed periodically in a nuclear power station. Commercial methods for detecting hydrogen in such cases generally employ gas chromatography, requiring the melting of a portion of the zircaloy tube in a carbon furnace. This method is time consuming and is not an *in-situ* analysis.

In our previous work, we reported a novel "selective detection of H" technique using the specific characteristics of a TEA CO_2 laser in order to address the difficulties associated with H analysis in zircaloy using the laser plasma method [13, 20]. Focusing a TEA CO_2 laser on a zircaloy sample containing hydrogen (H) and surrounded by helium gas at atmospheric pressure resulted in the production of a strong helium gas plasma. Only H atoms came out of the metal sample because the sample surface was slightly melted due to the heat of the gas plasma. The H atoms then moved into the

region of helium gas plasma to be excited by metastable helium atoms; however, no host emission line from the sample appeared as ablation of the host elements does not occur. This technique has great potential for the highly sensitive analysis of H due to the absence of host emission lines.

However, the disturbance of H emission from H_2O is still a difficult problem. In our previous work using a zircaloy sample with free hydrogen, H emission appeared to some extent at 65 μg/g levels. To realize practical application of H analysis on a zircaloy sample in nuclear power station, we must suppress the H emission disturbance to a level less of than 10μg/g levels. In this research, we clarified the origin of the H emission disturbance coming from H_2O molecules. Namely, the H emission disturbance was due to H_2O molecules in the sample surface and not H_2O in the surrounding gas. We also studied the emission characteristics for emission from the surface and for emission from inside the sample. A preliminary experiment to confirm the realization of the laser cleaning method without a heating effect was been carried out.

5.4.2. Experimental Setup

Figure 5.24 shows the experimental arrangement used in this study. A TEA CO_2 laser (Shibuya SQ-2000; 3 J pulse energy, 10.6 μm wavelength, 200 ns pulse duration, and 30 mm x 30 mm beam cross-section) was used as an irradiation source. During the experiment, the laser energy was set at 250 mJ by inserting an aperture in front of the focusing lens. The laser beam was focused on the sample's surface from the front through a ZnSe window by using a combinations of two ZnSe lenses, one with a focal length of 50 mm and the other with a focal length of 100 mm. When the laser cleaning was employed to remove H_2O from the metal surface, the lens with a focal length of 50 mm was shifted 15mm from the focusing condition. The spot size of the laser beam on the zircaloy surface was 0.5 mm x 0.5 mm for tight focus, resulting in a power density of 0.7 GW/cm^2. The laser was typically operated at 10 Hz; however, the laser was employed in manual single shot mode for some experiments.

The samples to be irradiated were cleaned with ethanol and attached to a sample holder in a metal chamber. The samples used in this experiment were zircaloy that had been doped with various concentrations of hydrogen (0, 11, 50 and 100 μg/g). Prior to the analysis, the chamber with an inner diameter of 115 mm was evacuated using a

vacuum pump to a pressure of approximately 2 Pa was heated to 150°C, and held at that temperature for 30 minutes to remove the H_2O attached to the chamber wall. During laser bombardment, high-purity He gas (99.99999%) was passed over the surface through a metal pipe with a diameter of 5 mm. The pipe exit was located close to the focusing point of the gas plasma (at a distance of 3 mm). The helium gas flowed into the chamber from the pipe exit. The pressure of the surrounding gas in the chamber was set to 0.11 MPa.

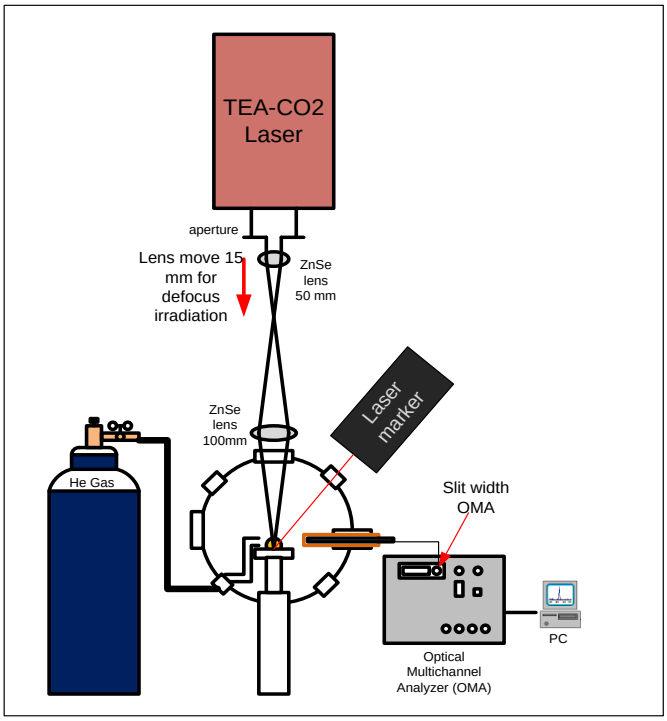

(a)

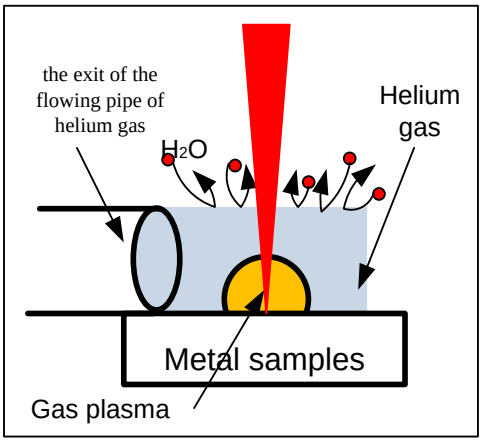

(b)

Fig.5.24 (a) Experimental set-up. (b) Metal-assisted helium gas plasma and helium gas flow system.

The emission spectrum of the plasma was obtained by detecting laser plasma radiation using an optical multi channel analyzer (OMA) system (ATAGO Macs-320) consisting of a 0.32 m focal-length spectrograph with a grating of 1200 grooves/mm, a 1024-channel photodiode detector array, and a micro-channel plate image intensifier. The spectral resolution of the OMA system was 0.2 nm and the spectral width to display was 60 nm. The light emitted from the laser plasma was collected by an optical fiber (27° in the solid angle) inserted in a quartz tube and placed 3 cm from the focusing point of the TEA CO_2 laser and perpendicular to the path of the laser beam. The other end of the fiber end was fed into the OMA system. In the case of photomultiplier detection, plasma emission was fed into a photomultiplier system consisting of a PMT H10304, amplifier, ADC converter, pulse delay generator C10149. Just in front of the photomultiplier, we put an interference filter (centre wavelength of 656.69 nm and bandwidth of 3.21 nm in FWHM).

5.4.3 Experimental Results and Discussion

In a previous experiment [13, 20], we reported a selective detection technique for H analysis in a zircaloy sample. The method has significant potential for sensitive analysis of H in a metal sample as it is not affected by the host emission lines that appear near the H emission line when the typical LIBS technique is used. In order to suppress the interference from H_2O, we intentionally generated a small-sized helium gas plasma, and high-purity helium gas was flowed using a small pipe (diameter of 2 mm), the exit of which was set near the gas plasma. In this study, we modified the helium gas flow system by using a large-diameter pipe (approximately 5 mm) so that the helium gas plasma was totally covered by fresh gas, which protected the helium gas plasma from being attacked by H_2O molecules as there are impurities in the surrounding gas, as shown in Fig. 5.24(b). In order to fully cover the helium gas plasma with fresh helium gas, the helium gas must be flowed with sufficient current.

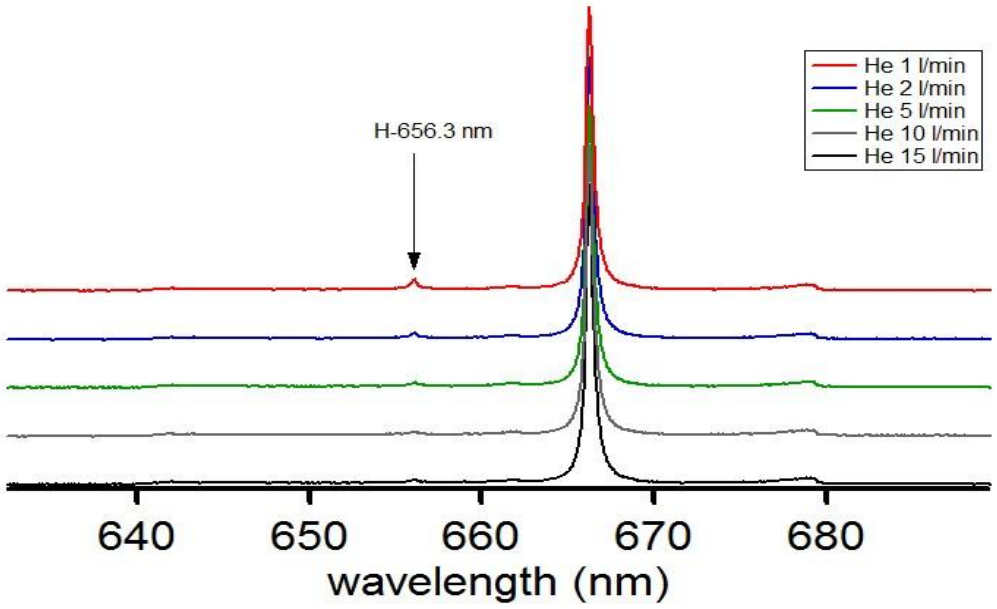

Fig.5.25 Hydrogen spectrum (656.3 nm) changes with helium flow rate in zircaloy sample with free hydrogen.

Figure 5.25 shows how the hydrogen spectra changes with helium flow rate and Fig. 5.26 shows how hydrogen emission intensity (656.3 nm) changes with helium flow rate which plotted from Fig. 5.25. The spectrum was acquired from the zircaloy sample with free hydrogen. Thus, the emitted hydrogen came from H_2O attached to the sample surface or contained in the surrounding gas. The delay time and gate width of the OMA system were set at 1 and 10 μs, respectively. Each data point plotted in the curve was obtained using ten shots of laser irradiation and data was acquired using a new position on the sample surface. The intensity of the H emission at 656.3 nm steeply decreased up to ten liters per minute and then become nearly constant with increasing He current. Based on this experiment, a He gas flow rate of ten liters per minute rate was used in subsequent experiments. This technique enables H emission to be suppressed to approximately 10μg/g.

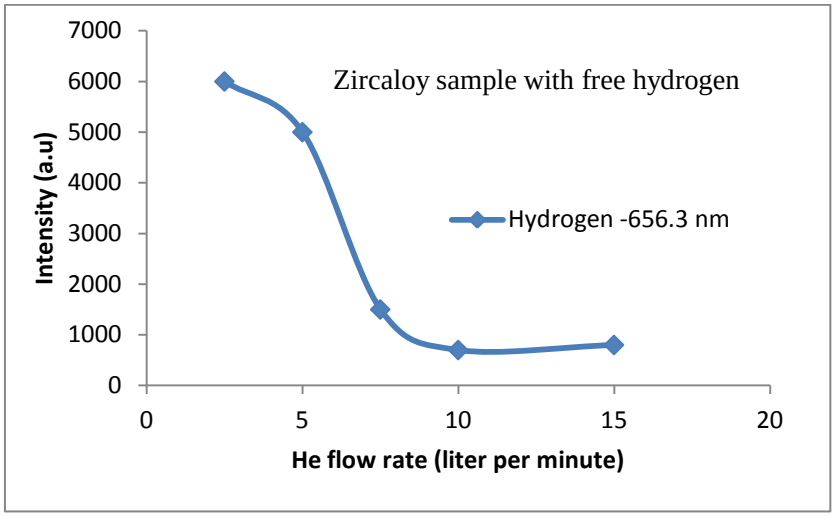

Fig.5.26 Hydrogen emission intensity (656.3 nm) as the function of helium flow rate in zircaloy sample with free hydrogen.

As described above, a host emission line did not appear near the H emission (656.3 nm) for this unique selective detection method, indicating that the slit width of the OMA could be opened further in order to improve the signal-to-noise (S/N) ratio. Figure 5.27 shows the emission spectra taken from a zircaloy sample containing 50 μg/g of H with the previously used slit width of 0.025 mm (red line) and with a slit width of 0.1 mm (blue line). The gate condition of the OMA system was set at 1–20 μs, and ten shots of the TEA CO_2 laser irradiation were used. With a slit width of 0.1 mm, the emission intensity was much greater and broader than that with a slit width of 0.025 mm. The S/N ratio using the slit width of 0.1 mm was four times greater than that using a slit width of 0.025 mm. When the slit width of the OMA was greater than 0.1 mm, a disturbance was generated due to the scattering of light in the spectrograph. Based on these results, we used a slit width of 0.1 mm in the subsequent experiments.

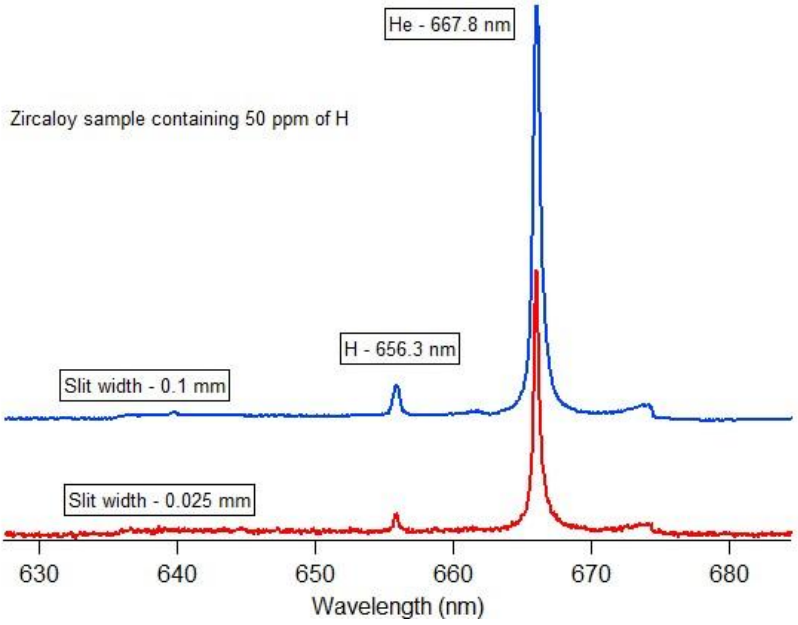

Fig.5.27 The emission spectra for zircaloy sample containing 50 µg/g of hydrogen using a slit width of 0.025 mm (red line) and a slit width of 0.1 mm (blue line).

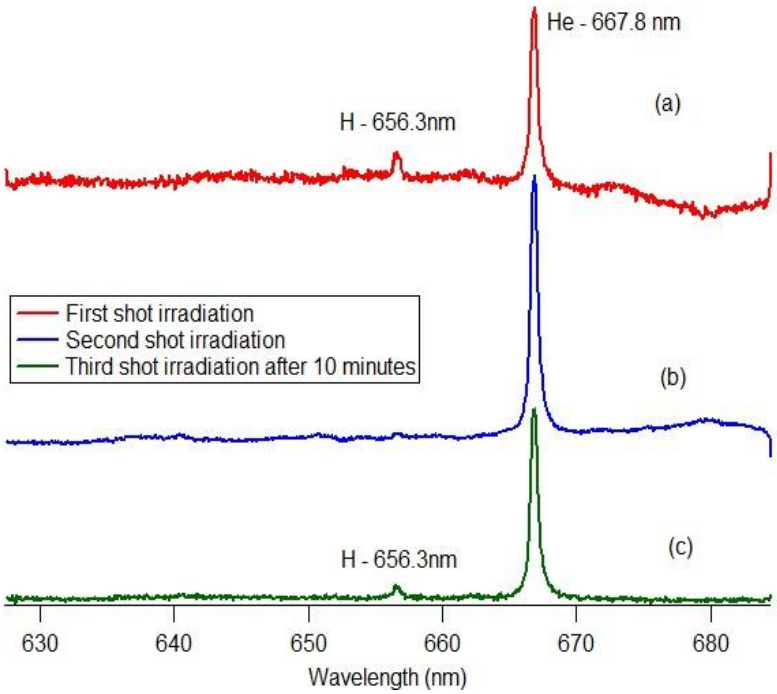

Fig.5.28 (a) The emission spectrum of a free hydrogen sample after the first single shot of laser irradiation. (b) The emission spectrum after the second single shot of laser irradiation administered a few seconds after the first laser irradiation. (c) The emission spectrum after the third single shot of laser irradiation applied approximately ten minutes after the second laser irradiation.

If a highly sensitive analysis of H with a detection limit of 1 μg/g is to be achieved, H emission from H_2O must be reduced further. For this purpose, the origin of H_2O, either from the sample's surface or the surrounding gas, must be understood as it is responsible for the H emission. As a result, emission spectra were collected using the manual single-shot irradiation mode. Figure 5.28(a) shows the emission spectrum of the first shot of laser irradiation on a free hydrogen zircaloy sample. The H emission (656.3 nm), which comes from H_2O, was relatively strong. Figure 5.28 (b) shows the emission spectrum of the second shot of laser irradiation a few seconds after the first laser irradiation. The laser irradiation was administered at the same position used in Fig. 5.28(a). The H emission nearly disappeared, indicating that the H emission is primarily due to H_2O molecules that are attached to the sample's surface and that the H_2O in the surrounding does not contribute directly to the H emission. If the origin of the H_2O responsible for H emission were the surrounding gas, H emission would always occur, regardless of previous laser bombardment. Figure 5.28 (c) shows the emission spectrum of the third shot of laser irradiation administered approximately ten minutes after the second shot. H emission was clearly observed, indicating that over the course of ten minutes, a considerable number of H_2O molecules had become attached to the sample's surface.

Another important factor to consider for suppressing H emission from H_2O is optimization of the gating time of the OMA system because there may be a difference in the emission time profiles between H emission from inside the sample and that from H_2O attached to the sample's surface. Figure 5.29 shows the time profiles of the H emissions from two different samples: a zircaloy sample containing 2600 μg/g of H (blue line) and a zircaloy sample with free hydrogen (H emission from the surface, red line). The gate width of the OMA system in this experiment was set at 0.5 μs, and the OMA slit width was 0.1 mm. Each data point plotted in the curve was obtained using ten shots of laser irradiation and was acquired using a new position on the sample's surface. In this experiment, we intentionally increased the amount of surface water to produce a sufficient signal corresponding to H emission by not heating the chamber. For the zircaloy sample containing 2600 μg/g of H, H emission increased steeply to 5 μs and then decreased to 20 μs. Because the H emission from the surface continues with a long lifetime, contribution of H emission from the surface increases when the gate width

of the OMA is increased. Therefore, the H emission must be measured at the initial stage of plasma production with the OMA gating time set at 1–3 μs.

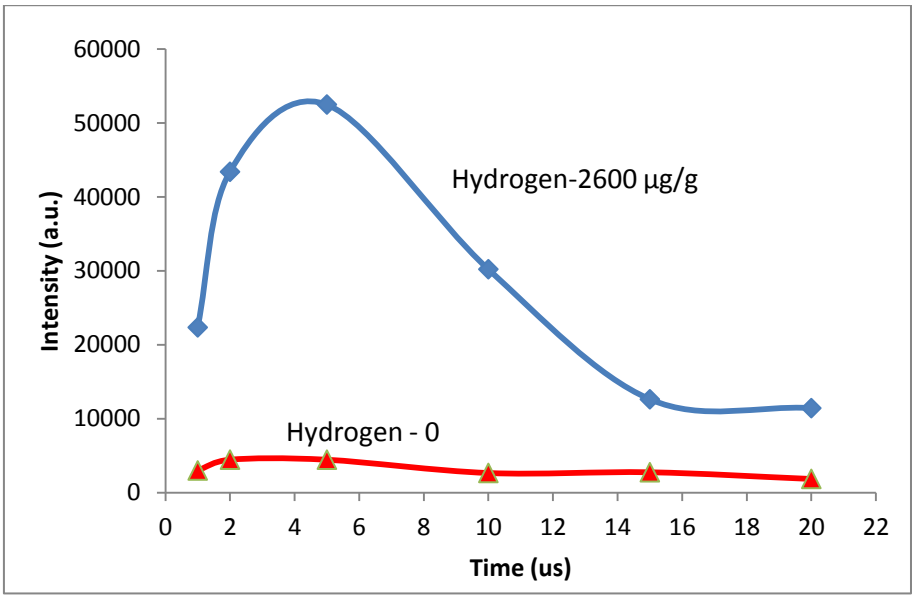

Fig.5.29 Time profile of H-656.3 nm emission taken from two different samples; namely, zircaloy sample containing 2600 μg/g of hydrogen (blue line) and zircaloy with free hydrogen (red line).

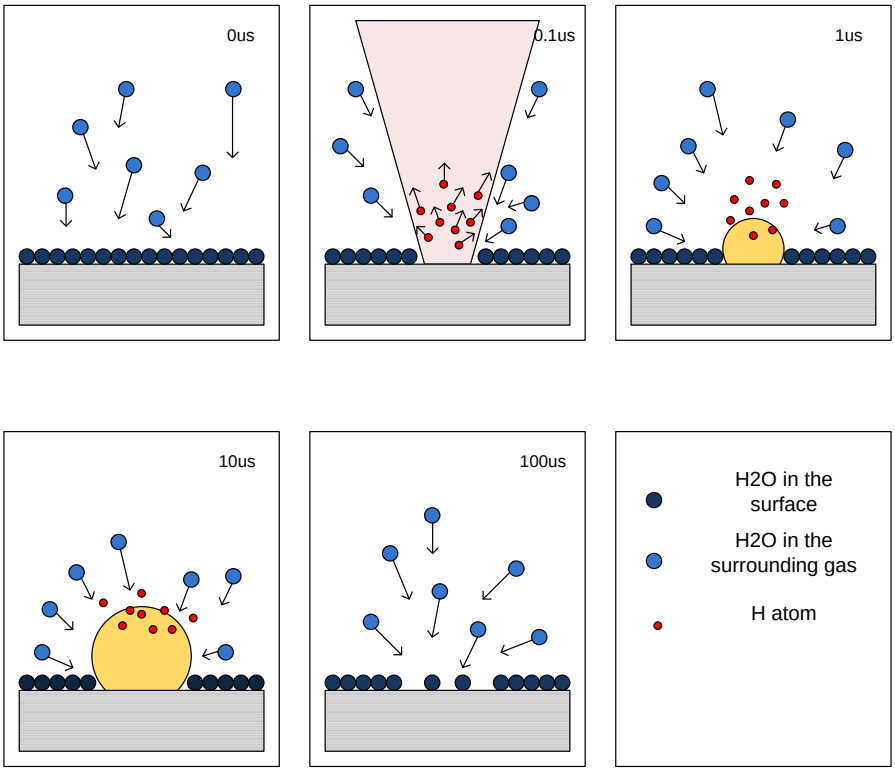

Fig.5.30 Illustration of the occurrence of H emission from H_2O attached on the metal surface when TEA CO_2 laser is irradiated on the metal surface.

The long lifetime of H emission from H_2O is explained as follows. As shown in Fig. 5.30, prior to laser irradiation, the sample surface is covered by H_2O molecules. During the initial stage (approximately 0.1 μs) of TEA CO_2 laser pulse irradiation when the helium gas plasma has not yet started to form, the H_2O molecules attached to the sample surface are dissociated by absorbing the TEA CO_2 laser energy to produce H and O atoms, and the atoms move out at high speed. After approximately 1 μs, the helium gas plasma expands until approximately 20 μs. Because the hydrogen is already distributed in the space in front of the helium gas plasma, the metastable helium atoms collide with the hydrogen atoms, resulting in H emission. When the plasma disappears after 100 μs, the H_2O molecules in the surrounding gas again start to attack the sample surface and become attached.

Based on these experiments, we conclude that the important factors for suppressing H emission from H_2O and increasing the sensitivity of H detection are a high He gas flow rate (ten liters per minute), which can be achieved using a large pipe, a wide slit width of 0.1 mm, pre-surface irradiation, and a suitable OMA gating time setting (1–3 μs). A preliminary H analysis experiment was performed under these optimized conditions using zircaloy samples containing different low-level concentrations of H (free hydrogen, 11 μg/g, 50 μg/g, 100 μg/g). Figure 5.31 shows the hydrogen emission spectra of zircaloy samples containing (a) 0 μg/g of H, (b) 11 μg/g of H, (c) 50 μg/g of H, and (d) 100 μg/g of H. Each spectrum was obtained after ten shots of laser irradiation at 10 Hz following two shots of pre-irradiation to remove the surface water. The gate time and the gate width of the OMA system were 1 and 2 μs, respectively. Hydrogen emission from the zircaloy containing 11μg/g H was observed with low background emission intensity, and the H emission from zircaloy 0 μg/g was very small.

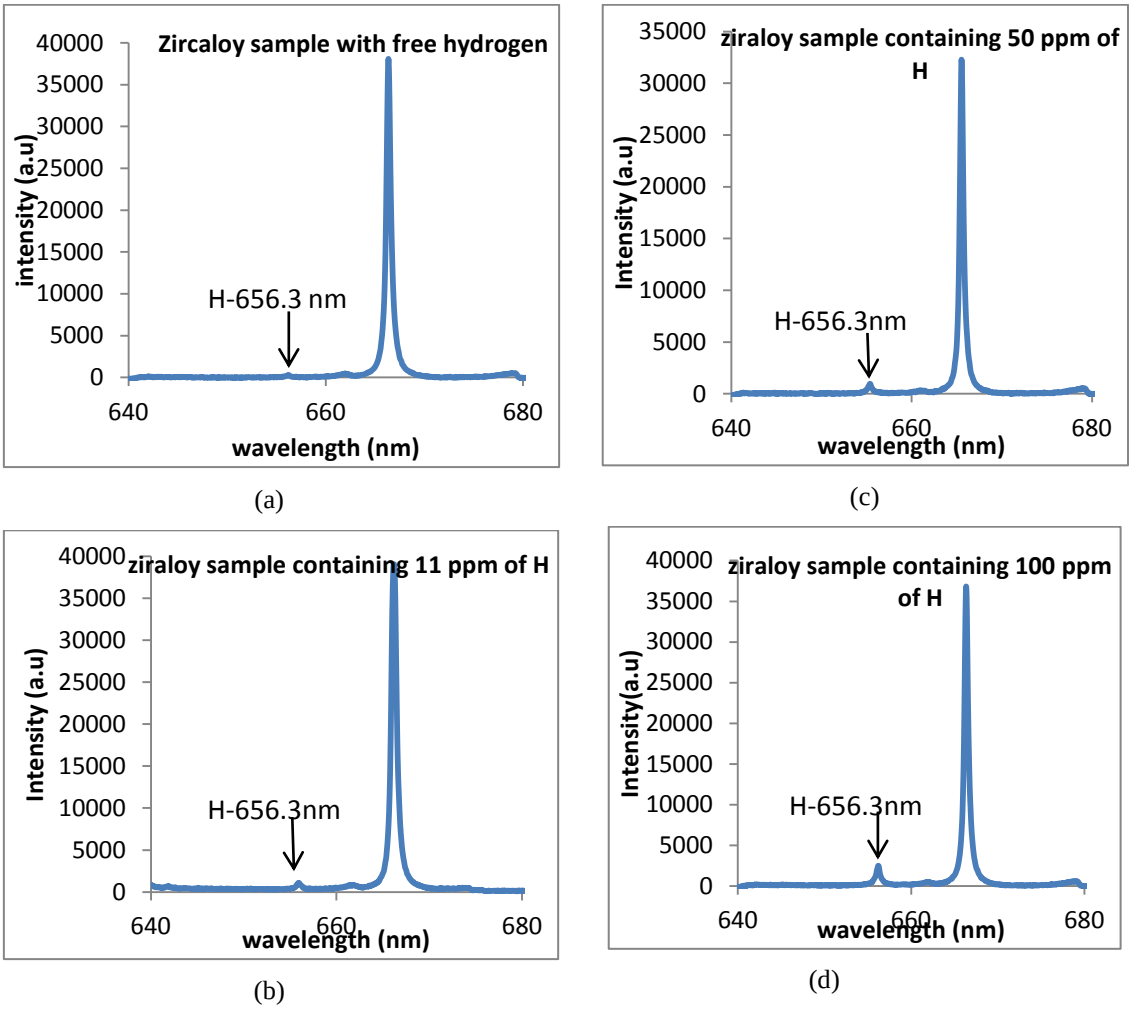

Fig.5.31 The hydrogen emission spectra taken from the zircaloy samples containing (a) 0µg/g of H, (b) 11 µg/g of H, (c) 50 µg/g of H, and (d) 100 µg/g of H.

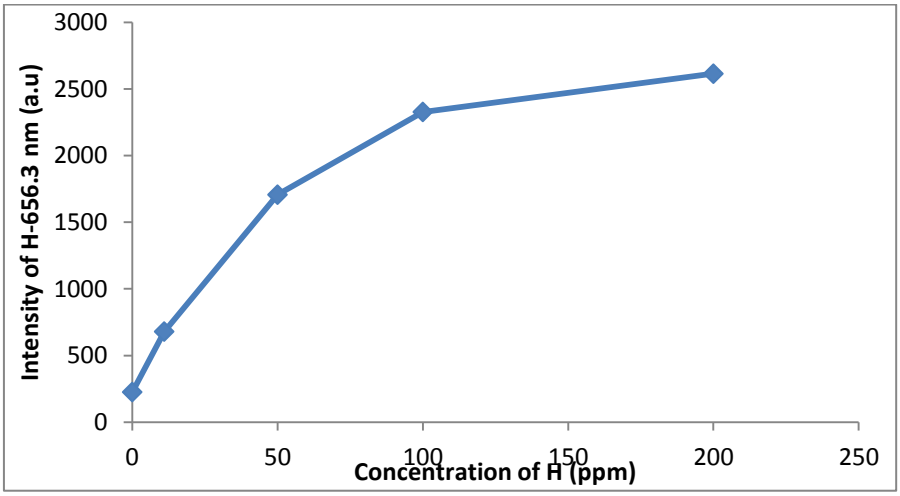

Fig.5.32 Calibration curve of hydrogen emission taken from zircaloy samples containing different concentrations of hydrogen in low concentration range between 11 µg/g and 100 µg/g

The data from Fig. 5.31 is plotted in Fig. 5.32 as a calibration curve. A standardization method was not used when generating this calibration curve because the helium emission intensity was nearly constant, regardless of the sample. As shown in Fig. 5.32, this calibration curve is not linear, especially at H concentrations greater than 100μg/g. This non-linearity is likely due to the heating effect. Some hydrogen atoms in the metal sample are removed by the heating effect during TEA CO_2 laser irradiation. Further study is required to improve this calibration curve. However, in this experimental stage, a reliable hydrogen analysis can be conducted in a low concentration range between 10μg/g and 100μg/g with a detection limit of at least 5μg/g. Notably, a calibration curve experiment with such low concentration levels of H have never been performed before due to the lack of H emission detection sensitivity and H_2O disturbance.

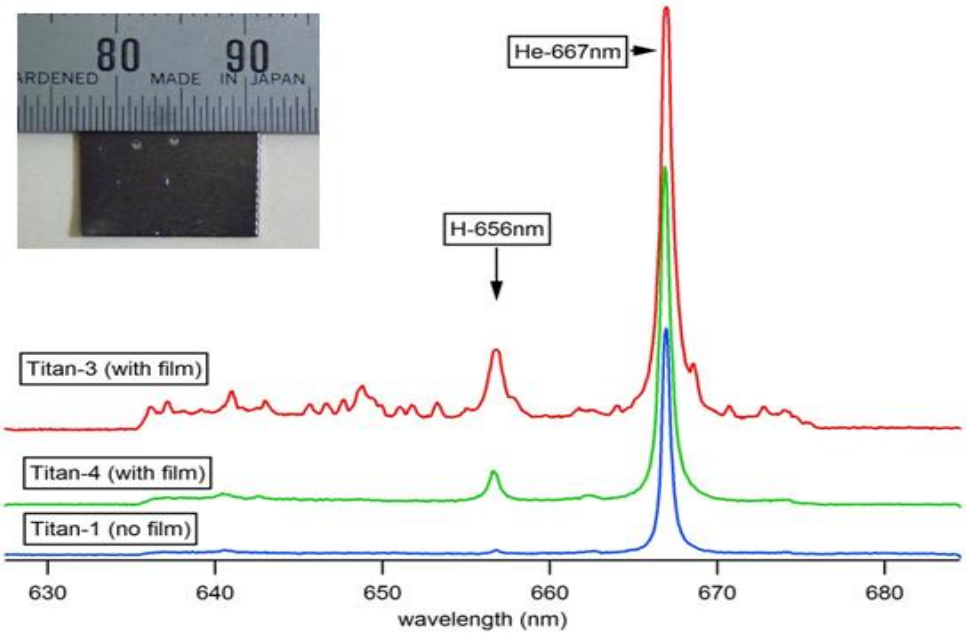

Fig.5.33 The emission spectrum taken from Titan samples which have different films on their surface; Titan-3 (red line) and Titan-4 (blue line) have coating films on the surfaces, while Titan-1 is pure Titan with free hydrogen (green line) and no film on it.

With confirmation of our technique's high sensitivity for suppressing the disturbance of H_2O, we fabricated a unique H analysis scenario in a Titan thin film sample. Figure 5.33 shows the emission spectra of Titan samples with different films on their surfaces (red line and green line), pure Titan with no film (blue line) and the inset figure is the titan sample after laser bombardment. The OMA gate condition of the

system was set at 1–3 μs, the slit width of the OMA was set at 0.1 mm and the helium gas flow rate was ten liters per minute. In this experiment, we did not use pre-irradiation because it would remove the thin film. The emission spectra of the Titan-3 and the Titan-4 samples are different due to the different surface coating treatment processes. In the spectrum for Titan-1 (blue line) shown in Fig. 5.33, the hydrogen signal is negligibly weak because there was no thin film on the surface, indicating that H elements in the film can be analyzed. This kind of film analysis is only possible with a TEA CO_2 laser because the induced gas plasma vaporizes only the thin film on the surface, without ablating the sample's body. If we had used a Nd:YAG laser, a strong host line would have appeared due to the ablation process. Additionally, ordinary H analysis using gas chromatograph is not possible because both the film and the sample will vaporize, causing loss in the film analysis.

By combining several techniques, we can suppress H emission from H_2O to approximately 5μg/g. The strict requirements of the nuclear power station industry can be satisfied using these techniques.

However, the present technique is still not sufficient for H analysis in steel samples, which requires a much greater H sensitivity with a few μg/g. In order to realize μg/g level analysis, complete removal of surface water is required. As illustrated in Fig. 5.28, the signal from H_2O can be reduced using a pre-irradiation technique. However, this method has a serious problem because one shot of irradiation already given influence to hydrogen inside the sample. To overcome this problem, the TEA CO_2 laser irradiation was made defocused condition. Figure 5.34 shows how the emission spectrum changed when the focusing lens was shifted; (a) tight focus, (b) defocus of 8 mm and (c) defocus of 15 mm after TEA CO_2 laser bombardment on the sample surface. These spectra were taken with ten shots of laser irradiation. The gate condition of the OMA system was set to 1–3 μs, the slit width of the OMA was 0.1 mm, and helium gas flow rate was ten liters per minute. When the lens defocus setting was set at 8 mm of defocus, hydrogen emissions increased causing the incremental of evaporation of H_2O molecules compared to the tight focus. However, when the lens was shifted at 15 mm of defocus, no emission lines appeared because no plasma was produced. Even if plasma is not generated, surface H_2O molecules will be removed through the absorption of the TEA CO_2 laser energy.

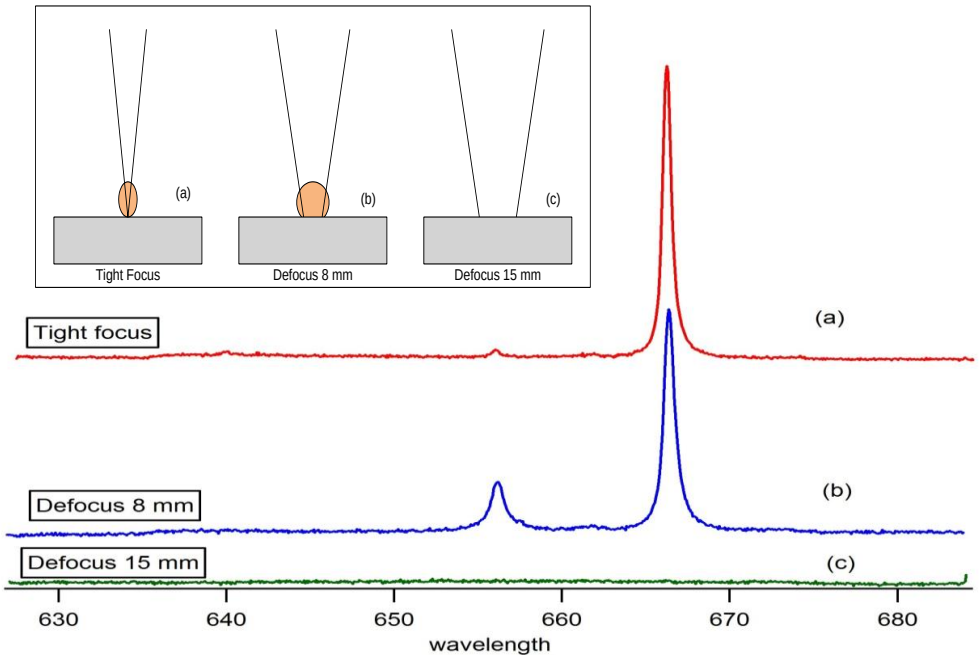

Fig.5.34 The emission spectra of hydrogen taken by zircaloy sample free hydrogen for tight focus (a), defocus 8 mm (b) and defocus 15 mm (c) after the TEA CO_2 laser bombardment.

In hydrogen analysis in steel sample, heating is not permitted because hydrogen is removed from inside. Therefore, the analysis must be conducted at room temperature. As a preliminary experiment to realize hydrogen analysis with μg/g level, we tried to reduce H emission from H_2O by employing the defocus cleaning method. In this experiment, we used zircaloy sample in place of steel.

Figure 5.35 shows the hydrogen emission spectra from the zircaloy sample with free hydrogen when laser irradiation was made by tight focusing (red line). The gate condition of the OMA system was set to 1–3 μs, the slit width of the OMA was 0.1 mm and helium gas flow rate was ten liters per minute. In this experiment, the heating treatment in the vacuum chamber was not applied. The remaining H emission, which comes from the surface water, is approximately 50μg/g. On the other hand, blue line spectrum was taken after defocusing cleaning; namely, ten shots of laser irradiation were performed under the defocusing condition, shifting the focusing lens at 15 mm, where almost no gas plasma generation was observed. Then, the lens was immediately set back for a tight focus to produce a helium gas plasma. H emission (blue line) is seen to be very weak (corresponding to approximately 10μg/g). Thus, the defocusing cleaning method was confirmed as being very effective for suppressing H emission

from H_2O on the sample's surface. However, our experimental system is not yet sufficient for practical applications because the time interval between the defocus laser cleaning and laser irradiation for plasma generation is approximately two minutes. This time interval is long, which causes many H_2O molecules to attach on the sample's surface. To solve this problem in the future, we will synchronize two TEA CO_2 laser with a suitable time interval (about 100 ms): one for the defocus laser cleaning and the other for the helium gas plasma generation.

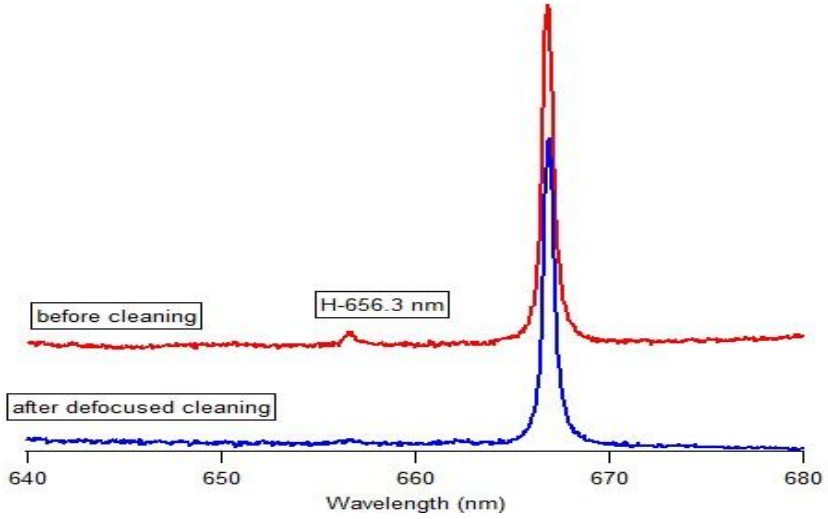

Fig.5.35 Hydrogen emission spectra taken from zircaloy sample with free hydrogen sample after the TEA CO_2 laser bombardment on the surface sample before cleaning (red line) and with the condition after defocusing laser cleaning (blue line)

In the future, in order to increase the sensitivity, we will employ a photomultiplier combined with an interference filter to pass H emission in place of the OMA system as shown in fig. 5.36 (a). Using this method, the S/N ratio will be improved at least 10^3 times over the OMA system case because the solid angle to collect H emission is significantly increased. A preliminary experiment was made. Fig. 5.36(b) shows hydrogen signal (656.3nm) from zircaloy sample containing 0μg/g and 50 μg/g of H using photomultiplier method. These signals were obtained with ten shots of laser irradiation at 10 Hz following two shots of pre-irradiation (not defocus cleaning) to remove the surface water and helium gas was flowed with 10l/min. Using this photomultiplier method, sensitivity was increased and noise decreased to the level of 0.2μg/g.

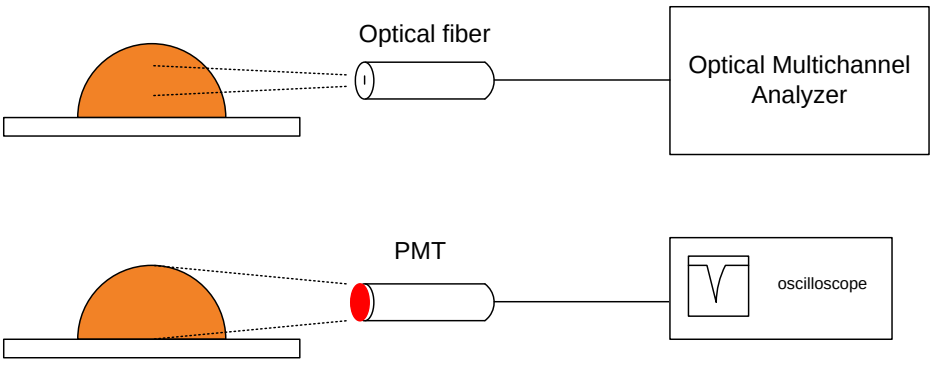

(a)

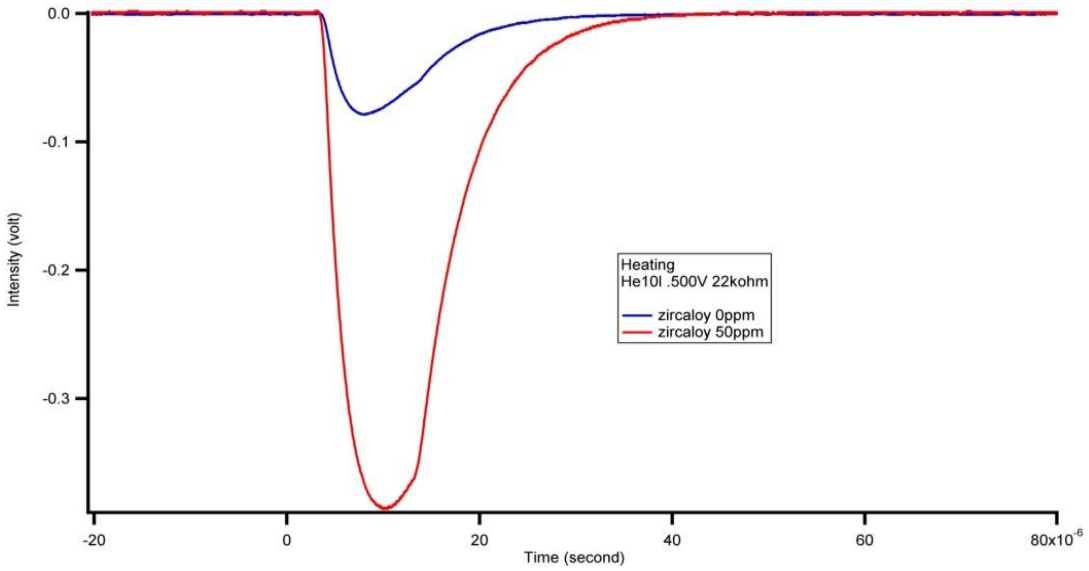

(b)

Fig.5.36 illustration of photomultiplier technique (a), Hydrogen-656.3nm intensity for zircaloy sample containing 0 and 50 μg/of hydrogen using photomultiplier technique (b)

5.4.4 Conclusion

In this study, we have developed a highly sensitive technique for the near *in-situ* analysis of hydrogen in a metal sample, which is typically difficult due to H_2O disturbance. For this purpose, the novel technique of "selective H detection" method using helium gas plasma was combined with several techniques. First, gas plasma was produced just near the exit of a large gas pipe (diameter of 5 mm) and high purity helium gas (99.99999%) was flowed at a high rate of ten liters per minute so that the

helium gas plasma was totally covered by the fresh helium gas. Using a pre-irradiation technique, H_2O on the surface was significantly removed. We confirmed that the origin of the H_2O causing the H emission was the H_2O located on the sample surface and not that in the surrounding gas. The time profiles of hydrogen emission from inside the sample and the sample surface were clearly different. The hydrogen emission from H_2O on the surface had a long lifetime compared to that from the sample itself. Therefore, in order to suppress the contribution of hydrogen emission from H_2O, the OMA gate condition was set at 1–3 μs. H calibration curve was made using a zircaloy sample containing a low concentration of hydrogen (11–100 μg/g). The results showed that the sensitivity of the H analysis was more than sufficient to assess hydrogen degradation in metal materials used in the nuclear industry. We also proved that this technique could be used for H analysis in thin films on Titan samples. In general, H analysis in films is very difficult because when conventional H analysis using gas chromatography is employed, the film and the sample will be vaporized, which causes loss of information of the H distribution. We confirmed that the defocused cleaning methods were very effective for suppressing the disturbance of the H emission from H_2O on the sample surface. By combining several techniques described above, we succeed in suppressing H emission from H_2O to the level of 10μg/g. In the future, to achieve H analysis with a precision of 1 μg/g, we will employ two TEA CO_2 laser systems which can be operated with suitable synchronized time. Namely, one laser is used for surface cleaning by defocused laser irradiation and the other is used for He gas plasma generation. Our final goal is to realize H analysis in steel sample, where the analysis of level of 1 μg/g is required.

References

1. D. A. Cremers, and L. J. Radziemski, Handbook of Laser-Induced Breakdown Spectroscopy, John Wiley and Sons, Ltd, England, 2006
2. K. H. Kurniawan, and K. Kagawa, Laser- Induced Shock Wave Plasma Spectroscopy, Applied Spectroscopy Reviews, **41** (2006), 1-36
3. N. Idris, S. Terai, T. J. Lie, H. Kurniawan, T Kobayashi, T. Maruyama, and K.Kagawa, Hydrogen Emission Induced by TEA CO_2 Laser Bombardment on Solid Samples at Low Pressure and Its Analytical Application, Appl. Spectroscopy, **59** (2005) 115-120

4. K. H. Kurniawan, M. Pardede, R. Hedwig, Z. S. Lie, T. J. Lie, D. P. Kurniawan, M. Ramli, K. Fukumoto, H. Niki, S. N. Abdulmajid, N. Idris, T. Maruyama, K.Kagawa, and M. O. Tjia, Quantitative Hydrogen Analysis of Zircaloy-4 Using Low-Pressure Laser Plasma Technique, Anal. Chem. **79** (2007) 2703-2707
5. M. Pardede, K. H. Kurniawan, T. J. Lie, R. Hedwig, N. Idris, T. Kobayashi, T. Maruyama, Y. I. Lie, K. Kagawa, and M. O. Tjia, Hydrogen Analysis in Solid Samples Using Laser-Induced Helium Plasma at Atmospheric Pressure J. Appl. Phys. **98** (2005) 043105 1-5.
6. M. Ramli, N. idris, K. Fukumoto, H.Niki, F. Sakan, T. Maruyama, K. H. Kurniawan, T. J. Lie, K. Kagawa, Hydrogen Analysis in Solid Samples by Utilizing Helium Metastable Atoms Induced by TEA CO2 Laser Plasma in Helium Gas at 1 Atmosphere, Spectrochim. Acta Part B: At. Spectrom. **62** (2007) 1379-1389.
7. M. Ramli, N. Idris, H. Niki, K. H. Kurniawan, and K. Kagawa, New Method of Laser Plasma Spectroscopy for Metal Samples Using Metastable He Atoms Induced by Transversely Excited Atmospheric Pressure CO_2 Laser in He Gas at 1 atm, Jpn. J. Appl. Phys., **47**, (2008) 1595 -1601
8. Bernstein, I. M. and Thompson, A. W. Hydrogen Effects in Metals, The metallurgical Society of AIME, New York, 1981
9. Oriani, R. A. Hirth, J. P. And Smialowski, M. Hydrogen Degradation of Ferrous Alloys Noyes Publications, New Jersey, 1985
10. Moody, N. R. and Thompson, A. W. Hydrogen Effects on Material Behavior, The Minerals, Metals & Material Society, Pennsylvania, 1990
11. F. *Boué*-Bigne, Laser-induced breakdown spectroscopy applications in the steel industry: Rapid analysis of segregation and decarburization, Spectrochim. Acta, Part B., **63** (2008) 1122-1129
12. M. Tran, Q. Sun, B. W. Smith, and J. D. Winefordner, Determination of F, Cl, and Br in Solid Organic Compounds by Laser-Induced Plasma Spectroscopy, Appl. Spectrosc., **55** (2001) 739-744
13. Z.S. Lie**,** Ali Khumaeni**,** H. Niki, K. Fukumoto, and K. Kagawa Hydrogen Analysis in Metal Samples by Selective Detection Method Utilizing TEA CO2 Laser-Induced He Gas Plasma, *Applied* Physics A, Springer **101**, (2010) 555-558
14. Ali Khumaeni, Zener Sukra Lie, Hideaki Niki, Kenichi Fukumoto, Tadashi Maruyama, and Kiichiro Kagawa. A Novel Double Pulse Laser Plasma Spectroscopy Technique for H Analysis in Metal Sample Utilizing Transversely Excited Atmospheric-pressure CO2 Laser-InducedMetastable He Atoms. Journal of optical review **17** (2010) 285-289
15. K. Kagawa, K. Kawai, M. Tani, and T. Kobayashi, XeCl Excimer Laser-Induced Shock Wave Plasma and Its Application to Emission Spectrochemical Analysis, Appl. Spectrosc. **48** (1994) 198-205.
16. A. W. Miziolek, V. Palleschi, and I. Schechter: Laser- Induced Breakdwon Spectroscopy (LIBS): Fundamental and Application, Cambridge University Press, New York, 2006
17. N. Omenetto, Role of lasers in analytical atomic spectroscopy: where, when and why, J. Anal. At. Spectrochem. **13** (1998) 385-399.

18. D. A. Rusak, B. C. Castle, B. W. Smith, J. D. Winefordner, Recent Trends and the Future of Laser-Induced Breakdown Spectroscopy, Trends in Anal. Chem. **17** (1998) 453.
19. J.M. Vadillo, and J. J. Laserna, Laser-induced plasma spectrometry: truly a surface analytical tool, Spectrochim. Acta B. **59** (2004) 147-161.
20. Zener Sukra Lie**,** Ali Khumaeni, Tadashi Maruyama, Ken-ichi Fukumoto, Hideaki Niki and Kiichiro Kagawa, Emission characteristics of Hydrogen in atmospheric helium gas plasma induced by TEA CO_2 laser bombardment on zircaloy sample containing hydrogen, Journal of Analytical Atomic Spectrometry, 26 (2011) *1451*
21. K.H. Kurniawan, T. J. Lie, M. M. Suliyanti, R. Hedwig, M. Pardede, M. Ramli, H. Niki, S. N. Abdulmadjid, N. Idris, K. Lahna, Y. Kusumoto, K. Kagawa, M. O. Tjia, The Role of He in Enhancing the Intensity and Lifetime of H and D Emissions from Laser-Induced Atmospheric-Pressure Plasma, J. Appl. Phys. **105** (2009) 103303 1-6.
22. A. F. Gibson, T. P. Hughes, C. L. M. Ireland, Numerical curve fitting of general order kinetics glow peaks, J. Phys. D: Appl. Phys. **4** (1971) 1527- 1534
23. T. R. Loree and L. J. Radziemski, Laser-induced breakdown spectroscopy: time integrated applications Plasma Chem. Plasma Process. **1**, (1981) 271-280.
24. L. J. Radziemski and T. R. Loree, Laser-induced breakdown spectroscopy: time resolved spectrochemical applications. Plasma Chem. Plasma Process. **1**, 281 (1981).
25. N. Konjevic, Plasma broadening and shifting of non-hydrogenic spectral lines: present status and applications, Phys. Rep. **316**, (1999) 339-401.
26. N. Idris, K. H. Kurniawan, T. J. Lie, T. Kobayashi, M. Pardede, H. Suyanto, R. Hedwig, K. Kagawa, and T. Maruyama, Characteristics of Hydrogen Emission in Laser Plasma Induced by Focusing Fundamental Q-sw YAG Laser on Solid Samples, Jpn. J. Appl. Phys. **43**, 4221 (2004).

Chapter 6

Summary and Conclusion

Laser-induced breakdown spectroscopy (LIBS) was recently shown to be promising techniques for rapid quantitative analysis of elements in many kinds of sample, including metals. On the other hand, hydrogen analysis was essential in the technology of nuclear power stations. Therefore, we want to use LIBS technique for implementation of hydrogen analysis in nuclear power station. However, highly sensitive and reliable analysis of hydrogen in metal samples is very difficult if we use the standard LIBS technique due to broadening of the H emission spectrum, a "mismatching effect", and the disturbance from ubiquitous water molecules (H_2O).

During our continuing study, it had been clarified that in order to overcome these difficulties, there are two options. One is laser-induced low pressure plasma and another is laser-induced helium gas plasma at atmospheric pressure. In this thesis, experimental study has been made and it was divided into five main topics:

1. High sensitive analysis of hydrogen (deuterium) using laser-induced low pressure plasma,
2. the proof of "mismatching effect" using atmospheric helium gas plasma,
3. high sensitive analysis of deuterium using Nd:YAG laser-induced atmospheric helium gas plasma,
4. high sensitive analysis of hydrogen (deuterium) using TEA CO_2 laser-induced atmospheric helium gas plasma (selective detection of H),
5. Excitation mechanism of atoms in atmospheric helium gas plasma.

Summary of this study was described as follows. In low pressure plasma, titan sample was used to determine the most favorable experimental parameters in UV laser (355nm) - induced plasma spectroscopy. An effective enhancement of the D impurity signal and effective elimination of the interfering hydrogen emission from the surface water were achieved with low laser energy (5mJ). Another kind experiment on low pressure was done to realize the depth profile of H analysis. Namely, the nanoseconds Nd:YAG laser has been replaced by picoseconds laser (pulse 20ps) using zircaloy samples. Using this picoseconds laser, we have succeeded in obtaining the more adequate calibration line applicable to quantitative hydrogen analysis because of less thermal effect. As the results, high sensitive hydrogen analysis with a limit of detection around 10μg/g was realized.

According to the shock wave model, by the laser irradiation, atoms gush out from the surface with super high speed and adiabatic compression takes place in the surrounding gas to make shock wave. Just behind the shock wave, high temperature plasma was produced and atoms are excited in the high temperature region. It is assumed that in high pressure, hydrogen gush out earlier with very high speed than other elements because hydrogen mass is extremely lighter than others, and when the shock wave starts the hydrogen already locates at the forward of the shock front. Therefore, no excitation of hydrogen happens. We called this as "mismatching effect". To prove this assumption, we used "helium metastable atoms probing technique"; namely helium gas plasma was produced in front of the sample surface by focusing fundamental Nd:YAG laser (110mJ). Then, 532 nm Nd:YAG laser was irradiated to sample surface with a suitable delay time to send the atoms to the cooled helium gas plasma, where metastable helium existed. When ground state atoms enter the cooled helium gas plasma, emission takes place by colliding with metastable helium atoms. By this method, we directly proved that H atoms come out much faster than other elements.

For highly sensitive analysis of deuterium using atmospheric helium gas plasma, we also used Nd:YAG laser-induced helium gas plasma to excite the ablated atoms, and the picoseconds Nd:YAG laser (pulsed of 20ps) was used to ablate the zircaloy surface sample. By controlling the timing between the generation of helium gas plasma and target ablation, we realized very sensitive D analysis by suppressing the disturbance of H_2O. Namely, atoms which are ablated by ps laser, are swept out the H_2O molecules from the helium gas plasma region. The detection limit was confirmed to be 20μg/g, approximately.

As we confirmed before, metastable helium atoms produced in Nd:YAG laser-induced helium gas plasma are very useful to excite hydrogen atom. To make a lot of metastable helium atoms, big helium gas plasma was required. For this purpose, TEA CO_2

laser was used due to the specific characteristics of a TEA CO_2 laser which has low frequency (long wavelength of 10.64 μm) and long pulse duration (200 ns). In early study, we have employed a unique double –pulse technique for H analysis in a zircaloy sample that combines a TEA CO_2 laser and a Nd:YAG laser. The Nd:YAG laser, which is synchronized with the TEA CO_2 laser, is focused onto the metal surface to ablate the atoms into the helium gas plasma induced by the TEA CO_2 laser. However, we found in this research that by conscientiously performing the experiment, in which we suppress the amount of the ubiquitous water molecules (H_2O) deposited on the sample surface and also populated in the surrounding gas, the H emission is still clearly detected from the zircaloy sample containing several hundred μg/g of H. Namely, this result indicates that zircaloy sample is faintly melted and only H atoms come out from the sample surface and subsequently move into the helium gas plasma to be excited through metastable helium atoms. We named this as "selective detection of H".

Using the "selective detection of H" technique, the H_α, H_β, H_γ, and H_δ emission lines can be detected clearly with very low background spectra and a very narrow spectral width using the zircaloy sample containing hydrogen. Based on these emission characteristics, which cannot be found in case of standard LIBS method, the excitation mechanism of H which is crucial issue for H analysis in metal samples was discussed. To clarify the excitation mechanism and characteristic of atoms in TEA CO_2 laser-induced helium gas plasma, Teflon was used as a sample because it contains carbon and fluorine as host elements and hydrogen as impurity. As the result, we concluded that not only impurity atoms but also helium atoms are excited through helium metastable atoms. This helium metastable atom is produced at initial stage of the helium gas plasma production through recombination process between ions and electrons. In the helium metastable state, there are two kinds; namely, triplet and singlet. It is important to know which one is the major contributor in excitation process. For this purpose, the helium emission spectrum was observed in wide-wavelength region. It was found that the helium emission of 587.6nm (due to the transition from 3d to 2p in triplet) is much stronger than that of 667.8 nm (due to the transition from 3d to 2p in singlet). This fact indicates during the recombination between ions and electrons, mostly triplet helium atoms are produced. Thus, we conclude that not singlet helium metastable atoms but triplet helium metastable atoms are major contributor in the excitation process.

In order to get highly sensitive H analysis using "selective detection of H" method, we combined several unique methods to suppress H emission from H_2O; the gas plasma was produced just near the exit of a large gas pipe and high purity helium gas was flowed at a

high current of ten liters per minute so that the helium gas plasma was totally covered by the fresh helium gas, and also a pre-irradiation technique was used. By these methods, H emission from H_2O was significantly reduced. We also demonstrated that defocus cleaning is very effective to remove H_2O without using the heating process.

It is naturally expected that the sensitivity of H analysis can be highly increased when we employ a photomultiplier combined with an interference filter to pass only H emission in place of the OMA system. Preliminary experiment was made in this study and the S/N ratio was improved at least 10^3 over the OMA system case because the solid angle to collect H emission is significantly increased. By combining this PMT method and TEA CO_2 laser defocus cleaning method, in the future H analysis in steel sample, where μg/g level are required, will be realized.